CAPILLARY LC-MS METHODS FOR TRACE LEVEL PEPTIDE DETECTION AND ITS APPLICATION FOR MONITORING NEUROPEPTIDES *IN VIVO*

by

Ying Zhou

A dissertation submitted in partial fulfillment
of the requirements for the degree of
Doctor of Philosophy
(Chemistry)
in The University of Michigan
2015

Doctoral Committee:

Professor Robert T. Kennedy, Chair
Professor Kristina I. Håkansson
Professor Adam J. Matzger
Professor Yoichi Osawa

DEDICATION

To my parents, Min Yang and Xiaoping Yang, and my husband, Junsi Gu, who constantly support me through all the obstacles encountered in my dissertation study.

ACKNOWLEDGEMENTS

I would like to express my deepest gratitude to my advisor Professor Robert T. Kennedy, who accepted me as his graduate student and offered enormous support and encouragement during my PhD study. I would like to thank him for always challenging me to achieve more; the training I received with his guidance has helped me grow tremendously. I would also like to thank my dissertation committees, Professor Kristina Håkansson, Professor Adam Matzger and Professor Yoichi Osawa for their expert input and insightful advices throughout my candidacy, data meeting and dissertation. I could not have achieved this far without their gracious help.

It has been great pleasure to work in Kennedy lab, embraced by the warm support and friendship given by all the colleagues I had overlap with, including Dr. Shunwen Sun, Dr. Claire Chisolm, Dr. Maura Perry, Dr. Anna Clark, Dr. Qiang Li, Dr. Peng Song, Dr. Gwendolyn Anderson, Dr. Thomas Slaney, Dr. Neil Hersey, Dr. Jing Nie, Dr. Meng Wang, Dr. Omar Mabrouk, Dr. Woog He Lee, Dr. Ting Zhang, Dr. Maojun Gong, Dr. Chunhai Ruan, Dr. Beixi Wang, Dr. Jim Grinias, Dr. Kennon Deal, Dr. Jeremy Felton, Dr. Mohamed Dawod, Dr. Mahmoud ElAzzouny, Dr. Alexandros Zestos, Cynthia Cipolla, Shi Jin, Shusheng Lv, Erik Guetschow, Colleen Dugan, Jenny-Marie Wong, Paige Malec, Thitaphat Ngernsutivorakul and Joanna Thielen. I am and will always be proud of being a Kennedian. I want to especially thank Dr. Omar Mabrouk and Jenny-Marie Wong for their generous help in keeping the capillary LC-MS system behaving and for the collaboration in the *in vivo* part of my projects.

Last but not least, I would love to give my sincere thanks to my family and friends for their continuous encouragement and support. I cannot thank my husband Junsi Gu enough for taking me as who I am, for his persistent faith in me and his unconditional love which led me through my toughest times in my research.

TABLE OF CONTENTS

LIST OF FIGURES

LIST OF TABLES

LIST OF APPENDICES

LIST OF ABBREVIATIONS

α-MSH	α-melanocyte-stimulating-hormone
Aβ	β amyloid
aCSF	artificial cerebrospinal fluid
AD	Alzheimer's Disease
AGC	automatic gain control
amol	attomole
ApoE	apolipoprotein E
Ang	angiotensin
AQUA	absolute quantification
AVP	arginine vasopressin
BDNF	brain-derived neurotrophic factor
BLAST	basic logical alignment search tool
BSA	bovine serum albumin
CCK	cholecystokinin
CeA	central amygdala
CID	collision-induced dissociation
cLC	capillary liquid chromatography
CNS	central nervous system
CRH	corticotropin releasing hormone
CRM	consecutive reaction monitoring
CSF	cerebrospinal fluid
Da	dalton
DynA	dynorphin A
EC	electrochemical detection
ELISA	enzyme-linked immunosorbent assay
EIA	enzyme immunoasssay
ESI	electrospray ionization
FT-ICR	Fourier transform ion cyclotron resonance
FWHM	full width at half maximum
Gal	galanin
GDNF	glial cell derived neurotrophic factor
GnRH	gonadotropin-releasing hormone
GP	globus pallidus
GRP	gastric releasing peptide
hBD-1	human β defensing-1

HPLC	high performance liquid chromatography
ICPMS	inductively coupled plasma mass spectrometry
I.D.	inner diameter
IL	interleukin
i.p.	intraperitoneal
ISF	interstitial fluid
KP	kisspeptin
LC	liquid chromatography
LDCV	large density-core vehicle
LE	leucine enkephalin
LF-IBBC	lateral flow integrated blood barcode chip
LIT	linear ion trap
LoB	limit of blank
LOD	limit of detection
MALDI	matrix assisted laser desorption ionization
ME	methionine enkephalin
MS	mass spectrometry/mass spectrometer
MS^n	multistage mass spectrometry
MW	molecular weight
MWCO	molecular weight cut-off
OFQ	orphanin FQ
NGF	nerve growth factor
NPY	neuropeptide tyrosine
NT-3	neurotrophin-3
O.D.	outer diameter
OXT	oxytocin
PAN	polyacrylonitrile
PEI	polyethyleneimine
PEO	polyethylene oxide
PPO	polypropylene oxide
PRISM	high-pressure, high-resolution separations coupled with intelligent selection and multiplexing
PS-DVB	polystyrene-divinylbenzene
PTFE	polytetrafluoroethylene
PTH	parathyroid hormone$_{1-34}$
PVN	paraventricular nucleus
Q-TOF	quadrupole-time-of-flight
QIT	quadrupole ion trap
RIA	radio immunoassay
RSD	relative standard deviation
SCX	strong cation exchange

SD	standard deviation
SELDI	surface enhanced laser desorption ionization
SEM	standard error of mean
SIL	stable isotopically labeled
SISCAPA	stable isotope standards and capture by anti-peptide antibodies
SMT	somatostatin
SRM	selected reaction monitoring
Sub P	substance P
TIMP-1, -2	tissue inhibitor of metalloproteinases-1, -2
SPE	solid phase extraction
TOF	time of flight
VEGF	vascular endothelial growth factor
VIP	vasoactive intestinal peptide
VTA	ventra tegmental area

ABSTRACT

Capillary liquid chromatography coupled to mass spectrometry detection (cLC-MS) is an emerging technique for detecting low abundance peptide from microliters of sample. Its practicality in monitoring peptides from *in vivo* microdialysate was limited to 10 out of more than 200 mammalian neuropeptides due to the slow analysis rate and uneven sensitivity for different peptides. The slow speed is not favorable for *in vivo* study which can generate many samples per day, while peptide degradation during storage requires immediate measurement after collection. The uneven sensitivity results in high limit of detection (LOD) of some neuropeptides, making them undetectable by cLC-MS at dialysate concentration. In this dissertation, cLC-MS's performance was improved in these two aspects.

The rate limiting step of cLC-MS was the long sample injection/rinsing process due to high back pressure using a 25 μm bore column. A method utilized large particle (10 μm) as LC packing and 75 μm bore column was developed to reduce column back pressure and enhance injection/rinsing speed. The method reached 4 min/sample throughput compared to previously reported throughput at 20-30 min/sample with similar LOD for enkephalins and dynorphin A_{1-8}. This was achieved by rapidly injecting sample under 14 μL/min and eluting the peptides slowly under 100 nL/min to maintain nanoESI sensitivity. This method was applied for monitoring enkephalins from rat globus pallidus (GP) dialysate.

To increase peptide detection sensitivity, acetonitrile (ACN) was used as organic additive in sample to increase neuropeptide solubility and decrease nonspecific adsorption. Adding ACN to optimal concentration improved LOD to low pM range (0.1-2 pM) from 8 µL sample for all 10 neuropeptides tested in the study. In addition, modification of the microdialysis probe using polyethyleneimine (PEI) increased sampling recovery by reducing electrostatic interaction between neuropeptides and microdialysis catheter. This method was applied for monitoring intact orexins from rat arcuate nucleus.

Application of cLC-MS can be extended to quantifying low abundance proteins using a peptide fragment produced from protease digestion (signature peptide method). In Chapter 4 a signature peptide method for brain derived neurotrophic factor (BDNF) was developed. For BDNF, chymotrypsin produced higher signature peptide signal than trypsin digestion, and concentrating the protein prior to denaturation, reduction and alkylation was necessary to achieve good signature peptide signal. The method had 5 pM LOD for BDNF and neurotrophin-3 (NT-3), and 10 pM LOD for glial cell derived neurotrophic factor (GDNF), and can be potentially applied for detecting these neurotrophins from *in vivo* sample.

Chapter 1

Introduction

1.1 Overview of neuropeptides and neuroproteins

Neuropeptides are peptides produced and released by neurons and are capable of exerting signaling effects by binding to neuronal receptors[1]. Neuropeptides are synthesized as biologically inactive protein precursors, called prepropeptide, at the ribosome of the neuron cell. Prepropeptides undergo proteolytic cleavage to form mature neuropeptides, which are packed into large density-core vehicle (LDCVs) and delivered to axons and dendrities for release. Neuropeptides are released via exocytosis upon strong stimulation in a Ca^{2+} dependent manner. Released neuropeptides can bind to their post-synaptic neuron receptors, or diffuse into extracellular space, where they can either bind to a receptor in neurons distant from the releasing neuron or be deactivated by peptidase. Neuropeptides can act as: (1) neurotransmitters that transmit signal between releasing neurons and receiving neurons; (2) neuromodulators that modulates small molecule neurotransmitter effects; (3) paracrine and autocrine regulators that are involved in cell-to-cell communication; and (4) hormones that are released into blood stream and exert impact on distant organs. Different functions of neuropeptides are depicted in Figure 1.1.

Neuropeptides constitute the largest and most diverse family of signaling molecules in the central nervous system (CNS). Over 70 genes encoding prepropeptides have been discovered, and each prepropeptide can produce several active neuropeptides[1]. They are involved in many physiological and pathological processes, such as learning and

memory[2], pain modulation[3], sleep regulation[4,5], appetite control[6], social interaction[7], drug addiction[4,6] and depression[8]. Research has been performed to understand neuropeptide function from different perspectives, including: (1) tissue distribution study by locating neuropeptide-producing neurons and neuropeptide receptors; (2) quantification from tissue extract or body fluids to evaluate disease state and pharmacological treatment; (3) in-brain administration for understanding their signaling circuit and potential as drug targets; (4) studying animal models lacking or over-expressing certain neuropeptide; (5) *in vivo* monitoring for direct correlation between their extracellular level and behavior, pharmacological treatment and other neurochemical changes in the brain.

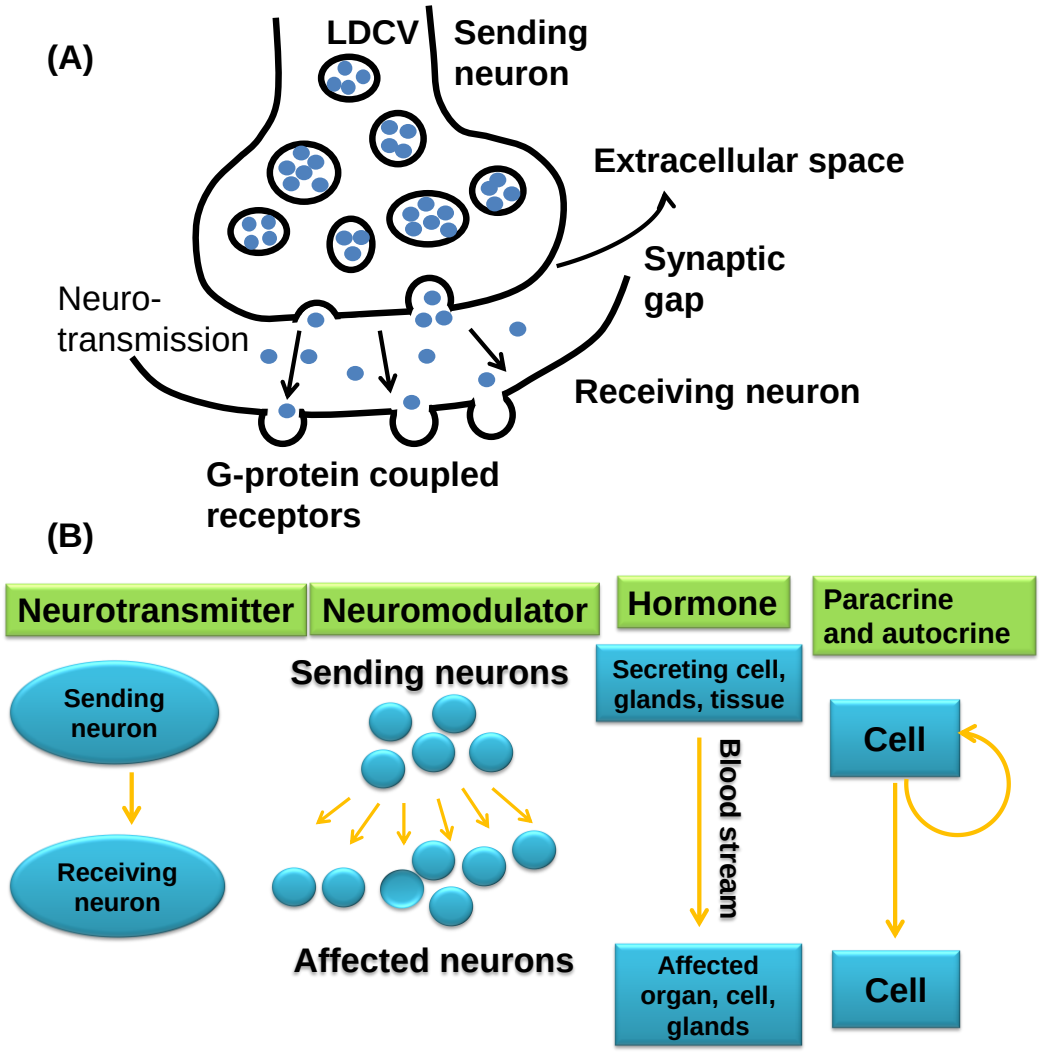

Figure 1.1 (A) Neuronal release of neuropeptides. (B) Neuropeptide signaling in the body.

Neuroproteins are proteins expressed in and associated with the nervous system. Unlike neuropeptides, neuroproteins do not act as neurotransmitters; they are usually involved in supporting neuronal growth, differentiation and protection. Mutation and improper post translational modification of neuroproteins can lead to pathogenesis of diseases[9], and cerebral lesion can cause "leaking" of neuroproteins into extracellular fluid, eg. cerebrospinal fluid (CSF) and blood[10]. Therefore, their concentration in body fluid can serve as marker for disease or brain trauma. For example, τ protein is a neuroprotein

that stabilizes microtubules. Hyperphosphorylation of τ leads to microtubule disorganization and τ aggregation, resulting in neurodegeneration and diseases such as Alzheimer Disease (AD)[11]. Studies have shown that elevated phosphorylated τ levels in CSF correlate with progression of AD, suggesting its potential as AD biomarker[12].

1.2 *In vivo* neuropeptide and neuroprotein quantification using microdialysis sampling

In vivo measurement of extracellular neuropeptide and neuroprotein release provides insights into their dynamics and regulation mechanisms in living subjects; therefore, this is an important approach to elucidate their biological functions. Emerging tools for *in vivo* neurochemical monitoring includes *in vivo* cyclic voltammetry and *in vivo sampling* coupled to highly sensitive analytical techniques.

In vivo cyclic voltammetry detects neuropeptides by monitoring their oxidation peak using a fiber implanted into the brain. It can achieve high spatial resolution and temporal resolution; however its application is limited to neuropeptides containing electroactive amino acid residues (tyrosine, methionine and cysteine) and has low specificity and poor electrode stability. For these reasons it has only been applied in limited number of *in vivo* or living tissue studies[13-15].

In vivo sampling has been applied more often because it allows assaying of fractions by highly sensitive analytical techniques such as radioimmunoassay (RIA), enzyme immunoassay (EIA) and high performance liquid chromatography (LC) with electrochemical (EC) or mass spectrometry (MS) detection. Most commonly utilized *in vivo* sampling methods include push-pull perfusion and microdialysis. Push-pull perfusion achieves sampling by simultaneously perfusing and withdrawing the perfusion

media through the sampling probe at identical flow rates, carrying neuropeptides in the extracellular fluid to the outlet for collection. Similarly, microdialysis also involves perfusion media flowing through a probe interior, except that the "pull" flow is not always required because a semipermeable membrane is incorporated at the tip end as fluid barrier. The membrane allows peptides smaller than its molecular weight cut-off (MWCO) to diffuse into the probe, driven by the concentration gradient across the membrane (Figure 1.2).

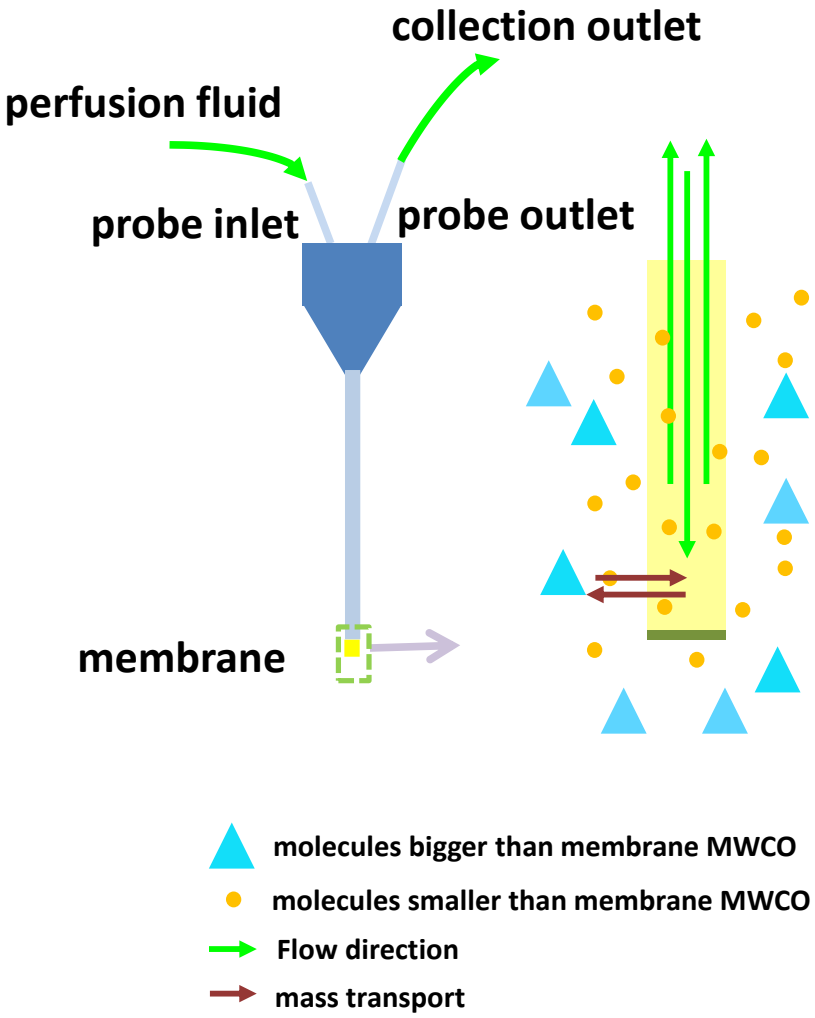

Figure 1.2 Scheme of microdialysis probe for sampling molecules from aqueous environment. The perfusion fluid is pumped into the probe inlet and flows to the outlet. Molecules smaller than membrane's

MWCO enter the probe through diffusion driven mass transport and are carried by perfusion media to the collection outlet.

Because of the membrane which sets a physical barrier between the perfusion flow and brain tissue, microdialysis has gained favorable attention over push-pull perfusion due to lower level of tissue damage and capability of generating cleaner sample[16]. Microdialysis is a non-equilibrium sampling technique based on analyte diffusion; therefore, the analyte concentration in dialysate is a fraction of the actual extracellular concentration. Relative recovery of the probe, defined as the analyte concentration in dialysate divided by the actual concentration from the sampling media, is affected by the membrane material[17], active sampling area (membrane length)[17], dialysis flow rate[18,19] and temperature. For proper estimation of extracellular concentration from dialysate concentration, the dialysis probe needs to be calibrated. Most commonly employed calibration method is *in vitro* calibration, where the probe samples from a solution with known analyte concentration, and analyte concentration in dialysate is measured to calculate probe's *in vitro* recovery. Other calibration methods were also developed to correct the impact of analyte *in vivo* dynamics on recovery, these methods include low flow method[20], no-net-flux method[21] and retrodialysis[22,23].

Microdialysis sampling has been applied to study neuropeptide *in vivo* signaling and its correlation with behavior, disease state and pharmaceutical treatment. One example is the *in vivo* microdialysis of orexin A and melanin-concentrating hormone (MCH) from human amygdala. This study revealed that the level of these peptides alters during sleep-wake cycle and between different emotions, indicating their link to specific emotions and state rather than simply arousal[7]. Using microdialysis coupled to capillary LC-MS, our lab demonstrated elevated enkephalin level in rat dorsal neostriatum, and concluded that

these peptides are able to signal consumption of sensory reward[6]. Summary of neuropeptides monitored with *in vivo* microdialysis till 2010 can be found in our previous group member's dissertation[24], and Table 1.1 lists a brief update for neuropeptides monitored with microdialysis in the last five years.

With the development of high MWCO membrane, the application of microdialysis can extend to *in vivo* quantification of big peptides and proteins. Cytokine dynamics and their relation to brain injury are perhaps the mostly studied using microdialysis[25-28]. For example, a study reported detection of 17 cytokines from human brain dialysate following brain tumor resection, and all the cytokines showed gradual decrease in concentration, indicating acute brain inflammatory response after surgery[27]. Moreover, microdialysis has been utilized in studying the *in vivo* dynamics of several important neuroproteins related to neurodegenerative diseases such as AD. Protein τ in mouse hippocampus interstitial fluid (ISF) was measured using microdialysis, and it was revealed that ISF monomeric τ level decreased over age (~200 ng/mL to 72.3 ± 28.0 ng/mL) and following the onset of τ aggregation, suggesting the extracellular τ is in equilibrium with the toxic τ aggregates[29] associated with AD. Microdialysis studies on a big neuropeptide β-amyloid (Aβ) also revealed important discovery of its ISF level regulated by synaptic activity[30] and the correlation to brain's regional vulnerability to Aβ aggregation in AD[31]. In addition, *in vivo* microdialysis on brain derived neurotrophic factor (BDNF) and nerve growth factor (NGF), has shown that intranasal administration of carnosic acid caused 3-fold increase in BDNF concentration and 2-fold increase in NGF concentration in rat hippocampus, indicating the potential of this drug in treating diseases caused by neurotrophin depletion[32]. *In vivo* microdialysis of α-synuclein (a

neuroprotein best known for its association with Parkinson's disease) and apolipoprotein E (ApoE, related to catabolism of lipoprotein constituents, linking to AD due to its impact on Aβ metabolism) were also reported[33,34]. The concentration for α-synuclein using *in vivo* microdialysis was 0.15±0.12 ng/mL in mouse striatum, and ranged from 0.5-8 ng/mL in human cerebral cortex[34]. The concentration of total exchangeable ApoE was 111.2±14.4 ng/mL in mouse hippocampus[33]. These studies show that monitoring neuroproteins in the brain of live subjects can lead to unique insight in a variety of important topics.

Table 1.1 *In vivo* neuropeptide monitoring studies published between 2010 and 2015

Peptide	MW (Da)	Animal/ Brain region	Quantification method	Dialysate basal concentration	Biological observation
Neuropeptide-S (NPS)	2210	Rat/ Amygdala	RIA	6.4±1.9 pM[35]	Increased release under stress (forced swim)[35]
β-amyloid $(Aβ)_{40}$	4330	Mouse/ hippocampus	ELISA	~13pM[36]	N/A, microdialysis method development[36]
$Aβ_{42}$	4514		ELISA	~16 pM[36]	N/A, microdialysis method development[36]
$Aβ_{x-40}$	N/A	Mouse/ hippocampus	ELISA	148.51 ± 17.93 pg/mL, ISF concentration	ISF Aβ levels in mice predict the degree of Aβ aggregation in specific brain region[31]
		Mouse/ striatum		47.4 ± 11.46 pg/mL, ISF concentration	
Arginine-vasopressin (AVP)	1084	Hamster/supra-chiasmatic nucleus (SCN)	ELISA	34±5 pM[37]	Circadian release both under dark-light cycle and constant darkness[37]
		Rat/paraventricular nucleus (PVN)	cLC-MS	11.1±2.9 pM[19]	Slow and persistent response to osmotic stress[19]
Oxytocin (OXT)	1007	Rat/PVN	cLC-MS	5.4±1.3 pM[19]	Rapid response to osmotic stress[19]
Methionine-enkephalin	573	Rat/GP	cLC-MS	14±1 pM[38]	N/A, cLC-MS method development

(ME)				64 ± 29 pM[39]	Amphetamine increased release, suggesting (with other data) inhibition on γ-aminobutyric acid and disinhibition on dopamine in GP to sustain locomotion[39]
		Rat/Dorsal Neostriatum	cLC-MS	2.61±0.56 pM[6]	Increased release during reward consumption[6]
Leucine-enkephalin (LE)	556	Rat/ GP	cLC-MS	7±1 pM[38]	N/A, cLC-MS method development
				15 ± 2 pM[39]	Amphetamine increased release, suggesting (with other data) inhibition on GABA and disinhibition on DA in GP to sustain locomotion[39]
		Rat/Dorsal Neostriatum	cLC-MS	2.32±0.30 pM[6]	Increased release during reward consumption[6]
kisspeptin-54 (KP-54)	5857	Monkey/ stalk-median eminence (S-ME)	RIA	61.4±15.3 fM[40] (prepuberty)	Developmental increase in release during the process of puberty[40]
gonadotropin-releasing hormone (GnRH)	1183	Monkey/ S-ME	RIA	8.3±3.3 pM[41]	N/A, microdialysis method development[41]
			RIA	1.3±0.4 pM (prepuberty) [40]	Developmental increase in release during the process of puberty[40]
vasoactive intestinal peptide (VIP)	3326	Hamster/ SCN	RIA	2.0-60.0 pg/sample[42]	Circadian release under dark-light cycle, release is stimulated by photic input and inhibited by serotonin[42]
β-endorphin	3466	Rat/central amygdala (CeA)	Solid phase RIA	12900±1000 pM[43]	β-endorphin and CRH release can be stimulated by alcohol, CRH release could modulate β-endorphin release in CeA[43]
Corticotropin-releasing hormone (CRH)	4758	Rat/CeA	Solid phase RIA	663±74 pM[43]	
		Rat/dorsolateral bed nucleus of the striaterminalis (dlBNST)	EIA	95.3±7.3 pM[44]	Formalin evoked pain increases CRH release[44]
Orexin A	3561	Rat/ hypothalamus, amygdala	RIA	11±2 pM in hypothalamus[7] 6±1 pM in amygdala[7]	Maximal release in amygdala during positive emotion, social interaction and

		Human amygdala	RIA	11±1 pM[7]	anger, minimal release during pain; increased release at wake onset
melanin-concentrating hormone (MCH)	2387	Rat hypothalamus, amygdala	RIA	10±3 pM in hypothalamus[7] 10±3 pM in amygdala[7]	Minimal release in social interaction and pain, increased release after eating and at sleep onset[7]
		Human amygdala	RIA	6±1 pM[7]	
Neuromedin B	1132	Rat hippocampus	cLC-MS	4 pM[45]	N/A, *in vivo* cLC-MS method development[45]
Neuromedin N	746			11 pM[45]	
	1673			3 pM[45]	
Neurotensin		Rat/ventral tegmental area (VTA)	cLC-MS	Not reported[46]	Activating lateral hypothalamus area neurotensin cells caused acute and transient increase in the VTA[46]
		Rat Striatum	RIA	144±26 pM[47]	Prolyl oligopeptidase is not responsible for cleaving neurotensin and Sub P *in vivo* [47]
Substance P (Sub P)	1348	Rat Stiratum	RIA	11000±800 pM[47]	
gastric releasing peptide (GRP)	2859	Hamster SCN	RIA	188±58 pM[37]	Circadian release under dark-light cycle, reversed rhythmicity at constant darkness[37]
Dynorhpin A_{1-8} ($DynA_{1-8}$)	981	Rat/Dorsal Neostriatum	cLC-MS	~4.5 pM[6]	Level remained unchanged during eating[6]
		Rat/CeA	Solid phase RIA	602±60 pM[48]	Alcohol-induced increase in release was attenuated by CRH receptor 2 antagonist[48]
Orphanin FQ (OFQ)	1809	Rat/ substantia nigra reticulate, human CSF	Solid phase extraction-RIA	~100 pM in rat, ~41 pM in human CSF[49]	Parkinsonian toxin induced release, increased level in CSF of Parkinson patients—linkage between OFQ and parkinson's disease[49]
Neuropeptide tyrosine (NPY)	4272	Hamster/ SCN	RIA and surface enhanced laser desorption ionization (SELDI)-TOF	lower detectibility ~0.39 pM[50]	Rhythmic release under dark-light cycle; can be stimulated by wheel running, intergeniculate leaflet - mediated release in SCN[50]

The biggest challenge in *in vivo* neuropeptide and protein monitoring using microdialysis is the extremely low level (~pM) of neuropeptides and proteins in the dialysate, which originates from limited probe recovery and low extracellular level of the

peptides. As a result, sampling techniques with higher recovery rate and analytical techniques able to quantify sub pM to low nM level of neuropeptide present in 5-100 μL dialysate are desired for reliable monitoring and absolute quantification of neuropeptide in extracellular space.

This dissertation focuses on developing analytical methods for *in vivo* microdialysis application for the following neuropeptides and neuroprotein. The peptides are selected because of our laboratory and collaborator's interest in studying their *in vivo* regulation of feeding behavior.

(1) Enkephalins. Leucine and methionine enkephalin (LE and ME) are two pentapeptides from the protein precursor preproenkephalin which contains six copies of ME gene and one copy of LE gene[1]. They belong to the opioid peptide family and mainly interact with μ and δ opioid receptors[51-53]. Enkephalins are involved in signaling reward consumption (such as eating palatable food)[6], pain modulation[3] and locomotors activity[54]. They are widely expressed in the brain, and can be measured by microdialysis from discrete brain regions such as striatum[6,18], globus pallidus (GP) [38,39] and nucleus accumbens[55] with RIA or LC-MS detection. Enkephalin concentration in dialysate can range from ~2 pM to ~130 pM.

(2) Dynorphin $A_{1-8,\ 1-17.}$ Dynorphin (A and B) are another type of opioid peptides, they derive from pre-prodynorphin and mainly bind to κ opioid receptor[51]. Dynorphin A consists of 17 amino acid residues ($DynA_{1-17}$), and can undergo further *in vivo* cleavage to form fragments such as $DynA_{1-8}$, $DynA_{1-13}$ and $DynA_{2-13}$ etc. DynA plays role in many physiological processes such as pain transmission[56], stress-induced and proactive behavior[57]. Previous study also discovered that infusion of $DynA_{1-8,\ 1-17}$ antibody into the

brain can cause elevation in feeding threshold[58]. $DynA_{1-17}$ was measurable in spinal perfusate[59]; however no *in vivo* microdialysis has been performed on it. $DynA_{1-8}$ is studied more with microdialysis, and it can be detected by LC-MS or RIA in different brain regions such as CeA[48,60], striatum[6,18] and PVN of hypothalamus[19]. $DynA_{1-8}$ concentration can range from ~4 pM to ~600 pM in dialysate.

(3) β-Endorphin. β-Endorphin is an opioid peptide originating from pro-opiomelanocortin (POMC)[1] and mainly binds to μ opioid receptor. The full-length peptide contains 31 amino acid residues. It can respond to alcohol[60] and nociceptive stimulation[61], and can stimulate food intake when injected into the brain[62]. β-endorphin can be measured by RIA or ELISA using microdialysis from striatum[18], CeA[43,60], arcuate nucleus of hypothalamus[61] and spinal cord[63] with dialysate concentration ranging from ~35 pM to ~12.9 nM. LC-MS detection of β-Endorphin is achieved by digesting the full-length peptide to a shorter peptide fragment, which had improved sensitivity[18].

(4) α-melanocyte stimulating hormone (α-MSH). α-MSH is a peptide hormone cleaved from POMC[1]. It belongs to the melanocortin system in the opioid gene family (including adrenocorticotropic hormone and α, β, γ-MSH) and is detected at high concentration in discrete neuronal clusters in hypothalamus[64]. In skin and hair α-MSH stimulates production of melanin, and in CNS it is involved in feeding behavior[65] and development of addiction[66]. It is suggested that N-acetylated α-MSH (the so-called α-MSH) and deacetylated α-MSH may have different effect on food intake[65]. No *in vivo* brain microdialysis has been performed on α-MSH, however it was detected by RIA from human dermal microdialysate[67] and rat hypothalamus push-pull perfusate[68,69]. The concentration was ~60 pM and ~30 pM in dialysate and perfusate respectively.

(5) Galanin (Gal). Gal is a peptide deriving from prerogalanin, it belongs to the galanin gene family and binds to three galanin receptors (GAL-R1, GAL-R2, GAL-R3) distributed in PVN, dorsal raphe nucleus, hippocampus and amygdala[70]. It is involved in learning and cognition[2], feeding[71], cardiovascular regulation[72] and tumor suppression[73]. *In vivo* microdialysis of galanin was reported in rat dorsal hippocampal formation[74] and spinal cord[75] with RIA or HPLC-RIA detection, the dialysate concentration in spinal cord was ~7.9 pM.

(6) Substance P (Sub P). Sub P derives from preprotachykinin A which belongs to the kinin and tensin gene family, and binds to neurokinin-1 receptor. Sub P is involved in pain/inflammatory response[67], sleep[76], emotional stress and psychological disorder[8,76,77], and could also alter feeding behavior through enhancing motor activity when injected to ventral tegmental area (VTA)[78]. Microdialysis of Sub P was reported in periaqueductal gray[79], preoptic anterior hypothalamus[79], basal ganglia[80], medial amygdala[77] and trigeminal ganglia[81]. Dialysate concentration measured by RIA ranged from ~4 pM to ~100 pM.

(7) Hypocretin/Orexins. Orexin A and orexin B derive from preprohypocretin, and they interact with orexin receptors OX_1R and OX_2R. OX_1R is selective for orexin A, and OX_2R binds nonselectively to both peptides. They are involved in sleep and feeding regulation, emotion and energy balance[4]. Orexin *in vivo* microdialysis was performed extensively on orexin A (hypocretin-1) in hypothalamus[5,7,82,83], basal forebrain[72], locus coeruleus[72] and amygdala[7], with dialysate concentration measured by RIA ranging from ~11-~75 pM. Orexin A *in vivo* concentration shows circadian fluctuation with elevated release during wakefulness and reduced release during sleep. Orexin B has not been

measured in *in vivo* setting yet, and this is possibly due to its fast degradation in the body[84].

(8) Nociceptin/Orphanin FQ (OFQ). OFQ derives from prepronociceptin and belongs to the orphanin gene family. It binds opioid receptor like-1 receptor and plays roles in modulating nociception[85], feeding regulation and anxiety[86]. Microdialysis on OFQ has been performed in rat hippocampus[87], thalamus[87] and substantia nigra reticulata[49] and concentration in dialysate as measured by RIA (or solid phase extraction, SPE coupled to RIA) ranged from ~60 pM to ~149 pM.

(9) Cholecystokinin tetrapeptide (CCK-4). CCK-4 is a tetrapeptide fragment of cholecystokinin (CCK) from the preproCCK, which belongs to the CCK/gastrin gene family. CCK-4 is involved in panic induction[88], memory deterioration and anxiety[89]. No *in vivo* microdialysis has been performed to detect this peptide, although other forms of CCK have been measured *in vivo* from rat anterior cingulated cortex[90] and rostral ventromedial medulla[91].

(10) Brain derived neurotrophic factor (BDNF). BDNF is a neuroprotein in the neurotrophin family. It plays critical role in neuron cell survival, differentiation and neuronal plasticity[92]. Its concentration in body fluid and tissue has correlation with AD[93-95] and several mental disorders such as major depression and bipolar disorder[96-99]. BDNF can also be measured *in vivo.* In a study measuring its release from supraoptic nucleus using push-pull perfusion, the basal level was below limit of detection using a commercial ELISA kit, and the level under osmotic stress was approximately 40 pg (3 fmol) per 15 min fraction[100]. Another *in vivo* microdialysis study reported its endogenous level in rat hippocampal region to be 207 ng/ml (15 pM)[32].

1.3 Recent improvement in *in vivo* neuropeptide/protein sampling technique

Relative recovery rates for neuropeptides and proteins typically range between <1% to 20%[18,19] depending on the analyte, probe membrane material, probe construction and flow rate used. Reasons for the low recovery of neuropeptides and neuroproteins include their low diffusion coefficient, non-specific adsorption loss and fluid loss across the dialysis membrane. Table 1.2 summarizes recent studies on improving the recovery of microdialysis-based sampling techniques focusing on solving the three problems.

1.3.1 Reducing non-specific adsorption by probe/tubing modification

Peptides and proteins are observed to bind to surface and microdialysis probes at μM level[101,102]. The adsorption can be described by Langmuir isotherm[102], meaning that adsorption loss can become more severe when being sampled at physiologically relevant concentration (pM to nM). Modification on the microdialysis tubing[5,82] and probe[103] to block active adsorption sites has been investigated for reducing adsorption loss. Particularly, a commercially available PEO_{98}-PPO_{67}-PEO_{98} triblock copolymer (Pluronic F-127) was utilized to reduce protein adsorption loss when sampling from human CSF. This polymer self-assembles onto hydrophobic microdialysis membrane and tubing through interaction with the hydrophobic moiety polypropylene oxide (PPO), leaving hydrophilic polyethylene oxide (PEO) chain to form a water-swelling, protein repelling layer on the surface. The modification increased average protein recovery of a 10 mm probe from 23.9% to 32.1% when sampling from human CSF[103].

Recent work in preparing fouling-resistant membranes for hemodialysis[104-108] suggests a route to producing low binding materials that can potentially be utilized in neuropeptide/protein microdialysis sampling. The polyethyleneimine (PEI) modification method on AN69 membrane is of particular interest to our laboratory. AN69 is a

hydrophilic polyacrylonitrile (PAN) membrane with embedded sulfonate group that has previously been shown to have excellent relative recovery for several small neuropeptides (LE, ME, $DynA_{1-8}$, OXT, AVP)[6,19]. Modifying the membrane by physical adsorption of a hydrophilic, polycationic PEI may offer a convenient way to reduce electrostatic interaction and improve recovery of bigger, positively charged neuropeptides. Evaluation of recovery change after PEI modification will be discussed in detail in Chapter 3.

Another simple alternative to reduce non-specific adsorption loss of neuropeptide and neuroprotein is to add a non-analyte protein (usually bovine serum albumin, BSA or human serum albumin, HSA) into the perfusion media to block the adsorption site. The protein additive also helps reduce fluid loss due to osmotic pressure difference (discussed in the next section), therefore has been widely utilized as a standard method in peptide/protein sampling[75,87,109-111]. Although being effective, the concentration of serum albumin (0.1-4% w/v) in perfusion media is much higher than the neuropeptide/protein concentration. Therefore additional sample clean-up may be required when quantifying dialysate using highly sensitive cLC-MS, because blocking protein can also be preconcentrated on the capillary column and interfere with analyte neuropeptide/protein retention and detection. In addition, leaking of blocking protein into the brain is possible (see below).

1.3.2 Reducing fluid loss across microdialysis membrane

Microdialysis for small molecules is typically performed using membranes with MWCO of 6-15 kDa. In contrast, the MWCO of microdialysis membrane for neuropeptide and protein sampling is usually between 20-1000 kDa due to their bigger

size compared to small molecule neurotransmitters. The higher MWCO membrane contains bigger through pores[112], which are more prone to leakage due to hydrostatic pressure and osmotic pressure of the perfusion media. Leakage is readily observable when using a 100 kDa MWCO membrane[103]; it causes bulk fluid movement from the microdialysis probe into the sampling space, resulting in both concentration and sample volume loss. Instead of solely pressurizing the perfusion media, microdialysis in "push-pull" format is proven to effectively reduce pressure difference across the membrane and achieved both ~100% fluid recovery and increased neuropeptide/protein recovery[36,113,114].

Another approach to reduce fluid loss is to add a macromolecule osmotic reagent (serum albumin or dextran) into the perfusion media to balance the osmotic pressure difference between perfusion media and the protein-containing extracellular fluid. Some studies have suggested that using the osmotic reagent alone can achieve ~100% fluid recovery and good protein recovery[115]; although it was recommended to always use push-pull microdialysis when sampling big neuropeptides/proteins. In addition to potential interference with subsequent analyte detection, concern associated with osmotic reagent is its potential to leak into sampling space when a probe with MWCO larger than the molecular weight of osmotic reagent is used. For example, BSA (MW = 66 kDa) may leak into the brain when flowing through a 100 kDa or higher MWCO probe. Such leakage could trigger undesired biological response that interferes with the ongoing *in vivo* study. Evaluation of possible leakage[116] was carried out based on the inflammatory response when microdialyzing in rat spinal horn with BSA, rat serum albumin (RSA), Dextran 70 and Dextran 500 as perfusion media supplement using a 100 kDa MWCO probe. Significant inflammation was observed with the use of Dextran 70, indicating that

it is leaking through the probe and should be eliminated in future *in vivo* microdialysis experiments.

1.3.3 Modified sampling technique to overcome limited peptide/protein diffusion

The non-equilibrium sampling of microdialysis has determined that molecules with larger diffusion coefficient have higher relative recovery, making this technique not as favorable when sampling bigger neuropeptides/proteins whose diffusion coefficient is low. To overcome this barrier, different approaches improving neuropeptide/protein delivery into the probe have been reported, including microdialysis-ultrafiltration sampling and affinity enhanced sampling.

Microdialysis-ultrafiltration sampling utilizes a push-pull microdialysis set up with the "pull" flow rate greater than the "push" flow rate to generate bulk fluid movement into the sampling probe that facilitates the recovery of neuropeptides/proteins. Studies have shown 50%-100% recovery achieved for peptides and proteins[113,117,118], and this technique is proven to be useful for *in vivo* studies where reduction of ~10-100 µL of extracellular fluid does not cause drainage or disturbance of extracellular fluid (eg. in human mucosa, blood etc)[117].

Affinity enhanced sampling methods improve analyte recovery by including in the perfusion media an affinity agent (cyclodextrin[119], antibody[120], conjugated heparin[121]) that binds selectively with high affinity to target analyte to increase concentration gradient and facilitate mass transport across the membrane. The affinity agent can be either in free solution or immobilized on microspheres. Antibody showed higher recovery over other agents[122-124] . Antibody immobilized microspheres also provides easier interface with multiplexed detection methods such as LC-MS[124] or flow cytometry[123].

Challenges in the wide application of antibody immobilized microsphere, in addition to its lengthy preparation and bead saturation issue, are bead settling and tubing clogging, which was still observed in a recent study[124] where nanospheres were utilized as intentin to solve these problems. A separate study utilized air-segmented flow plug to effectively prevented microsphere settling and clogging, and showed 10-fold improvement in GnRH's *in vitro* recovery[125]. However the safety and effectiveness of this method was not validated for *in vivo* sampling.

Table 1.2 Solutions to improve microdialysis sampling and examples

Targeted cause	Solution	Reported recovery (or improvement)
Non-specific adsorption	Using siliconized tubing	Orexin A recovery: 0.8±0.3% [5] at 0.3 µL /min
	Pluronic F-127 adsorption to create hydrophilic surface	transferrin recovery: 59.7 % β-hemoglobin recovery: 61.5 % [103] at 0.3 µL /min
	Polysulfone/phospholipid blend membrane	Reduced albumin, γ-globulin and fibrinogen adsorption visualized by immnogold-scanning electron microscopy[104]
	Modifying AN69ST membrane by heparin adsorption	Reduced coagulation due to reduced protein adsorption[105]
	New membrane material using polyethersulfone blended with 2-hydroxyethl methacrylate and acrylic acid	76% less BSA adsorption and 80% less bovine serum fibrinogen adsorption compared to polyethersulfone membrane[106]
	PEI physical adsorption onto PAN membrane	Reduced adsorption of high molecular weight kininogen [108]
	Adding blocking protein	5.5±0.2% for somatostatin (SMT) at 5 µL/min [109] 6.2 ± 0.3% for OFQ at 2 µL/min[87] 2.0±0.13%–2.6±0.27% for CCK-8 at 3.5 µL/min[110] 1.4%-1.5% for Gal at 3.5 µL/min[75] 6.6±1.3% for Sub P at 3 µL/min[111]
Fluid loss	"Push-pull" microdialysis	~15%-28% for cytochrome c, human serum albumin, ribonuclease A, lysozyme and α-lactalbumin [113] ~13% for $A\beta_{40}$, ~16% for interleukin (IL)-6[36] IL-1β:27.8±4.1%; IL-6:45.2±8.4%; NGF: 22.2±7.9% [114]
	Macromolecule as osmotic reagent	~100% fluid recovery using 10% BSA, IL-1β recovery ~2.7%[115] 94% and 100% fluid recovery with Dextran 60 and Albumin[126] ~100% fluid recovery with Dextran 250[103]

Diffusion limitation	Affinity enhanced sampling	64.8 ± 11.7% for chemokine ligand (CCL)-2[120] ~70% for interferon (IFN)-γ and ~35% for tumor necrosis factor (TNF) -α[121] 60.4 ± 5.8% for TNF-α; 25.8 ± 2.3% for IFN-γ; 4.9 ± 0.1% for IL-5; 78.8 ± 8.0% for IL-4; 19.8 ± 2.5% for IL-2[123] 55.2 ±5.29% for fibril-associated protein (FLP)-1, 87.3±5.09% for FLP-2, 92.1±3.45% for Sub P, 82.9±5.25% for SMT[124]
	Microdialysis-ultrafiltration	100% for LE, vasopressin and BSA[118] ~50%-~90% for cytochrome c, human serum albumin, ribonuclease A, lysozyme and α-lactalbumin[113] 52 ± 0.4%, 46 ± 1% and 38 ± 6% for myoglobin, soybean trypsin inhibitor and carbonic anhydrase[117]

1.4 Analytical methods for detecting low abundance intact peptide/protein

The low neuropeptide/protein concentration (Table 1.1) and very limited volume of dialysate sample (1-100 μL) require analytical method with good mass sensitivity. Most neuropeptide/protein quantifications rely on immunoassays, such as RIA and ELISA, which detect analyte based on the molecular recognition and binding between antigen and antibody. These techniques can achieve excellent mass LOD (<1-100 amol) with wide selection of commercially available kits, therefore require minimal method development. However, the entire detection process can take from 6 hours to 2 days. Although throughput can be enhanced by assaying in 96-well and 384-well format, the long analysis turnover can be problematic due to the degradation issue of neuropeptides. Single-analyte detection is another limitation of these methods, meaning extra sample volume is needed when monitoring more than one neuropeptide/protein, leading to elongated fraction collection between time points and subsequently reduced temporal resolution. Moreover, these techniques suffer from cross reactivity issue because they do not detect peptides and proteins based on their amino acid sequence; a non-analyte

peptide/protein with similar binding affinity to the antibody can also generate signal, leading to false positive.

Numerous studies have been conducted in improving the speed and multi-analyte capacity of immunoassays for peptides/proteins. A commercialized swirling micro-channel plate was utilized to enhance mass transfer in ELISA's incubation step, reducing detection time to ~2 h and sample/reagent consumption to 5 µL while maintaining ultrahigh sensitivity of ELISA (LOD= 13 fM for human IL-4)[127]. Microarrays, microbeads, nanoparticles were also popular media for realizing fast and multiplexed detection of neuropeptides/proteins, with limit of detection as low as 83 aM[128-132], and platform for simultaneous detection of up to 100 protein/peptides were already commercialized[133]. In addition, microfluidic platform such as lateral flow integrated blood barcode chip (LF-IBBC)[134] and centrifugal microfluidics[135] were applied to immunoassays to achieve accelerated and multiplexed protein detection. The assay time can be as short as 20-50 min with low pM LOD from 200 nL of sample[136]. Although supreme performance, in terms of sensitivity, throughput, speed and multi-analyte detection can be achieved by immunoassays, they still suffer from potential cross reactivity issue when structurally similar interference peptides/proteins are present in the sample, which may result in false positive in the measurement.

LC-EC or LC-MS are promising alternatives to immunoassays in detecting neuropeptides, due to their higher specificity and sensitivity to small peptides, especially peptides with MW < 2000 Da. In these methods, 4-10 µL of peptide-containing sample is injected onto a column packed with reverse phase separation media and retained on the head of the column. After rinsing the column with weak mobile phase (aqueous solution)

which removes unretained matrix components such as salt, the retained peptides are eluted by strong mobile phase (organic solvent such as methanol and acetonitrile) and detected by highly sensitive EC or MS. EC detects peptides containing electroactive residues such as tyrosine, cysteine and methionine. Derivatization procedure can be used for peptides not containing these residues[137,138]. On the other hand, the development of MS techniques, such as soft ionization (electrospray ionization, ESI and matrix assisted laser induced desorption ionization, MALDI) technique, advanced mass analyzer (ion trap, triple quadrupole) has enabled highly sensitive, sequence-specific detection of neuropeptides using multistage MS (MS^n). In addition, the application of a capillary LC (cLC) column (Figure 1.3), capable of preconcentrating microliters of peptide solution into 20-50 nL elution band, can further increase the sensitivity of LC-MS based detection. Combining preconcentration, LC separation with the sensitivity and specificity of MS detection, cLC-MS can achieve simultaneous monitoring of several neuropeptides with mass LOD as low as 2 amol and concentration LOD as low as 0.5 pM[18]. It has been successfully applied to monitor 10 neuropeptides from the brain, including Angiotensin IV (Ang IV)[139], ME[6,18,19,38,39,137,140,141], LE[6,18,38,39,140,141], $DynA_{1-8}$[18], neurotensin[45,46,142], β-endorphin[18], AVP[19], OXT[19], neuromedin N[45] and neuromedin B[45].

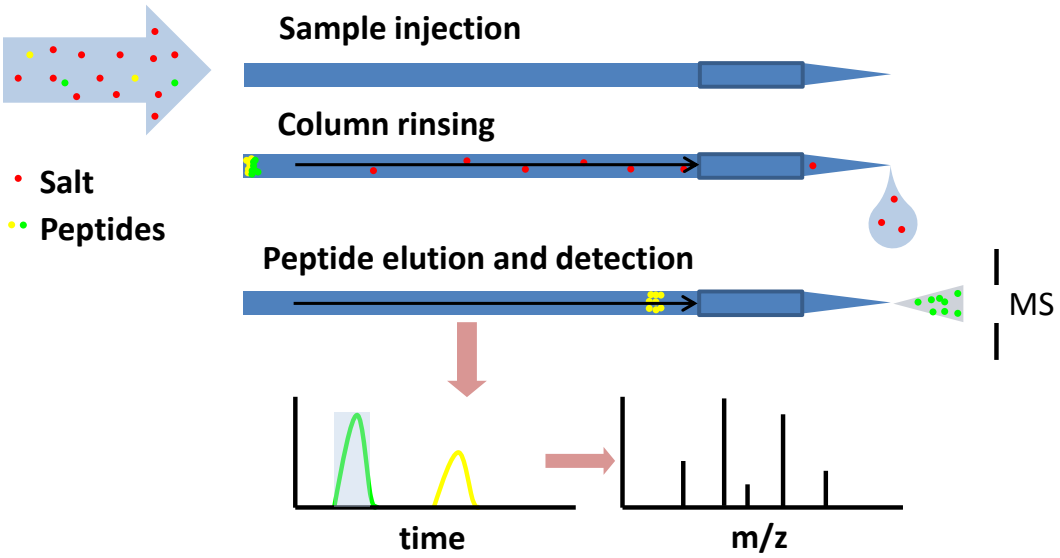

Figure 1.3 Scheme of preconcentration and capillary LC-ESI-MS analysis of neuropeptide.

Limitations do exist in the application of cLC-MS in routine *in vivo* neuropeptide/protein quantification. The highest sensitivity is achieved with the smallest bore column (25 μm I.D.), because it provides largest preconcentration ratio and lowest flow rate for highest nano-ESI signal. However the small bore columns are also subject to elongated analysis time due to slow sample injection and limited column stability (i.e. usually suitable for 20-40 injections in our laboratory), making cLC-MS impractical when analyzing large number of samples (eg. *in vivo* neurochemical monitoring). Improvement on cLC-MS analysis speed and column stability is discussed in chapter 2.

In addition, only 10 mammalian neuropeptides have been monitored *in vivo* using cLC-MS. Most of them have MW < 2000 Da, indicating the sensitivity might not be adequate enough for monitoring intact larger neuropeptides with molecular weight >2000 Da. In fact, a previous study has reported that β-endorphin (3466 Da) had an LOD of 5

nM when detected intact, which was far too high for *in vivo* work. A signature peptide method (discussed below) was required to quantify this peptide from *in vivo* dialysate[18].

Table 1.3 summarizes developments in LC-MS for trace level detection of intact neuropeptides since 2010. It shows a general trend in improving peptide detection sensitivity and preventing adsorption loss by using either organic additive[143,144] or protein-containing matrix[145-147] for higher sensitivity. With these improvements, low-to-high pM LOD for several neuropeptides larger than 2000 Da was achieved using large bore capillary column (300 μm I.D.)[144] and regular-size LC columns (1-2.1 mm I.D.). These peptides include orexin A (3561 Da)[144], orexin B (2936 Da)[144], parathyroid hormone$_{1-34}$ (PTH, 4118 Da)[144], salmon calcitonin (3432 Da)[148], Apelin-36 (4196 Da)[149], Aβ_{38} (4132 Da)[146,147], Aβ_{40} (4330 Da)[146,147] and Aβ_{42} (4514 Da)[145-147]. Although the mass LOD or lower limit of quantification (LLOQ) were still at low-to-mid fmol range, it could potentially be improved by using cLC column which is capable of preconcentrating peptides to smaller elution band.

Table 1.3 Improvement in LC-MS quantification of trace level neuropeptide from biological sample

Method highlight	MS	Sample matrix	LOD (converted to mole unless specified)
Highly sensitive cLC-MS^3 for *in vivo* monitoring of AVP and OXT	LTQ XL linear ion trap (Thermo)	*In vivo* dialysate	5 amol for AVP and OXT[19]
cLC-MS^3 with large particulate phase to reduced injection backpressure, increasing analysis speed to 4 min/sample for *in vivo* monitoring of ME and LE	LCQ Deca XP Plus quadrupole ion trap (Thermo)	*In vivo* dialysate	15 amol for LE and ME 50 amol for DynA_{1-8}[38]
nanoUPLC-MS^2 with organic additive to reduce adsorption, optimized dilution solvent in standard preparation	Quattro Premier triple quadrupole (Micromass-Waters)	*In vivo* dialysate	LLOQ: 200 amol for neurotensin and neuromedin N,600 amol for neurmomedin B [133]
	Xevo TQ-S triple quadrupole (Waters)	*In vivo* dialysate	LLOQ: 2.5 amol for neurotensin and neuromedin N,15 amol for neurmomedin B[45]

LC-MS^2 with optimized gradient to reduce matrix suppression	TSQ EMR quantum quadrupole ion trap (Thermo-Finnigan)	Rat plasma	80 pM (200 µL rat plasma extracted to 100 µL,50 µL injected, corresponding to 8 fmol) for KP-10[150]
Solid phase extraction (SPE)- UPLC-MS^2 for direct detection of intact large peptide	Xevo TQ-S triple quadrupole (Waters)	Human plasma	LLOQ: 3 pM (500 µL plasma extracted to 150 µL,20 µL injected, corresponding to 200 amol) for salmon calcitonin[148]
Reduced nonspecific adsorption with ACN addition; elution from trap column w/ 10 ×online dilution to refocus peptide to a cLC column	LTQ linear ion trap (Thermo)	Human plasma	50 pM (37.5 fmol) for α-MSH, GnRH, Sub P and OXT 250 pM (187.5 fmol) for brain natriuretic peptide (BNP), C-Peptide , PTH, orexin B 750 pM (562.5 fmol) for orexin A[144]
High-throughput SPE coupled to 2D-LC-MS^2 to reduce matrix suppression	API 4000 tandem quadrupole (Applied Biosystems)	Human plasma, Rat plasma	1 pM (1400 µL human plasma extracted to 100 µL,15 µL injected, corresponding to 210 amol) 50 pM (200 µL rat plasma extracted to 100 µL, 15 µL injected corresponding to 1.5 fmol) both for OXT[151]
Electromembrane extraction coupled to LC- MS^2 for fast sample preparation and sensitive detection	triple quadrupole (unspecified model) (Thermo)	Human plasma	57 pM for Ang II, 43 pM for LE, 39 pM for endomorphin 1 (2 mL human plasma extracted to 60 µL acceptor solution, 50 µL injected)[152]
Weak cation exchange (WCX) extraction using magnetic microbeads coupled to LC- MS^2	TSQ Quantum Ultra triple quadrupole (Thermo)	Human plasma	7 pM, 14 pM, 9 pM, 12 pM for Apelin-12, -p13, -17, -36 (500 µL human plasma extracted to 50 µL, 30 µL injected corresponding to 2.1 fmol, 4.2 fmol, 2.7 fmol, 3.6 fmol)[149]
SPE - UPLC- MS^2, optimized MS^2 setting for neuropeptide detection	Xevo TQ-S triple quadrupole (Waters)	sea lamprey brain tissue, plasma	8 pM, 6 pM, 24 pM for GnRH-I,-II,-III (1000 µL tissue supernatant extracted to 100 µL, 10 µL injected, corresponding to 800 amol, 600 amol, 2.4 fmol)[153]
Development of surrogate matrix to mimic CSF and minimize adsorption, SPE of denatured sample followed by 2D-UPLC-MS^2 with stable isotopically labeled (SIL) internal standard to minimize matrix effect	API 5000 triple quadrupole (ABSciex)	4 mg/mL BSA in aCSF	LLOQ: 11 pM (200 µL sample extracted to 100 µL, 50 µL injected, corresponding to 1.1 fmol) for $A\beta_{42}$[145]
Use of SIL internal standard for reverse calibration to eliminate matrix effect, SPE of denatured sample coupled to LC-MS^2 for simultaneous quantification of $A\beta_{38}$, $A\beta_{40}$, $A\beta_{42}$	TSQ Vantage triple quadrupole (Thermo)	Human CSF	LLOQ: 61 pM, 14 pM, 13 pM (200 µL sample extracted to 25 µL, 20 µL injected corresponding to 9.8 fmol, 2.2 fmol, 2.1 fmol) for $A\beta_{38}$, $A\beta_{40}$, $A\beta_{42}$[147]

Development of surrogate matrix to mimic CSF and minimize adsorption, SPE of denatured sample followed by UPLC-MS^2 with SIL to minimize matrix effect	Xevo TQ triple quadrupole (Waters)	aCSF w/ 5% rat plasma	LLOQ: <0.1 ng/ml (200 µL sample extracted to 75 µL, 10 µL injected) for $A\beta_{38}$, $A\beta_{40}$, $A\beta_{42}$[146]

In addition to adsorption loss, bigger neuropeptides and proteins may suffer from compromised sensitivity due to multiple charge state that disperses signal in ESI-MS and poor ion transmission at high m/z. Recent advances in quadrupole-time of flight (Q-TOF), orbitrap and Fourier transform ion cyclotron resonance (FT-ICR) mass analyzer have allowed detection of intact protein approaching one mega Daltons with modification in source design, source pressure, electronics and detectors[154-157]. Zeptomole LOD for small proteins (8-20 kDa)[157] and low amol LOD of intact IgG (146 kDa)[154] have been achieved when directly infusing protein standard into MS. However, such modifications are usually built-in-house and are not readily available on commercial MS, and they have no demonstrated application in real biological samples. Improvement in analytical methods based on other type of MS also enabled highly sensitive protein detection. Element tagged immunoassay and element tagged affinity labeling strategy labels protein with metal ions for inductively coupled plasma mass spectrometry (ICPMS) detection, and can be coupled to various separation techniques such as HPLC and CE to achieve sub fmol to low amol detection of proteins[158,159]. Advantages of this method include high sensitivity, wide dynamic range, ease of generating internal standard and signal independency of chemical species; drawbacks are lack of sequence-specific information (therefore highly specific antibody or high resolution separation must be used) and labeling efficiency issue at low protein concentration. MALDI is another option to circumvent the multiple charge issue encountered using ESI. However it is also associated with poor

quantification due to heterogeneous crystallization of sample across the spot and mismatch between sample spot size (1-2 mm) and size of the laser spot (~200 μm). Improvement of MALDI target plate design[160-163], surface chemistry[164,165] and liquid dispensing techniques[160,166] enabled confinement of protein sample into ~100-500 μm dry spot, minimizing ionization heterogeneity across sample spot and achieving low amol detection of protein[160]. A recent *in vivo* study utilized a variation of MALDI, called surface enhanced laser desorption ionization (SELDI) to detect NPY. This method used antiNPY coated target plate for peptide capture and enrichment, resulting in lower NPY detectability of 0.1 pg from 60 μL microdialysate[50].

1.5 Signature peptide method for low abundance protein quantification

Currently the most popular non-immunological method for low abundance protein quantification is signature peptide method. This method digests large protein into fragment peptides that serve as analytical surrogates of the protein (Figure 1.4). The most widely used protease in signature peptide method is trypsin, because it has high activity and specificity at the carboxyl side of lysine and arginine. By converting protein into signature peptides, this method in theory possesses all the advantages of (capillary)LC-MS including specificity, sensitivity and multi-analyte capacity. Also, absolute quantification (AQUA) can be achieved by introducing a synthesized, stable isotopically labeled (SIL) signature peptide during the digestion process[167]. In reality, reaching similar performance as small peptide detection can be challenging for several reasons.

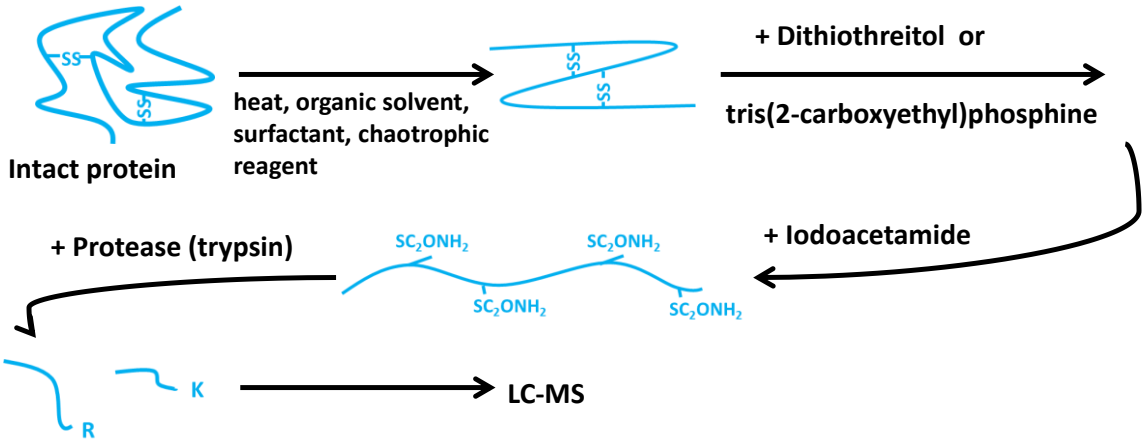

Figure 1.4 Scheme for protein digestion and signature peptide method

First (and fundamentally), the selected signature peptide must properly represent the target protein. Sequence similarity search should always be performed in database such as the basic logical alignment search tool (BLAST) to confirm the uniqueness of signature peptide to target protein[168]. Also it is advised that signature peptide selection should avoid sequence containing sites with possible posttranslational modifications (eg. methionine, cysteine and tryptophan)[169] , possible miscleavage sites (KK, RR, RP, KP)[170], and the signature peptide should be monitored for 3 daughter ion transitions in MS^2 mode to ensure specificity[171].

Second (and more important in the practical side), even for optimally selected signature peptide, its production and detection from low abundance protein in a complex biological sample can be difficult: the digestion may not reach completeness to fully release signature peptide for protease resistant protein presenting at trace level, and the sample matrix can further interfere with signature peptide yield and detection[148,172]. Impact of protease[173], protease format[174-176] and denaturing conditions[177-179] have been studied for improving digestion efficiency, revealing that these factors all affect

completeness of digestion. However, the impact of these parameters on signature peptide production at trace concentration is not frequently assessed when developing signature peptide methods. In chapter 4 of this dissertation, the impact of these factors will be studied on signature peptide production from BDNF at low concentration as a proof of concept study for highly sensitive signature peptide method for this protein.

Another key factor in successful signature peptide methods is use of purification and concentration strategies. When applied for complex samples such as whole blood, plasma, tissue homogenate and CSF[168], sample fractionation both before and after digestion may be required. Protein purification prior to digestion can be achieved based on its intrinsic properties including size, isoelectric point and hydrophobicity, with techniques such as solid phase extraction (SPE)[180], size exclusion chromatography (SEC)[181], ultracentrifugation (UC)[182] and organic precipitation[170]. Immunopurification techniques such as immunodepletion which removes abundant protein from sample[183], or immunocapture which selectively concentrates target protein[184], have also been applied for protein purification. Purification of signature peptides can be achieved by similar approaches. Particularly, stable isotope standards and capture by anti-peptide antibodies (SISCAPA) was developed to capture signature peptide along with its SIL internal standards using anti-peptide antibody for simultaneous sensitivity enhancement and absolute quantification[169].

For application in low abundance protein quantification, immunocapture usually gives higher sensitivity due to the high binding affinity of antibodies towards target protein/signature peptides. For example, an approach utilizing double immunoaffinity enrichment of target protein and online immunoaffinity chromatography-RPLC-MS^2 of

signature peptide gave LLOQ at 0.05 pM for IL-21 from 500 µL plasma (~50% injected)[185], equaling to 12.5 amol mass LLOQ. In another study, immunoprecipitation in 96-well ELISA format (IPE) followed by microwave-assisted protein digestion have shown LLOQ at 17 pM for N-terminal prohormone of brain natriuretic peptide from 50 µL serum (mass LLOQ 850 amol)[186]. Measurement of τ protein from CSF has also been realized by signature peptide method. This study employed immunoaffinity purification of τ protein along with a recombinant, SIL protein that served as internal standard to account for variability of the entire sample preparation and analysis process. The limit of quantification (LOQ) was 0.25 pM from 150 µL CSF and the method was able to detect significantly higher τ concentration in AD CSF[187]. Despite its high sensitivity, one potential drawback of immunocapture method is the availability of antibody for proteins and (especially) signature peptides, and the development of such antibody can take long time.

Non-immunocapture methods have also been explored for low abundance protein quantification. A method utilizing a single extraction step with acidic isopropanol to remove endogenous plasma protein yielded LLOQ at 190 pM for a protein drug from 50 µL plasma[170]. Another method using strong cation exchange (SCX) fractionation of tryptic digest prior to LC injection improved sensitivity by reducing matrix effect, and LOQ of 1-10 ng/mL (100-200 amol injected on column) was achieved for proteins spiked into immunodepleted plasma[183]. With recent advances in high resolution separation, an "antibody-free" (although immunodepletion was still used) signature peptide method was reported to have LOD at low pM range, using high-pressure, high-resolution separations coupled with intelligent selection and multiplexing (PRISM)[188]. In this approach, the

digested protein was spiked with SIL signature peptide internal standard for locating the signature peptide-containing fraction in the first dimension LC using a split flow design, and only the signature-peptide-containing fractions were injected to the second dimension LC column. This method achieved <50 pg/mL LOD for four proteins (for prostate-specific antigen 50 pg/mL=1.7 pM), owing to the improvement in separation and subsequently reduced matrix interference. This method was further evaluated with non-immunodepleted serum, and the LOQ was in low ng/mL range[189].

1.6 Dissertation overview

The work presented in this dissertation focuses on improving the analytical practicality and sensitivity of cLC-MS in neuropeptide/protein detection, with application in *in vivo* monitoring of neuropeptide enkephalins and orexins.

Chapter 2 studies analytical speed enhancement of cLC-MS by increasing the sample loading speed. The speed increase is achieved by reducing column's backpressure, enabling higher injection flow rate and shorter sample injection, which is the rate limiting step for cLC-MS analysis of neuropeptides. In this chapter, capacity of 75 μm I.D. capillary column packed with 10 μm reversed phase particles is evaluated for increasing throughput in cLC-MS^n based neuropeptide measurement. Coupling a high injection flow rate for fast sample loading/desalting with a low elution flow rate to maintain nano-ESI sensitivity, this column reduces analysis time from ~20-30 min to 3.8 min for 5 μL sample, with 3 pM LOD for enkephalins and 10 pM LOD for $DynA_{1-8}$. The use of isotopically labeled internal standard lowers peptide signal variation to less than 5%. This method is validated for *in vivo* detection of LE and ME with microdialysate collected

from rat GP, and has been published in *Journal of the American Society for Mass Spectrometry* (2013, volume 24, page 1700-1709) .

Chapter 3 focuses on improving *in vivo* detection of neuropeptides by both increasing cLC-MS's sensitivity and recovery of microdialysis sampling. Enhancement in sensitivity is achieved by adding ACN as organic modifier to peptide sample that reduces pre-injection loss caused by non-specific adsorption, reducing LOD for 10 tested neuropeptides to 0.1-2 pM from 8 µL sample. Improvement in microdialysis recovery is realized by modifying the hydrophilic, negatively charged AN69 membrane and fused silica tubing by polycationic PEI. The modification shows significant improvement in recovery for 7 positively charged neuropeptides, and is likely due to reduced electrostatic interaction. This method is then validated for *in vivo* monitoring of orexins from rat arcuate nucleus, and low pM level of orexins are quantified from the dialysate. This chapter has been prepared for publication in *Analytical Chemistry*.

Chapter 4 will discuss about the development of a signature peptide method for BDNF. BDNF has high structural stability and does not generate good tryptic peptide signal; while chymotrypsin is found to produce higher signature peptide signal. Concentrating the protein before denaturation and using immobilized chymotrypsin also helps increase the production of signature peptide. Using BDNF's optimized digestion protocol, two other proteins in the neurotrophin family, NT-3 and GDNF, can also be detected at trace level by signature peptide method. The LOD is approximately 5 pM for BDNF and NT-3, and 10 pM for GDNF, corresponding to 40 and 80 amol protein digest injected to the cLC-MS system. This method is potentially useful for realizing sensitive and multiplexed quantification for neurotrophin.

Chapter 5 will discuss about possible future directions and will include some preliminary data.

Appendices will document supplemental figure for chapter 3 and several other projects including:

(1) Signature peptide and micro-channel ELISA methods for measuring trace level protein markers in the spent medium of *ex vivo*–produced oral mucosa equivalent (EVPOME).

(2) Polymer monolithic column fabrication for neuropeptide extraction.

(3) BDNF ELISA result.

The merits and limitations of each method will be discussed.

Chapter 2

Rapid Preconcentration for LC-MS Assay of Trace Level Neuropeptides

2.1 Introduction

Neuropeptides act as neurotransmitters, neuromodulators, growth factors and hormones in the central nervous system. They are involved in physiological and pathological pathways such as learning, appetite control, depression, addiction, and reproduction[2,190-193]. Monitoring extracellular concentrations of neuropeptides can provide insights into their dynamics and physiological roles within the brain[6,50,194]. Such measurements are performed by microdialysis sampling followed by assay for peptides of interest in collected fractions. Measurement of neuropeptides is challenging due to their low extracellular concentration (usually pM level) and tendency to degrade during storage[195]. The difficulty is further exacerbated by low recovery of microdialysis sampling[196]; although recent developments have illustrated routes to improved recovery[119,120,125]. Measurement is also hampered by slow analysis times. Thus, despite their importance, neuropeptides are infrequently measured *in vivo* relative to other neurotransmitters. In this work, we describe an approach to increase the throughput of neuropeptide measurements while maintaining sufficient sensitivity.

Capillary zone electrophoresis[197,198], high performance liquid chromatography (HPLC) [137,141,199-202] and radioimmunoassay[203,204] have been applied for determining the *in vivo* concentration of neuropeptides. Since seminal work by Caprioli[142], electrospray

ionization (ESI)-multistage mass spectrometry (MS^n) has gained popularity for such measurements due to low amol detection limit from microliters of samples, high specificity, and multi-analyte capacity[19,140,142,205]. Although ESI-MS^n is a useful method, the high salt content and low concentration of neuropeptide mean that they must be preconcentrated, desalted, and separated, typically by LC or solid phase extraction, for analysis[206]. Use of cLC columns is critical because it allows the microliter samples to be concentrated on packed beds with nanoliter volumes to improve sensitivity[142]. This method has achieved limits of detection (LOD) as low as 0.5 pM from 4 μL volume samples of opioid neuropeptides, making it suitable for *in vivo* measurements.

A limitation of cLC-ESI-MS^n for high sensitivity neuropeptide measurements is its low throughput. When using columns with small bore (25-50 μm) packed with 5 μm reversed phase particles, loading a few microliter sample can take as long as 15 min, even at high pressures (4000 psi), and yield overall analysis time of 20-30 min/sample[18,19]. Narrow bore columns may also be prone to clogging, especially when repeatedly loading large volume of samples, which can further reduce throughput due to frequent column changes. Low throughput is a significant concern because microdialysis generally produces many sample fractions over the course of a single experiment. Neuropeptide degradation, which is frequently observed for trace concentrations found in brain samples[207], places a further premium on rapid analysis.

To accelerate analysis in capillary LC-MS^n, flow rate during preconcentration and column rinsing must be increased since these are rate limiting steps; however, it is unclear if more rapid preconcentration can be achieved while maintaining the low LOD needed. At a given pressure (e.g., the maximal pressure of the system) flow rate is

directly proportional to the square of both column I.D. and particle diameter [208]. In this chapter we improved throughput of neuropeptide analyses by: (1) using larger bore capillary columns (75 μm I.D.) packed with larger diameter (10 μm) reversed phase particles for lower pressure loading and rinsing; (2) determining the flow rate limits for operation; and (3) developing a periodic column washing scheme to maintain column stability under repeated injections. As a demonstration of the method, LE and ME) were detected in microdialysis samples collected *in vivo* from rat GP. The enkephalins are endogenous opioid ligands with important roles in many processes such as pain inhibition [209], addiction[210], feeding[6], and movement[51]. Rapid assays for these and related peptides will facilitate studies of their role in normal and pathological brain chemistry.

2.2 Materials and methods

2.2.1 Chemicals and materials

Fused silica capillary was from Polymicro Technologies (Phoenix, AZ). Solvents for capillary LC were Burdick and Jackson from Honeywell (Muskegon, MI). Alltima C18 packing materials (10 μm, 5 μm) were from Grace Davison (Deerfield, IL). Formic acid, hydrofluoric acid and isopropanol were from Fisher Scientific Inc. (Ann Arbor, MI). Enkephalins, high purity acetic acid and formamide were purchased from Sigma-Aldrich (Saint Louis, MO). $DynA_{1-8}$ was from Phoenix Pharmaceutical Inc. (Belmont, CA), Kasil^{TM} 1624 and K^{TM} sodium silicates were from PQ Corporation (Malvern, PA). Artificial cerebrospinal fluid (aCSF) used for making neuropeptide standards and microdialysis perfusion was made to a final concentration of 145 mM NaCl, 2.68 mM KCl, 1.10 mM $MgSO_4$, 1.22 mM $CaCl_2$, 0.50 mM NaH_2PO_4, and 1.55 mM Na_2HPO_4 with MiliQ^{TM} water (EMD, MiliporeBillerica, MA), and pH was adjusted to 7.4 using 1

M NaOH. High potassium aCSF solution has the same composition as regular aCSF except a combination of 75 mM KCl and 70 mM NaCl was used to substitute the 145 mM NaCl in regular aCSF. aCSF was stored at 4 ^{0}C and was filtered with 0.2 μm pore filters (GE, Piscataway, NJ) to remove particulates prior to experiment.

2.2.2 Capillary LC

Capillary columns were prepared in house using 75 μm I.D. /360 μm outer diameter (O.D.) fused silica capillary. A 1 mm silica sol-gel frit was placed at one end of the column using a slightly modified version of a method previously described[19]. In brief, a 20 cm long capillary was filled with a mixture of 3:1:1 (v/v/v) Kasil^{TM} 1624: K^{TM} sodium silicate: formamide up to 5 cm by capillary force, and then placed in an oven (100 ^{o}C) overnight for polycondensation of the silica sol-gel network. The capillary was cut by a ceramic capillary cutter (Polymicro Technologies) to leave a ~1 mm section of the sol-gel network as a single-ended frit. The capillary frit was flushed with water and methanol prior to packing. The column was packed with a slurry of 10 μm Alltima^{TM} C18 reversed phase particles (5 mg/ml particles in acetone) at 200 psi to 3.6 cm. The open end of the capillary was also cut to leave only 0.4 cm void capillary to minimize dead volume, resulting in 4 cm total column length. The electrospray emitter was prepared in house using 20 cm of 40 μm I.D./360 μm O.D. fused silica capillary. A 1 cm section of polyimide coating 10 cm away from one end was removed with flame to expose bare silica that was pulled into two separate tips by a P-2000 CO_2 laser puller (Sutter Instruments, Novato, CA). The tip was etched with 49% hydrofluoric acid for 3 minutes to create the electrospray emitter, and the emitter was cut at the open capillary side to a length of 1.3 cm. The column and emitter tip were joined by a 2 cm long

polytetrafluoroethylene (PTFE) tubing (1/16”X0.010”, Grace Davison, Deerfield, IL). The LC method is performed semi-automatically using the system depicted in Figure 2.1 as follows: (A) manually load 5 μL sample loop with sample using syringe and while (re)equilibrating column with loading solvent (0.1% formic acid) under 3600 psi; (B) switch injection valve and inject peptide standard under 3600 psi plus rinse with additional 5 μL loading solvent; (C) switch injection valve out of line and rinse column with another 5 μL loading solvent to remove remaining salt from column; and (D) switch selection valve to lower pressure pump with mobile phase to elute peptide(s) for detection.

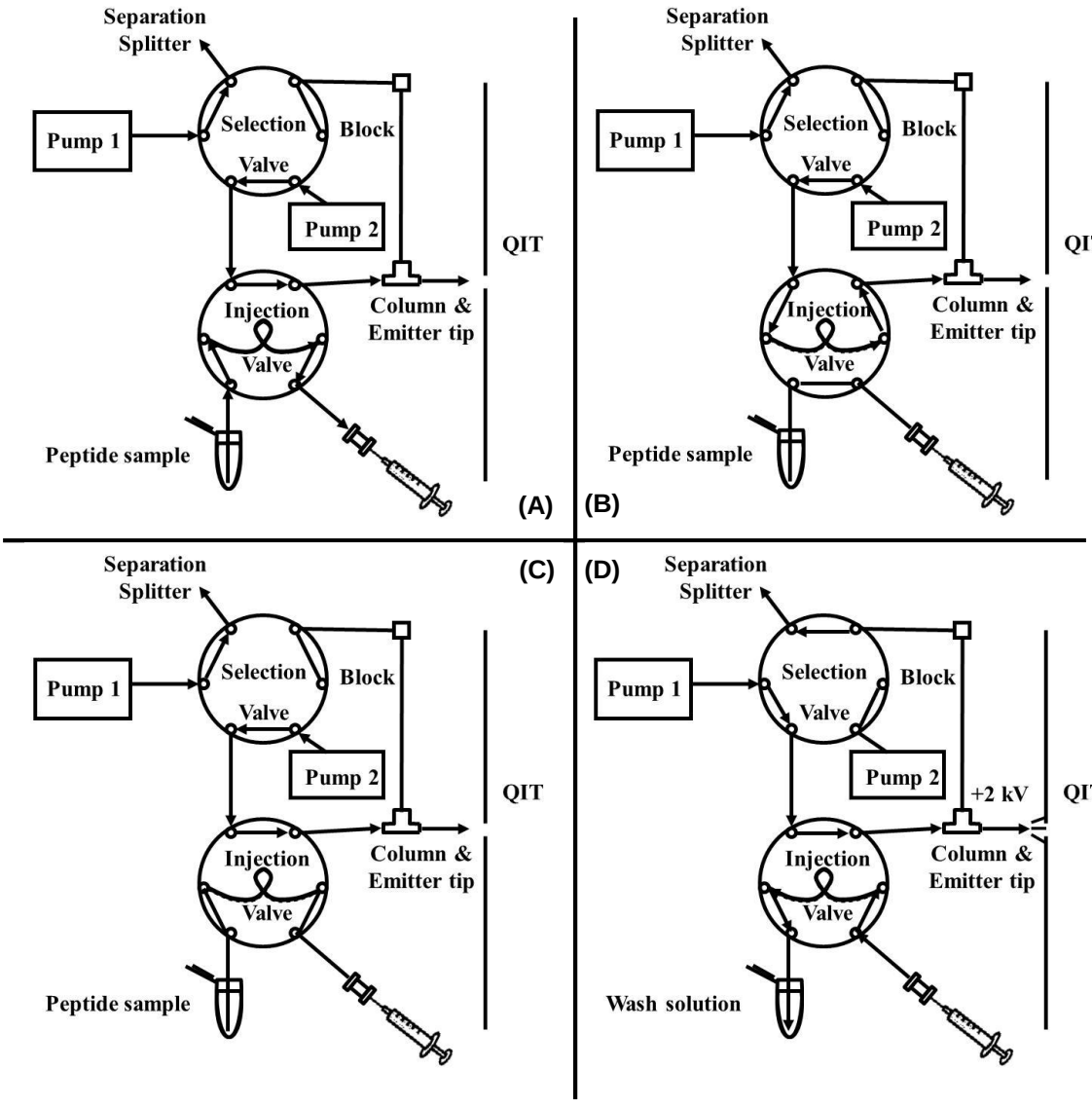

Figure 2.1 Diagram and operation scheme of the dual valve dual pump LC-MS^n system. Valve positions shown for filling sample loop (A), sample injection onto column (B), rinsing column (C), and peptide elution and detection (D). Pump 1 is a Waters 626 HPLC pump (Waters Corporation, Milford, MA) operated with elution mobile phase and pump 2 is a Isco 100D high pressure syringe pump (Teledyne Isco Inc., Lincoln, NE) to drive loading solvent through the column. Detailed description is given in the text.

2.2.3 MS detection

The LC system was coupled to a quadrupole ion trap (QIT) mass spectrometer (LCQ Deca XP Plus, Thermo Fisher, Waltham, MA) operating at positive mode with a Finnigan nanospray ionization source (Thermo Fisher Scientific, Waltham, MA). All measurements were made with the following setting: automatic gain control (AGC) on,

collisional induced dissociation (CID) q = 0.25, isolation width m/z = 3, activation time 0.25 ms, number of micro scan = 2, maximum injection time = 400 ms. Normalized collision energies were 38%, 33% for LE (MS^3), 36%, 33% for ME (MS^3) and 34% for $DynA_{1-8}$ (MS^2). Optimization of optics for best sensitivity was done monthly with constant infusion of 2 μM ME into the mass spectrometer with a flow rate of 100 nL/min. The MS^n pathways were: 556→397→278+323+380 for LE, 574→397→278+323+380 for ME as discussed in our previous work[18,140], 491→435 for $DynA_{1-8}$. Ions were detected under consecutive reaction monitoring mode (CRM) or selected reaction monitoring mode (SRM) with the following mass range: 277-279,322-324,379-381 for ME and LE, 434-436 for $DynA_{1-8}$.

2.2.4 *In vivo* microdialysis

Adult male Sprague–Dawley rats (Harlan, Indianapolis, IN) weighing between 250 and 350 g were used. Rats were housed in a temperature and humidity controlled room with 12 h light/dark cycles with food and water available *ad libitum*. All animals were treated as approved by the University of Michigan Unit for Laboratory Animal Medicine (ULAM) and in accordance with the National Institute of Health (NIH) Guidelines for the Care and Use of Laboratory Animals. Prior to surgery, rats were anesthetized with an intraperitoneal (i.p.) injection of a ketamine (65 mg/kg) and dexdormitor (0.25 mg/kg) mixture prepared in an isotonic salt solution. Concentric microdialysis probes with 1.5 mm long PAN active membrane (AN69 from Hospal, Bologna, Italy) with recoveries calibrated *ex vivo* of 9.6% for LE and 8.3% for ME at 0.6 μL/min flow rate were implanted under anesthesia into the GP according to the following coordinates from bregma and top of the skull: AP -1.3 mm, ML ±3.3 mm, DV -7.0 mm[211]. Probes were

secured to the skull by acrylic dental cement and metallic screws. Following surgery, rats were allowed to recover and experiments were run 24 h after probe implantation. Microdialysis probes were flushed at a flow rate of 1.5 μL/min with aCSF for 2 h using a Chemyx Fusion 400 syringe pump (Chemyx, Stafford, TX). Perfusion flow rate was then reduced to 0.6 μL/min and samples were collected every 20 minutes into vials containing 0.5 μL acetic acid to preserve peptide stability as previously described[18]. Samples were immediately injected on the LC-MS^n system following collection. High K^+ aCSF (75 mM) was perfused for 40 min through the probe after 3 baseline samples were collected. Lines were then switched back to standard aCSF and 3 more samples were collected (Figure 2.6).

2.3 Results and discussion

2.3.1 Influence of column bore size and particle size on sensitivity

The procedure for analysis by on-column preconcentration LC-MS^n is based on previous work which has been successful for several neuropeptides[18,140,141]. The dual pump system with selection valve allows sample to be loaded onto the column at high flow rate but then eluted at a lower flow rate that gives better ESI sensitivity[212,213] and LC performance without requiring an extensive pressure equilibration. Despite these steps, the rate limiting step of analysis is preconcentration and rinsing[18,139,140]. In prior work, when using a 25 μm I.D. by 4 cm long column packed with 5 μm reversed phase particles, 15 min was required to inject a 5 μL sample and rinse the column with 10 μL loading solvent (i.e. ~1 μL/min). The total analysis time was 30 min when including gradient dwell time (i.e. time for the elution gradient to reach the column), gradient elution, and column re-equilibration[18].

Injection flow rate could potentially be increased by increasing applied pressure; however, without specialized fittings and valves, the system is prone to leakage at pressures over 5000 psi. (Pumps with significantly higher pressure are also available but much more expensive.) Another solution is to use shorter columns; however, preliminary experiments revealed that shorter columns tended lose sample during preconcentration, perhaps due to elution during the injection step. To facilitate faster loading, we therefore explored larger bore (75 μm I.D.) capillary columns packed with larger diameter (10 μm) reversed phase particles to reduce column back pressure. Potential issues associated with this method are: (1) worse separation efficiency of larger particles[214] might result in broader elution band that affects detection sensitivity; (2) when the same volumetric flow rate is applied for elution, 75 μm I.D. capillary columns have a 9-fold decrease in linear flow velocity compared to 25 μm I.D. column. The change in linear velocity also changes separation efficiency [214], further complicating system performance determination.

To explore these effects, we made LE calibration curves comparing columns with different I.D.s and particle sizes under the same loading and elution flow rate. As shown in Figure 2.2 A, increasing column diameter from 50 μm to 75 μm resulted in an 18% increase in calibration curve slope while increasing particle size from 5 μm to 10 μm resulted in a 6% decrease in calibration curve slope. Since the calibration curve slope variation was already 10% between columns with the same I.D. and particle size, these data show that column and particle size had minor effects on detection sensitivity. The full width at half maximum (FWHM) of the LE peak using 10 μm particles was 7.4% ±6.2% (n=3) wider than with 5 μm particles (Figure 2.2B). This small change is likely due to the strong dependence of peak width on gradient slope for peptides. (Peptides were

eluted with a fixed mobile phase of 53% methanol; however, because the column was flushed with aqueous solution prior to elution, a "step" gradient was generated in the column.) Although 75 μm I.D. columns packed with 10 μm particles gave similar performance as the other two tested columns, the flow resistance on this column was much smaller, resulting in 15 μL/min injection flow rate at 4000 psi and potential to load and desalt 5 μL sample in one minute. However, under the same applied pressure, the injection flow rate was 6 μL/min on 50 μm I.D. columns packed with 10 μm particles and 4 μL/min on 75 μm I.D. columns packed with 5 μm particle, requiring at least 2.5 min and 3.8 min to load and desalt the same 5 μL sample, respectively. Previous studies[18,19] required 10-15 minutes to load and desalt 4-5 μL samples using smaller bore (25-50 μm) column with 5 μm column packing.

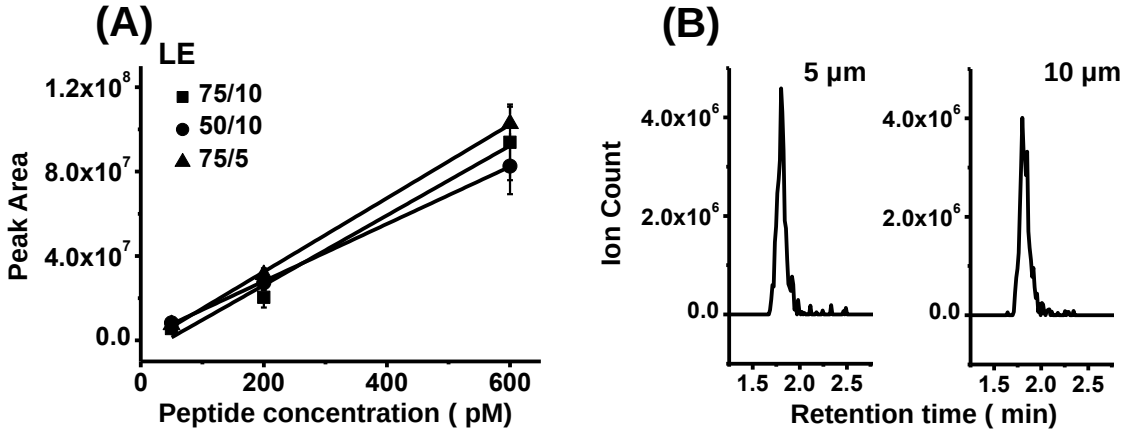

Figure 2.2 Influence of column I.D. and particle size on detection sensitivity. (A) Calibration curve showed column I.D. and particle size had little influence on sensitivity under the same volumetric elution flow rate. (B) Chromatogram of LE (5 μL 200 pM injected) showed no obvious peak broadening using column packed with 10 μm particle compared to column packed with 5 μm particle. All measurements were done with 3 replicates.

2.3.2 Influence of loading flow rate and elution flow rate on sensitivity

After establishing that 10 μm particles in 75 μm I.D. columns could be used with little effect on sensitivity but at lower pressures, we investigated the relationship between peptide signal and sample injection/rinsing flow rates to determine how rapidly the assay could be performed. For these experiments we used a sample volume of 5 μL and 10 μL of loading solvent to rinse the column. (The volume of rinsing solution needed was determined in separate experiments. If lower volumes were used, less stable signals were achieved, presumably due to interference from salts and other sample constituents that are not fully washed away.) The experiments revealed that peptide peak area remained stable for loading flow rate from 2.6 to 14 μL/min (Figure 2.3A). Interestingly, above 14 μL/min signal began to decrease for at least one of the peptides. The reason for this effect of higher flow rates is not clear. It seems unlikely to be a kinetic limitation to binding since the residence time of an unretained species was ~0.5 s under these conditions. Calibration curve of all three peptides also showed no sensitivity change when comparing injection under low (2.7 μL/min) and high (14 μL/min) flow rates (Figure 2.3B).

Another way to increase analysis speed is to increase separation flow rate; however, increasing volumetric flow rate may also cause dilution of the eluted peptide band and worse ESI efficiency[212,213]. We found that peptide signal from a 200 pM standard decreased 68%, 57% and 78% for ME, LE and $DynA_{1-8}$, respectively, when elution flow rate increased from 80 nL/min to 225 nL/min (Figure 2.3C). In theory, higher sensitivity could be obtained by pushing the electrospray flow rate lower [212,213]; however, in practice, further lowering flow rates will require an extended time period for elution, thus lowering throughput. An elution flow rate of 100 nL/min was selected as a compromise between

time and sensitivity. This flow rate allowed baseline separation of 3 peptides in 2 min (Figure 2.3D) while maintaining a LOD of 3 pM for enkephalins, and 10 pM for $DynA_{1-8}$.

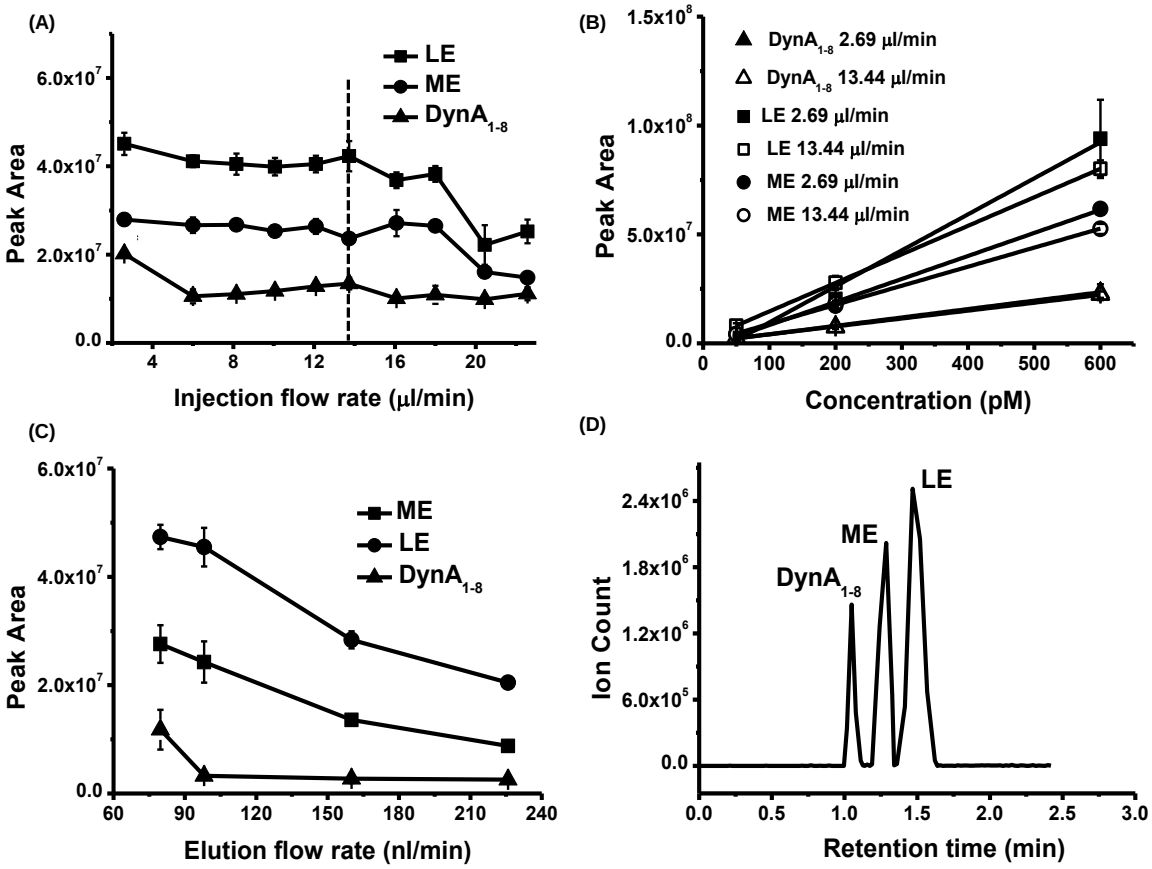

Figure 2.3 Influence of flow rates on detection sensitivity. (A) Peptide signal remained stable within the injection/rinsing flow rate range of 2.6 μL/min to 14 μL/min. (B) Calibration curve under different injection/rinsing flow rate (2.69 μL/min v.s. 13.44 μL/min) suggested no major sensitivity decrease when injecting peptide under high flow rate. (C). Increasing elution flow rate decreased peptide signal. Peptide standard: 200 pM LE, ME and $DynA_{1-8}$ dissolved in aCSF with 5% HAc. Injection volume: 5 μL. (D). Reconstructed ion chromatogram (RIC) of 5 μL 60 pM neuropeptide being injected onto the column. All measurements were done with 3 replicates.

The total analysis time under these conditions was 3.8 min/sample (0.4 min for sample loading and column re-equilibration, 0.4 min for injection/preconcentration, 0.8 min for rinsing, and 2.2 min for elution). In previous work using a 25 μm I.D. column with 5 μm packing, a total analysis time of 30 min was needed for analyzing one sample

with 4-5 μL volume, with approximately the same LOD when using the same quadrupole ion trap MS as used in this work. (Better LODs were obtained by using newer MS, eg. linear ion trap MS that has higher sensitivity.)[18] Thus this approach achieves similar sensitivity compared to previous results, but in 13% of the time. For an experiment which results in collection of 100 samples, analysis could potentially be completed in 6.3 h rather than 50 h, saving substantial amount of time.

Lower detection limit and higher multi-analyte capacity could potentially be achieved by using triple quadrupole MS, which has higher duty cycle and higher sensitivity under selected reaction monitoring (SRM) or multiple reaction monitoring (MRM) mode. It was reported that 16 neurotransimitters were detected in one LC run under MRM mode using a triple quadrupole MS. The sensitivity was sufficient to achieve lower pM to nM detection limit without preconcentration[215]. However, due to the reported better specificity of MS^3 in detecting enkephalins [140] and the fact that triple quadrupole MS is not capable of MS^n detection , ion trap type MS remains the best option when MS^3 or higher stage MS is desired for detecting several neuropeptides.

2.3.3 Improved stability during serial injections

To test system stability and injection reproducibility, we performed serial injections of 30 peptide standards containing 60 pM ME, LE and $DynA_{1-8}$. The relative standard deviation (RSD) was higher than 10% for all three peptides, and the RSD for ME was higher than 40% (Table 2.1). We considered several possibilities for this large RSD including: (1) loss of particles from the column due to the sudden pressure drop between sample injection and elution causing backflow of particles to the inlet side; (2) partial clogging causing decreased amount of sample injection and rinsing; (3) build-up of

impurities from peptide sample and solvent on the column causing a change in system response (e.g. by eluting with peptide or altering preconcentration capacity). By inspecting the column and tip assembly under a light microscope, assumptions (1) and (2) were eliminated since no clogging or bed length reduction was found.

Supporting the idea that accumulation of impurities affected the RSD, we found that in a similar series of injections in which a "wash" was applied (injection of 20 μL of wash solvent containing 60% (v/v) isopropanol, 30% (v/v) ACN and 10% (v/v) water) after every 6 assays the peak area RSD was reduced to less than 10% for the enkephalins and less than 20% for $DynA_{1-8}$ (see Figure 2.4A and Table 2.1). Peak area RSD of $DynA_{1-8}$ still remained > 10% could be the result from using SRM while enkephalins are detected by CRM. The reason for using SRM to detect $DynA_{1-8}$ is that it produced an easily identifiable daughter ion (c7, m/z = 435), while the MS^3 spectrum showed no major granddaughter ions for quantification. Previous paper[18] published by us also showed mediocre detection limit for $DynA_{1-8}$ using MS^3, urging us to use the SRM method as alternative for higher sensitivity. However, since SRM is essentially MS^2, whose specificity is lower than MS^n based CRM method, the higher variation in $DynA_{1-8}$ peak area is not unexpected. Although adding the wash step decreased system throughput from 3.8 to 4.4 min per sample, it proved to be effective in improving long term performance. Improvement of reproducibility could also be obtained through adding internal standards. As a demonstration, we monitored the peak area of 60 pM LE and deuterated LE we have in lab (dLE, m/z 560) under serial injection. Although using deuterated internal standard has potential issue such as chromatographic isotope effect, we have carefully examined the retention time of LE and dLE and found the difference

was negligible. These experiments showed that the RSD of peak area ratio of LE versus dLE was reduced to <5%, while peak area RSD of individual peptide was still around 8-9% (Table 2.1). Based on these results, we presume that use of stable isotopes of other peptides would also aid detection, but this was not tested for cost savings.

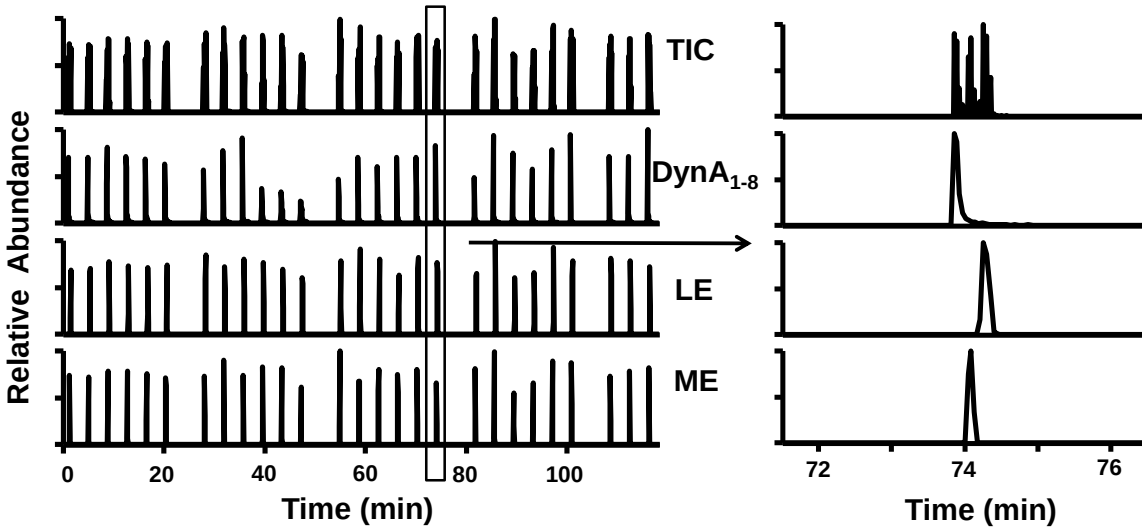

Figure 2.4 Chromatogram of serial injections of 60 pM peptide standards in series. A wash injection with 20 μL60:30:10 (v/v/v) isopropanol: ACN: H_2O injected onto the column was carried out every 6 injections. The right image shows a zoomed-in view of one injection where 5 μL peptide standard was preconcentrated, rinsed, and separated for detection within 4 minutes.

Table 2.1 Peak area RSDs of tested neuropeptides under different injection protocols. Adding wash injection and injecting peptide with internal standard significantly improves injection reproducibility.

Injection type	**Peak Area RSD ($DynA_{1-8}$)**	**Peak Area RSD (LE)**	**Peak Area RSD (ME)**
No column rinsing (n=30)	20.2%	18.5%	46.0%
Wash injection every 6 injections (n=27)	15.4%	8.4%	9.1%
	Peak Area RSD (dLE)	**Peak Area RSD (LE)**	**Peak Area ratio RSD (LE/dLE)**
Injection of LE and internal standard (with wash injection) (n=27)	9.2%	9.3%	4.3%

The larger columns with rinsing were also found to be resistant to clogging. Under these conditions, one column could be operated stably during two 2-hour long series

injections with 60 samples injected onto the column. After 60 injections, reduction in both injection and elution flow rate and retention time shift was frequently observed, indicating partial clogging. Therefore one column was typically used within one day. While potentially cumbersome, the ease of packing one such column (~10 min after frit preparation), negligible column-to-column retention time shift and small variation in calibration curve shape (~10%) mean that these columns are "disposable". Previous work found that 25 μm columns could only survive 20-40 injections, with column-to-column peak area variation up to 50%[18].

2.3.4 Detecting enkephalins in microdialysate

To demonstrate the feasibility of this method for *in vivo* peptide measurements, we used it to monitor enkephalins in microdialysis fractions collected at 20 min intervals under basal conditions and while perfusing 75 mM K^+ aCSF through a probe implanted in the GP brain of freely moving rats (n = 3), as summarized in Table 2.2. Microdialysis flow rate was set to be 0.6 μL/min, and 5 μL of the 12 μL dialysate collected over 20 min was actually injected onto the column. Excess dialysate was required to overfill the loop. More efficient use of such precious samples may be achieved by partial loop and "microliter pickup" mode using commercial autosamplers[18]. The concentration of peptides in dialysate samples was determined by external calibration using standard solutions of peptide dissolved in aCSF (5% HAc added) with the following concentrations: 5 pM, 50 pM, 800 pM, and 3 nM. Calibrations were linear with correlation coefficients of 0.99.

Table 2.2 ME and LE's basal and stimulated concentration in *in vivo* dialysate. *In vivo* concentration was corrected by the relative recovery of the microdialysis probe.

Collection condition	[ME] ± SEM (pM) (n = 3)	[LE] ± SEM (pM) (n = 3)
Basal, dialysate	14.2 ± 1.3	7.1 ± 0.9
Stimulated, dialysate	1833 ± 149	412 ± 71

To determine if concentration determined by external calibration was accurate, we also performed study on matrix effect. Spiking 5 pM, 50 pM, 800 pM, 3000 nM LE into dialysate gave a similar calibration curve as the same concentration in aCSF (Figure 2.5A). This suggests that matrix effects were negligible in the calibration of peptide concentrations. To better examine this effect at low concentrations, we compared peak area of 5 and 50 pM LE standards to that found for spiking the same concentrations into dialysate. The difference in peak area between the aCSF and spiked dialysate corresponded to 5.0 ± 2.8 (SD) pM (n = 3, from 1 rat) (Figure 2.5B), while LE's concentration in dialysate was determined to be 7.1 ± 0.9 (SEM) pM (n = 9, from 3 rats) by external calibration, which was not significantly different. This result further suggests minimal matrix effect on signal and that external calibration can be used.

Stability of the dialysate sample signal was examined under serial injection conditions. 9 basal dialysate fractions collected from 1 rat over 3 h were serially injected over 37 min (9 samples plus 1 wash injection). These samples showed 21% and 22% peak area RSD for LE and ME, respectively (Figure 2.5C). The RSD was higher than standards possibly because of natural variation of brain peptide concentration over this period. Average concentrations of LE and ME in serial injection were determined to be 5.8 ± 1.3 (SD) pM and 14.4 ± 3.2 (SD) pM, respectively. The basal dialysate

concentration determined from 3 rats were 14.2 ±1.3 (SEM) pM and 7.1± 0.9 (SEM) pM for ME and LE, again showed no significant difference.

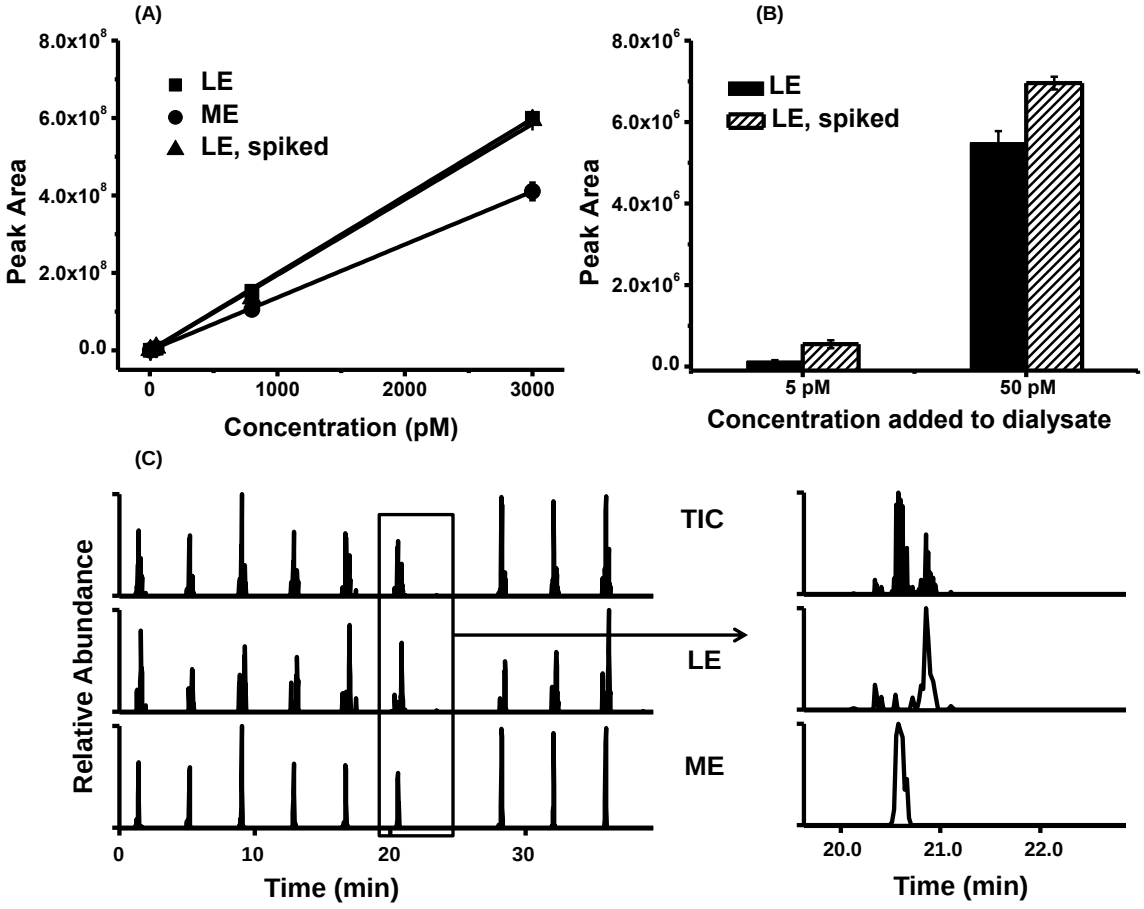

Figure 2.5 *In vivo* measurement of LE and ME from rat brain dialysate. (A). Calibration curve of LE and ME from 5 pM to 3 nM (n = 3) (B) LE's peak area in 5 pM/50 pM standard and dialysate spiked with 5 pM/50 pM LE. (C). Serial injection of 9 basal dialysate sample in 37 minutes. Injection volume: 5 µl.

The basal extracellular concentration for ME and LE was 171±22 (SEM) pM and 74±12 (SEM) pM when correcting for *in vitro* recoveries (8.3% for ME and 9.6% for LE). Peviously published results reported that the total enkephalin concentration in rat globus pallidus/ventral pallidum was 150 pM, with ME/LE ratio ranging from 1.3:1 to 3.0:1. Our data gave a total of 245 pM, indicating reasonable agreement.

K^+ stimulation causes depolarization of the neuronal cell membrane and subsequent neuropeptide level into the extracellular space [216,217]. In this study, perfusion of 75 mM K^+ aCSF into the brain caused 129 fold and 58 fold increase in ME and LE's *in vivo* concentration, respectively (Figure 2.6). Previous microdialysis-RIA based method reported that turning on K^+ stimulation for only 2 min in a 30-min long collection period caused collected opioid peptide (majorly enkephalins) increase from 1.5 fmol to 43.9 fmol in globus pallidus/ventral pallidum[195]. Another study using microdialysis coupled online to capillary LC-MS^2 reported K^+ stimulation over 30 minutes caused 32 and 19 fold increase in ME and LE concentration in GP, respectively[141]. The variation in enkephalin level increase could be contributed to the fact that previous results were obtained from anesthetized rats using 4 mm probe, while our results were from freely moving rats with 1.5 mm probe. Freely moving rats tend to have different response under potassium stimulation [140], and longer probes are less likely to be placed accurately in the targeted brain area. In addition, the K^+ concentration in this study was 75 mM, while previous studies used 100-150 mM K^+ for stimulation. Nonetheless, the reported results along with our observation was in agreement with the fact that the GP is the primary target of striatopallidal neurons which express high levels of enkephalins [218,219]. Thus, depolarizing the neurons directly at the terminal site of enkephalin release likely yields higher release levels compared to measuring in other areas such as the striatum where the cell bodies of striatopallidal neurons reside.

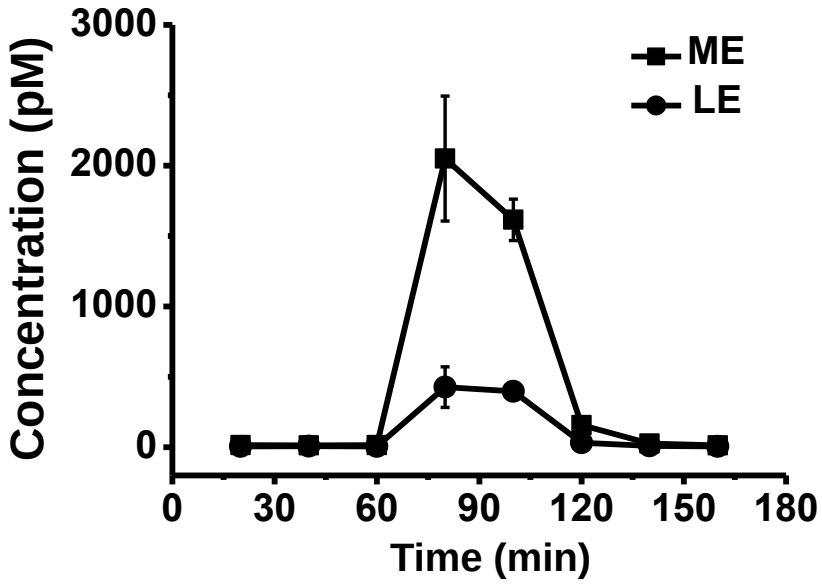

Figure 2.6 K^+ stimulation profile of ME and LE. Potassium concentration: 75 mM. Stimulation time: 40 minutes. Number of replicates: 3. Error bar represents standard error of mean (SEM).

Other studies also had suggested milder increases in enkephalin levels upon K^+ stimulation in striatum. For example, enkephalins increase in rat striatum was less than 10 fold under K^+ stimulation[18,140].

2.4 Conclusions

The method described in this chapter has demonstrated fast neuropeptide analysis with low pM detection limits. With ~4 min cycle time per sample, the throughput was improved 5-8 fold over previous work. This method was also validated for *in vivo* measurement where lower amol of enkephalins could be detected from rat brain dialysate. The enhanced analysis speed and column stability suggest the possibility of routine processing of many *in vivo* samples. SIL peptides will likely be needed for cases where small changes in peptides are to be measured. Further, as characteristic peptides are

increasingly used to quantify proteins, the general approach of rapid loading and rinsing may be of utility for trace analysis in other applications as well.

Chapter 3

Improving Capillary LC-MS Detection and Microdialysis Sampling for *in vivo* Monitoring of Intact Orexins

3.1 Introduction

Neuropeptides are an important class of signaling molecules in the brain that are implicated in functions as diverse as feeding, stress, pain, and sleep. Neuropeptides, which are formed by processing precursor proteins translated from genes, are released into the extracellular space by exocytosis from neurons to exert effects on neighboring neurons through binding to cell surface receptors. Regulation of neuropeptides can be studied by measuring tissue content of peptide or mRNA; however, better understanding of their regulation and function can be achieved by monitoring their extracellular concentration dynamics *in vivo*. Such measurements allow for direct correlation between extracellular concentration and behavior, drugs, disease state and other signaling or modulation processes[6,8,60,80,220]. A potentially useful technique for such measurements is microdialysis sampling. In this technique, a semi-permeable membrane probe is inserted into a specific brain region. The probe interior is perfused so that molecules released into extracellular space can diffuse across the membrane, enter the probe, and be collected for analysis.[221,222] Collecting a series of fractions allows temporal information to be obtained.[223,224] Microdialysis is favored over other sampling methods because it disturbs relatively little tissue[225,226] and produces sample that is free of proteins and tissue debris. Although microdialysis is routinely used for small molecule neurotransmitters, its use for

monitoring peptides remains relatively rare and challenging due to low extracellular concentration of peptides (1-100 pM) and small samples generated (1-10 µL). Analytical challenges are exacerbated by low recovery of neuropeptides through microdialysis probes. In this chapter we describe procedures to improve sensitivity and recovery of neuropeptides.

Historically neuropeptides have been assayed in dialysate by radioimmunoassay (RIA) or enzyme linked immunosorbant assay (ELISA). Although immunoassays with 9-100[40] attomole mass limit of detection (LOD) have been reported for neuropeptides, it can be difficult to develop and maintain assays with this sensitivity. Furthermore, immunoassays lack sequence specificity leading to potential false positives in quantification and inability to discern modified or degraded peptides[199,227].

An emerging method for trace neuropeptide detection is capillary liquid chromatography coupled to mass spectrometry (cLC-MS)[17-19,142,205,228,229]. With this method, microliter samples of low abundance peptides can be concentrated onto a nanoliter volume column to enable detection of specific peptides at low picomolar concentration (attomole quantity)[18,19,38,140]. Despite its potential for high sensitivity and specificity, only 10 of the over 200 known mammalian neuropeptides have been quantitatively measured at their endogenous concentration *in vivo* using this technique[18,19,38,39,139-142,205,228]. Successes have been mostly limited to small peptides (molecular weight, MW < 2000 Da). (An exception was β-endorphin, which was enzymatically digested to form a signature peptide fragment that was easier to detect with cLC-MS[18].) One reason for difficulty in applying cLC-MS to determination of

neuropeptides is widely disparate detection limits. A previous study showed that a selection of 10 neuropeptides had LODs from 0.5 pM to 10 nM from 4 µL sample[18].

Work on peptide drugs and tryptic peptides for shotgun proteomics applications has shown that adsorption to surfaces, such as sample vials, causes peptide loss and poor injection repeatability[102,230]. Addition of organic solvent, including ACN[143,231], ethanol[102], and dimethylsulfonate (DMSO)[232] to sample was shown to be effective in preventing non-specific adsorption loss and improved LOD to mid-to-high amol range[29] for peptides with MW < 2000 Da. This concept was extended to 3 neuropeptides in standard samples and dialysate[143]. Although promising, it remains questionable how widely applicable this approach is and whether organic additive to dialysate samples can provide enough improvement for *in vivo* detection of larger neuropeptides such as β-endorphin and orexins, where poor LC-MS sensitivity may have more complicated origin, such as multiple charge state in ESI-MS.

Another challenge for *in vivo* neuropeptide monitoring is low recovery of peptides by microdialysis probes. Previous studies have reported relative recovery from 0.28%-1.5% for β-endorphin (3467 Da), orexin A (3561 Da) and Gal (3157 Da)[5,63,75]. Ways to improve recovery include using high molecular weight cut-off (MWCO) membranes, blocking protein in perfusion media, push-pull microdialysis, and affinity-enhanced microdialysis[36,120,124,233]. While potentially effective, these methods do not prevent adsorption to the membrane itself and in some cases may complicate cLC-MS analysis. Microdialysis catheter modification has been investigated for reducing adsorption loss; however, published methods focus on reducing adsorption loss to hydrophobic membrane

and tubing surface[5,101,103]. Preventing sample loss when using an already hydrophilic membrane (such as AN69 membrane) and tubing has not been reported.

In this chapter, we evaluate and combine two methods to improve neuropeptide detection by reducing their loss during transport from brain to mass spectrometer. Adding ACN to dialysate sample was found to make LODs more similar and improved all LODs to 0.1-2 pM for 8 µL samples for a selection of 10 neuropeptides. The ACN percentage for each individual peptide was found to have an optimal value that correlated with peptide MW and retention time on a reverse phase LC column. We also improved probe recovery for several peptides by treating the dialysis membrane and fused silica tubing with polyethyleneimine (PEI). The effect appeared to be due to reducing electrostatic interaction between peptides and the microdialysis probe since modification increased recovery for peptides that carried net positive charge.

As a demonstration of utility of these approaches, we show that the method allows recovery and detection of intact orexin A and orexin B (2936 Da) from rat arcuate nucleus *in vivo*. Orexins are neuropeptides that regulate sleep-wake cycle and feeding behavior[4,234]. Monitoring their concentration *in vivo* may provide useful information on their *in vivo* processing and function. From the same samples we also detected a fragment of rat POMC that has a sequence identical to mouse β-endorphin. This result demonstrates the power of using sequence specific detection.

3.2 Materials and methods

3.2.1 Chemicals and materials

Orexin A, B, β-endorphin (mouse, rat), CCK-4, Gal, and OFQ were from Phoenix pharmaceuticals (Burlingame, CA). α-MSH, deacetylated α-MSH and $DynA_{1-17}$ were from American Peptide Company (Sunnyvale, CA). HPLC grade solvent, including water, methanol (MeOH) and ACN were purchased from Honeywell (Muskegon, MI). LC-MS grade formic acid (FA) and glass auto sampler vials, inserts were from Fisher Scientific (Waltham, MA). PEI (average Mn = 1800 by gel permeation chromatography, average MW = 2000 by light scattering, 50 wt% in H_2O) and Sub P were from Sigma-Aldrich (St. Louis, MO). Ringer'a solution consisting of 148 mM NaCl, 2.7 mM KCl, 1.2 mM $CaCl_2$ and 0.85 mM $MgCl_2$ was used as microdialysis perfusion media for both *in vivo* and *in vitro* experiments. High K^+ Ringer's solution was the same except that KCl's concentration was raised to 100 mM with NaCl concentration reduced to keep the same ionic strength. Fused silica capillaries were purchased from Molex (Phoenix, AZ) and 5 µm Alltima^{TM} C18 packing was from Grace Davison (Waltham, MA).

3.2.2 Microdialysis probe modification and *in vitro* recovery determination

Microdialysis probes for both *in vitro* and *in vivo* studies were constructed in-house in concentric style using AN69 polyacrylonitrile membrane (Hospal, Bologna, Italy) with 300 µm outer diameter (O.D.), 2 mm active membrane length. The probe inlet was connected to a section of 127 µm inner diameter (I.D.) FEP tubing with 10 µL dead volume (Zeus, Orangeburg, SC), and the outlet to a 100 µm I.D./360 µm O.D. fused silica capillary. PEI modification of the probe was achieved by immersing the probe into a stirring vial containing 5% PEI and pumping 5% PEI solution through the probe and

tubing at 0.5 µL/min for 12 h. After modification, the catheter was washed by Ringer's solution at 1 µL/min for 8 h to remove unabsorbed PEI. To measure *in vitro* recovery, the probe was placed in a stirring vial containing 1 nM peptide in Ringer's solution. Fractions were collected for 20 min while perfusing the probe at 0.5 µL/min. The collection vial was pre-loaded with the proper volume of ACN and FA to result in optimal ACN percentage and 0.5% FA in the fraction.

3.2.3 *In vivo* microdialysis sampling from freely moving rats

Adult Sprague-Dawley rats (Harlan Laboratories, Inc.) were used for all experiments. Rats were housed in a temperature and humidity controlled room with 12 h light/dark cycles with access to food and water *ad libitum*. Animals were treated as approved by the University of Michigan Unit for Laboratory Animal Medicine (ULAM) and in accordance with the National Institute of Health (NIH) Guidelines for the Care and Use of Laboratory Animals. In addition, all animal experiments were conducted within the guidelines of Animal Research Reporting *in vivo* Experiments (ARRIVE). Prior to microdialysis probe insertion, rats were anesthetized using an isoflurane vaporizer and placed in a Model 963 stereotaxic frame (David Kopf Instruments, Tujunga, CA, USA). Probes were inserted into the arcuate nucleus immediately after completion of removing excess PEI, using the following coordinates from bregma and top of skull (Franklin and Paxinos 2008): AP -2.2 mm, ML ±1.0 mm, DV -10.0 mm implanted at 3.5° angle. The probes were secured with skull screws and acrylic dental cement. Following surgery, rats were allowed to recover for 24 h with free access to food and water. Microdialysis probes were flushed at a flow rate of 2 µL/min with Ringer's solution for 1 h using a Fusion 400 syringe pump (Chemyx, Stafford, TX, USA). Perfusion flow rate was then

reduced to 0.5 µL/min and allowed to flush for an additional 1.5 h prior to baseline collections. Microdialysis fractions were collected at 20 min intervals. For each experiment, 4 fractions were collected at baselines, 3 during high-K^+ perfusion, and 2 post-stimulation. When experiments were completed, animals were sacrificed and the brains were extracted for histology.

3.2.4 Capillary LC-MS

Column and emitter tip preparation are described in detail elsewhere[38]. Briefly, a 8 cm length of 75 /360 µm I.D./O.D. fused silica capillary (frit length of ~0.5 mm in the exit end) was slurry-packed with a 5 mg/mL 5µm Alltima™ C18 slurry to a length of 4 cm. The frit end was connected to a fused silica electrospray emitter tip through a Teflon tubing connector. The tip-column assembly was connected to a dual-valve, dual-pump LC system as depicted in Figure 3.1. The system consisted of two 6-port Cheminert valves (Valco, Houston, TX), a high pressure syringe pump (Teledyne Isco, Lincoln, NE) and an Agilent 1100 HPLC pump (Santa Clara, CA). All tubing connections, including sample loop and sample needle, were made from 360 µm O.D. fused silica capillaries. Operation of the system has been described elsewhere[18]. Mobile phase A (MPA) was 0.1% FA in water and mobile phase B (MPB) was 0.1% FA in MeOH. The high pressure pump operated at 3500 psi to deliver loading solvent (0.1% FA) at 5 µL/min onto the column. The auto sampler was equipped with a 16 µL sample loop and operated at partial loop mode. 8 µL sample was loaded into the sample loop and injected, retained and rinsed on the column head using 3 min injection time and 2 min rinsing time. The LC plumbing in contact with peptide solution was highlighted in Figure 3.1. After injection the sample needle was washed by 100 µL wash solvent containing 50% MeOH, 50% water and 0.2%

FA to prevent carry-over. The HPLC pump was then switched to the column to elute peptides with the following gradient: 0.0-1.5 min: 5%-95% MPB, 1.5-7.0 min: 95% MPB, 7.0-7.1 min: 95%-5% MPB, 7.1-10.0min: 5% MPB. Elution flow rate was 150 nL/min.

The capillary system was coupled to a linear ion trap (LTQ XL, Thermo Scientific) mass spectrometer operating at positive ion mode. Peptides were detected either in MS^2 or MS^3 mode by collision induced dissociation depending on the sensitivity of each mode on individual peptide. Detection was achieved with the following parameters: spray voltage = 2.0 kV, capillary temperature = 150 ^oC, automatic gain control (AGC) on, q = 0.25, isolation width = 3 m/z, activation time = 0.25 ms, number of micro scan = 1. Fragmentation pathways of each peptide were listed in Table 3.1. To maintain ion optics for best peptide sensitivity, the linear ion trap was tuned bi-monthly by infusing 2 μM orexin A solution dissolved in 50:50 MeOH: water, 0.2% FA, and monitoring daughter ion at m/z = 854.

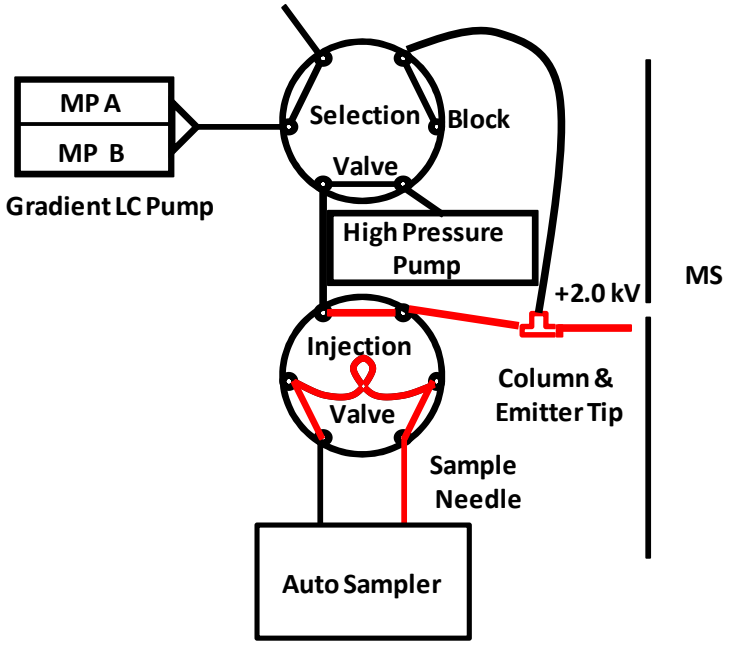

Figure 3.1 Dual pump dual valve system connection. Tubings in contact with peptides are highlighted in red. Sample needle, sample loop and connection tubing between the injection valve and column were all made from fused silica capillaries.

3.3 Results and discussion

3.3.1 Addition of organic additive to reduce post collection, pre-column peptide loss

Previous work showed that using 25 µm bore columns, 90 nL/min elution flow rates, and extensive on-column concentration with large volume injections (4-5 µL loaded onto 8 nL volume columns), it was possible to obtain detection limits as low as 0.5 pM-1 pM for enkephalins. However, detection limits were uneven, with other peptides having higher LODs such as Sub P (10 nM) and intact β-endorphin (5 nM). Subsequent study revealed that many of the peptides with poor LODs also generated significant carry-over, i.e. signals for peptide during injections of blank solutions after a sample injection (Appendix D). These observations suggested that adsorption to surfaces as peptides were transported from vial to column were causing both effects. Organic modifier added to samples had previously been shown to improve sensitivity for tryptic peptides[231,232] and 3

neuropeptides[143]. Therefore we investigated the effect of acetonitrile added at different concentrations (5-30%) to a panel of 10 neuropeptides with MW ranging from 597 to 3561 (see Table 3.1) dissolved in ringer solution.

Table 3.1 MS^2 or MS^3 pathways for selected neuropeptides. Daughter ions and granddaughter ions were selected based on intensity with direct infusion of 2 μM peptide standard. Three most intense transitions were selected for quantification unless the peptide only produced one or two predominant fragments, in which case only 1-2 daughter ions were selected.

Peptide	**M.W.**	**MS pathway**
CCK-4	596.7	597.7→580 (b4)→552(b4-CO),449(WMF-NH_3),334(WM)
OFQ	1809	453.4 ($[M+4H]^{4+}$)→536($y15^{3+}$),555($b16^{3+}$)
α-MSH	1665	556($[M+3H]^{3+}$)→513($y8^{2+}$), 687($y11^{2+}$), 544($[b13-NH_3]^{3+}$)
Deacetylated α-MSH	1623	406.8($[M+4H]^{4+}$)→458.5($y11^{3+}$)
$DynA_{1-17}$	2147.5	538($[M+4H]^{4+}$)→529.3,($b13^{3+}$) 630.0($b15^{3+}$), 668.1($b16^{3+}$)
Sub P	1347.6	450.0($[M+3H]^{3+}$)→600.3($b10^{2+}$)→254.0 (RP), 591.5 ($[b10-H_2O]^{2+}$), 946.5(KPQQFFGL-H_2O)
Gal	3164.5	528.5($[M+6H]^{6+}$)→554.7($y20^{4+}$), 581.7($a27^{5+}$), 609.7 ($y22^{4+}$)
Mouse β-endorphin	3436	688.7($[M+5H]^{5+}$)→754.4($y27^{4+}$), 805.5($y29^{4+}$) ,819.9 ($y30^{4+}$)
Orexin A	3561	713.3($[M+5H]^{5+}$)→854($[y32- H_2O]^{4+}$),858.5($[b32- H_2O]^{4+}$)
Orexin B	2936	735($[M+4H]^{4+}$)→693.5($[b27-H_2O]^{4+}$)

As shown in Figure 3.2 A and B, adding ACN to samples increased signal for all peptides tested; but, adding too much decreased signal so that each peptide had an optimal ACN percentage. We found a positive correlation of the optimal ACN concentration to both MW and retention time (Figure 3.2C and D). None of the peptides has optimal ACN percentage exceeding 25%. The maximal optimal percentage was also

observed in another study using DMSO as organic additive[232], where the observed threshold was 50% for 10 cytochrome c tryptic peptides in that study. These results can be understood by considering that increasing organic modifier decreases the tendency of a peptide to interact with solid surfaces by hydrophobic interactions during the injection process; however, adding organic modifier also increases the elution strength of the sample on the reversed phase LC columns. This in turn reduces the ability of the column to capture and stack peptide during large volume injections. Therefore peptides have an optimal concentration that increases with potential for hydrophobic interactions, as measured by retention. Because increasing molar volume increases dispersion interactions, this effect also correlates with MW.

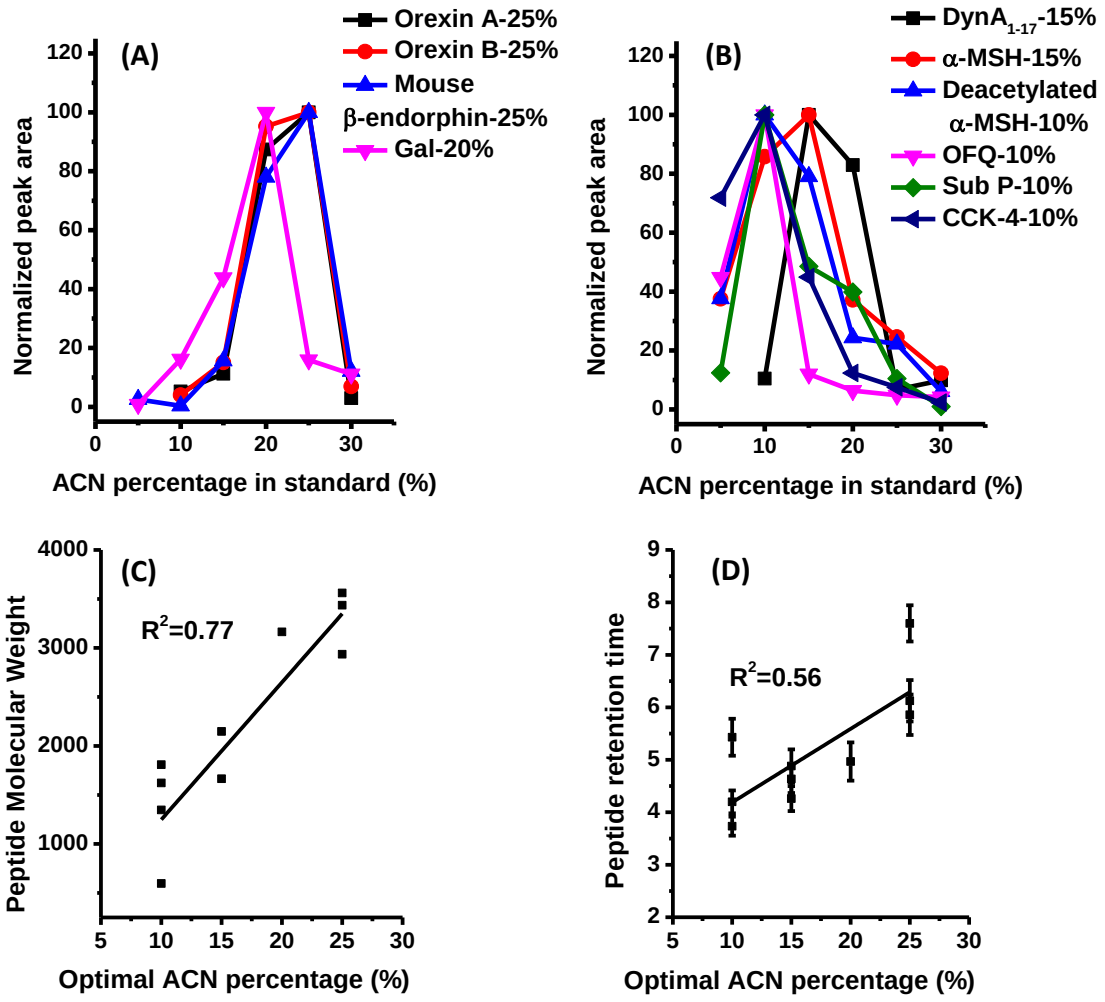

Figure 3.2 Adding ACN reduced peptide nonspecific adsorption loss prior to injection. (A), (B): Peptide signal (represented by normalized peak area averaged from triplicate injection) affected by ACN volumetric percentage at 5% interval, optimal ACN percentage for each peptide is labeled in the graph. (C): Impact of peptide molecular weight on the optimal ACN percentage of peptides. (D): Impact of peptide hydrophobicity (represented by retention time on a reverse phase column) on the optimal ACN percentage of peptides. To correlate retention time with optimal ACN percentage, ACN with 0.1% FA was used as MPB and a shallower gradient than the detection gradient was used to better separate peptides: 0-1 min: 2%-20% MPB, 1-9 min: 20-30% MPB, 9-10min: 30-90% MPB, 10-12min: 90% MPB, 12-12.1min: 90-0% MPB, 12.1-15min: 0% MPB. Graph was obtained from 9 replicated injection on three columns.

Improvement in peptide quantification was also evaluated by comparing the sensitivity and LOD for peptide standard dissolved in totally aqueous solvent and its optimal ACN concentration. Table 3.2 shows that adding organic solvent to the sample increased peptide detection sensitivity (as indicated by calibration curve slope) up to 23

fold, and decreased LOD by 1.4 to 60 fold. The biggest improvement came from the biggest peptides such as orexins and mouse β-endorphin, which are more likely to be lost due to adsorption as indicated by their optimal ACN percentage. This effect also tended to normalize the LODs giving a narrower range (0.1-2 pM) than when injecting from ringer solution with 0.5% FA (0.2-30 pM). Figure 3.3 shows that when injecting orexins and mouse β-endorphin with 25% ACN, the linearity of calibration curve (represented by R^2) increased from ~0.8 to above 0.98. Peptide signal reproducibility was also improved as indicated by the relative standard deviation (RSD) of the highest concentration injected: without ACN, the peak area RSD was as large as 70% at 200 pM for these three peptides, while injecting peptides with 25% ACN lowered the RSD down to 3% and 7% at 20 pM for β-endorphin and orexin A, and 16% at 10 pM for orexin B, respectively. Injection carry-over was also reduced from 20-50% to 1-2% when adding ACN to 25% for orexins. It should be noted that without ACN addition, orexin signal could still be observed after 3-4 blank injections (Appendix D), indicating that in addition to sample vial, the LC tubings also serve as active sites for adsorption and subsequent peptide loss.

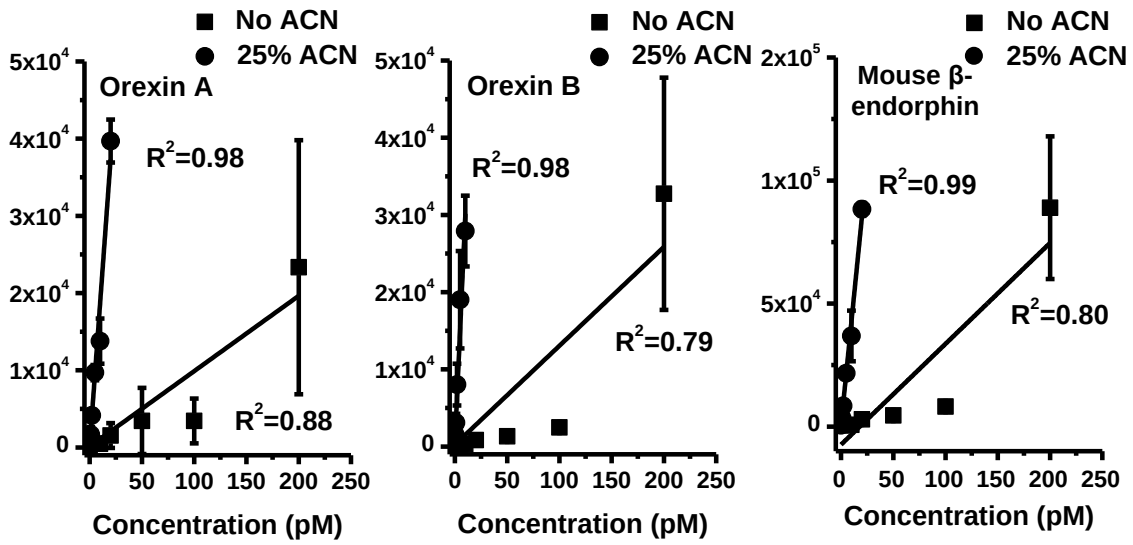

Figure 3.3 Representative calibration curve of the biggest peptides tested, injected with no or 25 % ACN added. 25% ACN calibration curve was obtained by triplicate injection of 0, 0.5, 1, 2, 5, 10, 20 pM (for orexin A and mouse β-endorphin) or 0,0.5, ,2,5,10 pM (for orexin B) peptide standard in ringer solution containing 25% v/v ACN, and 0% ACN calibration curve was done by triplicate injection of 0, 5, 10, 20, 50, 100, 200 pM peptide standard in ringer solution (0.5% FA).

Table 3.2 LOD and calibration curve slope for injections with totally aqueous standard or standard spiked with ACN to individual peptide's optimal value. LOD was calculated by using equations: LoB = $mean_{blank}$ + 1.645(SD_{blank}), LOD = LoB + 1.645($SD_{low\ concentration\ sample}$), LoB=limit of blank, SD=standard deviation. To confirm peptide detection at LOD, peptide calibration curve was made by triplicate injections of standards whose lowest concentration was close to the calculated LOD.

Peptide	Optimal ACN%	LOD with 0% ACN	LOD with optimal ACN%	Slope (pM^{-1}) with 0% ACN	Slope (pM^{-1}) with optimal ACN%
orexin A	25	30 pM	0.5 pM	98	1858
orexin B	25	5 pM	0.6 pM	128	2991
Mouse β-endorphin	25	4 pM	0.6 pM	353	4233
Gal	20	5 pM	1 pM	251	882
$DynA_{1-17}$	15	20 pM	2 pM	54	557
α-MSH	15	2 pM	0.8 pM	518	1188
SubP	10	0.5 pM	0.1pM	242	802
Deacetylated α-MSH	10	0.2 pM	0.1 pM	462	2426

CCK-4	10	1 pM	0.7 pM	56	153
OFQ	10	1 pM	0.3 pM	729	3847

3.3.2 Modifying microdialysis probe to increase peptide *in vitro* recovery

Initial *in vitro* relative recovery measurements were conducted either using in-house constructed mirodialysis probes with 2 mm length of AN69 membrane (MWCO = 80 kDa) or CMA 12 probe with 4 mm long PAES membrane (MWCO = 20 kDa). Orexins and β-endorphin recovery was lower than 1% for both probes (Table 3.3 and Figure 3.4). AN69 is a hydrophilic membrane with large MWCO[235], therefore poor peptide recovery was unlikely due to adsorption to the membrane through hydrophobic interaction or inadequate pore size. AN69 membrane carries negative charge owing to the embedded sulfonate group, while most selected peptides in this study have positive charge at pH 7.4 (Table 3.3) suggesting the possibility that electrostatic interaction affected recovery. AN69 has a positively charged version which employs physical adsorption of polycationic PEI onto the membrane[95,98], however, this version, called AN69ST, is mainly used in hemodialysis to reduce coagulation and has no demonstrated application in neuropeptide microdialysis. In addition, only switching the charge characteristic of the membrane does not result in elimination of negative potential in the other parts of the microdialysis catheter, such as silanol group on the inner wall of the fused silica capillary, which PEI is known to adsorb to[231,232]. These negatively charged sites might still cause electrostatic interaction and loss of peptides.

To modify the probe membrane and tubing at the same time, we pumped 5% PEI through the microdialysis catheter with probe attached prior to use. As shown in Figure 3.4, PEI-treatment improved recovery for 10 out of 11 neuropeptides tested and the

recovery increase was statistically significant for 7 peptides: rat β-endporpin, mouse β-endorphin, orexin B , Gal, Sub P, deacetylated α-MSH and OFQ (paired *t* test, $p < 0.05$). CCK-4 was the only peptide which showed slight decrease in recovery after treatment, and it carries zero net charge at pH 7.4, while all other peptides carry positive charge. Table 3.3 shows the value of relative recovery and recovery improvement after PEI treatment, it displays a general trend that smaller peptides with lower charge tend to have less improvement in recovery, while bigger peptides with larger net positive charge benefit more from the PEI treatment (Appendix D).

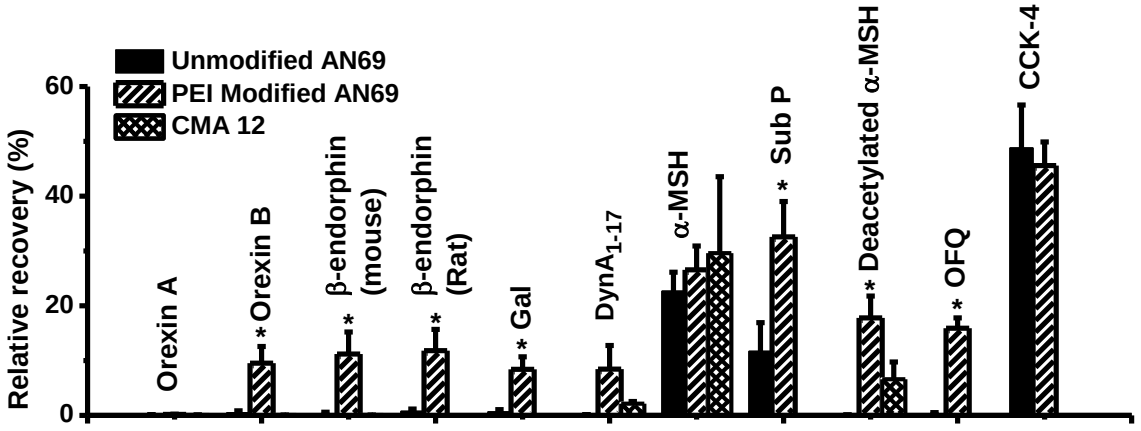

Figure 3.4 *In vitro* recovery comparison of in-house constructed AN69 probe treated or untreated by PEI solution. N = 4 for each type of probe. PEI modification significantly increased recovery for orexin B, mouse β-endorphin, rat β-endorphin, Gal, Sub P, Deacetylated α-MSH and OFQ (*p<0.05) . *In vitro* relative recovery values for orexins, mouse β-endorphin, α-MSHs and $DynA_{1-17}$ using 4mm CMA 12 probe (n=3) were also plotted. Error bar represents standard error of mean (SEM).

Table 3.3 *In vitro* recovery value for each peptide, peptide size and calculated net charge at pH 7.4. Net charge was estimated using equation $\mathbf{z} = \sum_i \boldsymbol{Ni} \frac{10^{pkai}}{10^{pH}+10^{pkai}} + \sum_j \boldsymbol{Nj} \frac{10^{pH}}{10^{pH}+10^{pkaj}}$, where N represents number of residue/termini and i and j represent basic or acidic residue/termini, respectively.

Peptide	Recovery – untreated probe (n = 4) (%)	Recovery— PEI treated probe (n = 4) (%)	Improvement in relative recovery (%)	Peptide MW	Net charge at pH 7.4
$DynA_{1-17}$	0.1 ± 0.04%	8 ± 4%	8300%	2148	+4.0
OFQ	0.3 ± 0.2%	16 ± 2%	5000%	1809	+4.0
Deacetylated α-MSH	0.7 ± 0.04%	18 ± 4%	3600%	1623	+2.1
β-endporpin (mouse)	0.3 ± 0.3%	11 ± 4%	3400%	3436	+4.0
orexin B	0.5 ± 0.3%	10 ± 3%	2700%	2936	+4.0
β-endporpin (rat)	0.8 ± 0.4%	12 ± 4%	1400%	3466	+4.0
Galanin	0.7 ± 0.4%	8 ± 2%	1200%	3165	+1.2
Sub P	12 ± 5%	33 ± 6%	180%	1348	+3.0
orexin A	0.08 ± 0.05%	0.2 ± 0.03%	130%	3561	+1
α-MSH	23 ± 3%	27 ± 4%	17%	1665	+1.1
CCK-4	49 ± 8%	46 ± 4%	-7%	597	0

3.3.3 Detecting neuropeptide using unmodified and PEI-modified AN69 membrane probe

To validate this method for *in vivo* study, neuropeptide orexins and β-endorphin were selected to be monitored from rat arcuate nucleus. Orexins regulate wakefulness and feeding behavior[4]. Orexin B has not been measured under *in vivo* setting, while orexin A has been measured in a few cases[5,82]; however, quantification has only been achieved with immunoassays which lack sequence specificity. Therefore it remains unclear whether intact orexin sequence can be detected *in vivo*. β-endorphin was previously

reported detection from this brain region[61]. Orexin A, orexin B, and β-endorphin can be readily assayed simultaneously by the LC-MS assay since they have the same optimal ACN%.

A pilot study that compared analysis of dialysate from unmodified AN69 probe (n = 2) and PEI-modified AN69 probes revealed interesting discoveries: 1) PEI-modified probe yielded baseline signal for orexin B, while its signal from unmodified probe was much lower. Orexin A's signal intensity was more comparable between unmodified probe and modified probe. This finding was in agreement with our previous *in vitro* recovery comparison that PEI treatment significantly enhanced recovery for orexin B, but not for orexin A; 2) PEI-modified probe also allowed recovery and detection of a peptide that has identical MS^2 transition to mouse β-endorphin from rat brain; but, this peptide was not detected from rats implanted with unmodified probe (Figure 3.5A). This also agrees with *in vitro* probe recovery data that PEI modification resulted in 32 times higher recovery for β-endorphin than unmodified probe. Therefore, PEI-modified probes were used for further *in vivo* study of peptides since it recovered higher *in vivo* signal. Rat β-endorphin, however, was not detected in the initial pilot study using either probe. Since mouse and rat β-endorphin possess different amino acid sequence (Ala26→Val26), we investigated the potential origin of the mouse β-endorphin sequence in rat brain by searching its sequence against rodent data base in Uniprot, and found this sequence in an unreviewed rat POMC (entry: Q8K422), which had experimental evidence of existence at transcript level. The discovery of mouse β-endorphin sequence in rat brain showed capillary LC-MS^2's high sequence specificity, without MS^2, this difference might not be able to be distinguished using immunoassay based methods.

The validity of external calibration was also examined for its capability of correctly monitoring *in vivo* concentration change. Comparison between dialysate spiked with 0-10 pM peptides to that of a standard calibration curve revealed no significant difference for mouse β-endorphin and orexin B, suggesting that matrix effect was negligible and external calibration could be used for quantifying these two peptides. For orexin A, however, the standard addition curve had flatter slope compared to standard curve, indicating matrix effect suppressed orexin A's signal at higher concentration, and the quantification can potentially be improved by including isotopically labeled orexin A as internal standard (Figure 3.5 B).

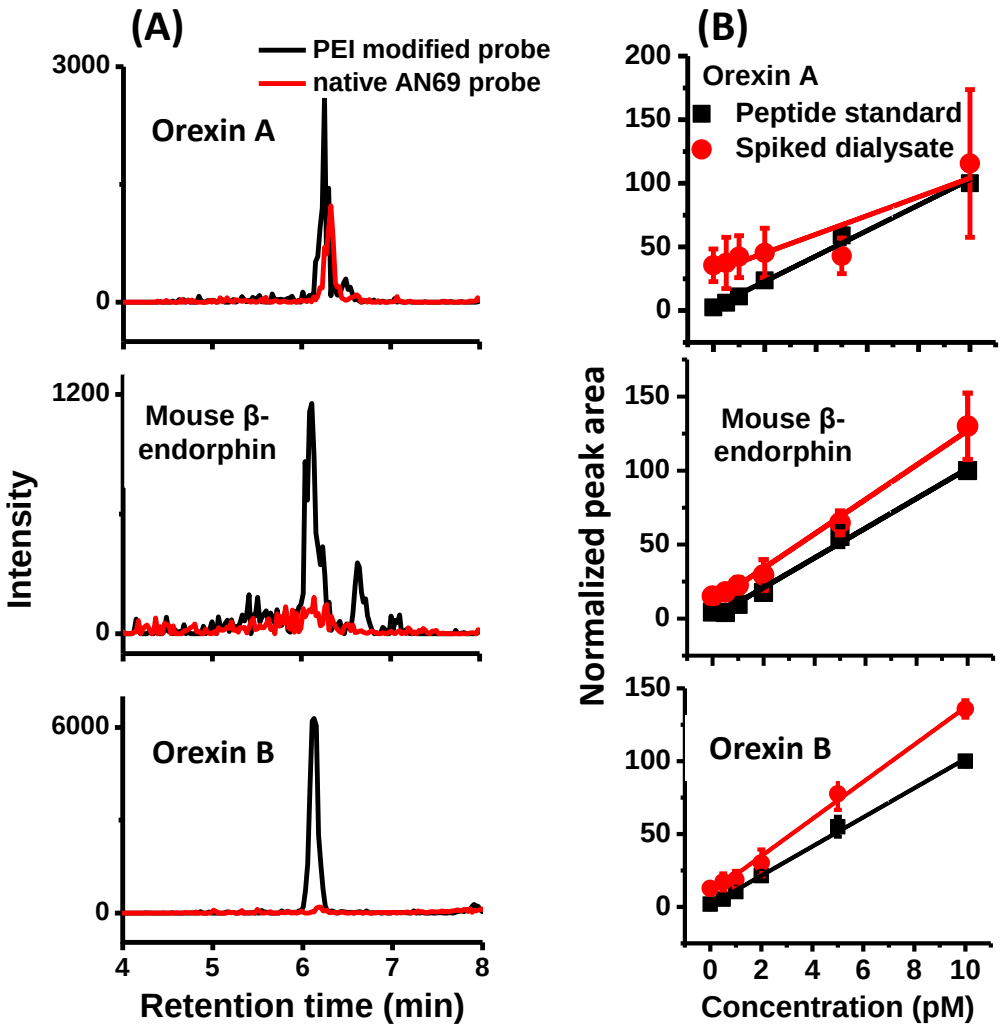

Figure 3.5 Detecting orexins and mouse β-endorphin from rat arcuate nucleus. **(**A) Overlaid, reconstructed ion chromatogram (RIC) for orexin A, β-endorphin and orexin B from *in vivo* dialysate collected using either PEI modified AN69 membrane or unmodified AN69 membrane. (B) Comparison between standard addition curve and standard calibration curve. 60 µL dialysate was collected and spiked with proper volume of ACN and FA to produce 25% ACN and 0.5% FA in final sample, aliquoted to 6 vials and spiked with peptide standard to a final concentration of 0, 0.5, 1, 2 ,5,10 pM. The peptide signal from spiked dialysate was normalized to the peptide signal from highest standard (10 pM), and this experiment was repeated in triplicates using of 3 rats.

3.3.4 *In vivo* neuropeptide monitoring in rat arcuate nucleus

To test the approach for monitoring the neuropeptides *in vivo*, we monitored orexins and β-endorphin during a treatment with high K^+, a method that can stimulate neuronal depolarization and exocytosis (Figure 3.6 A). Baseline concentration of orexins and mouse β-endorphin were detectable, however, rat β-endorphin was not detected from any of the 6 rats, in either baseline or K^+ stimulated fractions, despite good *in vitro* recovery of the probe (12 ± 4%) and low LOD (0.8 pM). The fact that rat β-endorphin was previously detected using ELISA from this brain region[61] but not detected in this study can be possibly explained by capillary LC-MS's higher sequence specificity towards intact rat β-endorphin, which suggests that the previously detected β-endorphin could be another molecule that had similar immunoreactivity. Neuropeptides' concentration in dialysate and extracellular basal concentration are listed in Table 3.4. Orexin A's extracellular concentration was estimated to be 1500 ± 350 pM in this brain region, while orexin B's concentration was only 23 ± 6 pM. The difference here may be contributed by the peptides' different stability against metabolism[7,84].

Table 3.4 Basal concentration of peptide orexins and mouse β-endorphin (n = 6). Basal dialysate concentration was calculated by external calibration and corrected for dilution of dialysate by adding ACN and formic acid. Basal extracellular concentration was estimated according to average *in vitro* recovery.

Peptide	Basal ± SEM dialysate concentration (pM)	Basal ± SEM extracellular concentration (pM)
Orexin A	3.0 ± 0.7	1500 ± 350
Orexin B	2.3 ± 0.6	23 ± 6
Mouse β-endorphin	2.5 ± 0.3	23 ± 3

100 mM K^+ stimulation caused increase in orexin A and B release, but not in mouse β-endorphin (Figure 3.6 A), which might indicate the non-synaptic release nature of this peptide fragment. For orexins, the increase was only statistically significant ($p < 0.05$) in the third K^+ stimulation fraction. The orexin level was also kept elevated 1-2 fractions post K^+ stimulation. To investigate the origin of slow response to K^+ stimulation, *in vitro* probe response to step concentration change was measured. Figure 3.6 B showed that it took 3 fractions for neuropeptide level to stabilize upon a step change of sampling solution concentration from 1 nM to 6 nM, this observation was in accordance with the *in vivo* data that the third K^+ fraction had highest peptide level. After sampling solution's peptide concentration dropped from 6 nM to 0 nM, peptide concentration in the dialysate fraction showed slow decrease, and did not reach balance after 80 min. Therefore the delay in peptide concentration increase under K^+ stimulation was likely caused by the slow response of the probe. Since the microdialysis probe and outlet tubing had a dead volume of ~7 μL, the response time of the microdialysis system can potentially be improved by using lower-dead-volume probe and outlet tubing to allow more column volume to be flushed using fewer fractions.

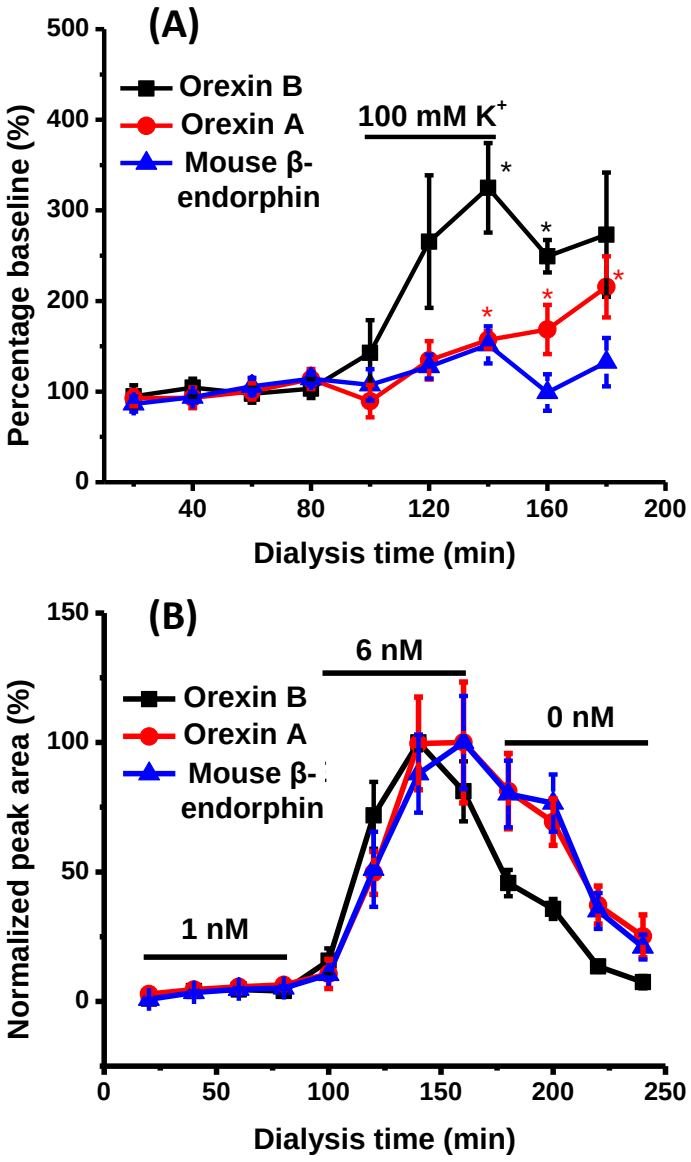

Figure 3.6 *In vivo* K^+ stimulation profile and in vitro probe response to co **(**A) K^+ stimulation profile for orexin A, β-endorphin and orexin B from in vivo dialysate collected using PEI modified probe. N=6, error bar represents SEM. **t* test, $p<0.05$. (B) *In vitro* probe response to concentration change. Probe was sequentially placed in stirring vial containing 1 nM, 6 nM and 0 nM peptide standards. Fraction collection started immediately after the catheter's dead time. Four fractions were collected from each concentration. N = 4 probes, error bar represents SEM.

3.3.5 Dialysate stability during storage

One challenge faced by neuropeptide *in vivo* monitoring is peptide stability after sample collection. Previous study showed decreased neuropeptide signal after storage in -80 ^{o}C for 24 h, and acidifying dialysate was reported to extend the storage period for enkephalins and neurotensin to 4 days[18]. In our study, we found that storing dialysate at its optimal ACN percent with 0.5% FA also helped to stabilize orexins and mouse β-endorphin signal up to day 3 post sample collection (Figure 3.7). The elongated storage time offers better flexibility of the analytical method when many dialysate fractions are generated within one experiment.

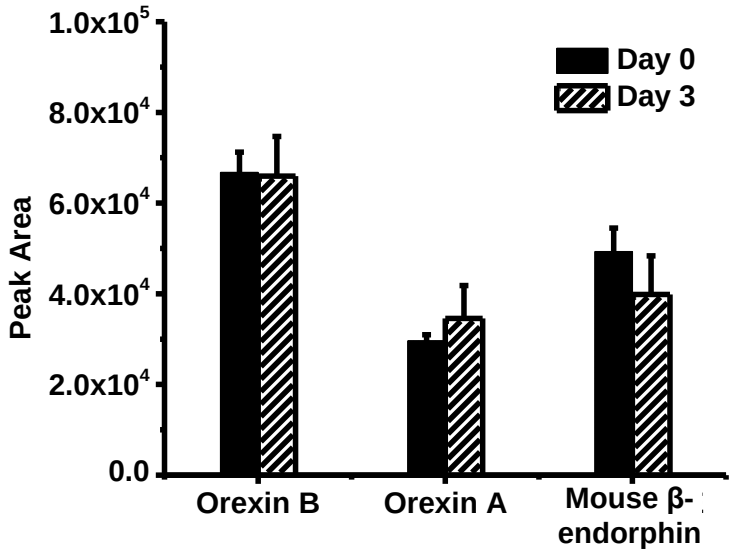

Figure 3.7 Neuropeptide stability after -80 ^{o}C storage for 3 days. Dialysate was collected from two rats and pooled, spiked with 1 nM peptide standard to a final concentration of 10 pM, and aliquoted to auto sampler vials. 4 vials were chosen in random for analysis on day 0 to day 3 to examine neuropeptides' stability over storage.

3.4 Conclusion

In this study we have successfully demonstrated *in vivo* detection of large neuropeptides including orexin A, orexin B and a rat POMC fragment which has identical sequence as mouse β-endorphin. This was achieved by enhancing cLC-MS's sensitivity using organic modifier to reduce peptide adsorption loss, and by modifying the probe to reduce electrostatic interaction and increase microdialysis recovery. With these improvements we were able to detect intact orexins and mouse β-endorphin from *in vivo* dialysate at low pM level. We also demonstrated potential applicability of this method to 7 other peptides which also benefit from the organic modifier strategy. Further improvement in quantification and sampling response is possible by including isotopically labeled peptide internal standard and using probe/tubing that has lower dead volume.

Chapter 4

Development of a signature peptide method for BDNF detection with picomolar detection limit

4.1 Introduction

Signature peptide method is an emerging substitute for enzyme linked immunosorbent assay (ELISA) in protein quantification. This method detects protein by measuring one or several of its peptide fragments produced from enzymatic digestion (usually trypsin) of the protein using liquid chromatography-mass spectrometry (LC-MS)[236]. Comparing to immunoassays which detects a single analyte, the signature peptide method can simultaneously quantify multiple proteins from one sample[237]. In addition, signature peptide method can potentially achieve ultrahigh sensitivity with LOD down to amol range when using cLC-MS[18]. Absolute quantification (AQUA) is possible by using isotopically-labeled internal standard[167].

Although quantification of low abundance protein at low amol range is possible, the development of such signature peptide method is usually challenging. The presence of protein matrix in the sample can interfere with signature peptide detection and quantification by generating highly abundant peptide fragments from other proteins[148]. Sample preparation such as immunodepletion[183], organic solvent precipitation[170] and immunocapture[184] can simplify mixtures to facilitate target protein detection. After extensive fractionation, low-to-mid amol LOD could be achieved[185,188]. Another issue is

that at trace concentrations, low protein digestion efficiency and incomplete digestion can result in low signature peptide production and reduced sensitivity. This issue is more profound for low abundance protein digestion because of Michaelis-Menten kinetics[238] of proteases such as trypsin, meaning low substrate (protein) concentration leads to lower digestion rate and even termination of digestion before completion due to protease self-digestion. Increasing protease concentration has been applied for improving digestion efficiency at low protein concentration, for example, an unconventionally high enzyme-to-protein ratio (4000:1) was needed to digest N-terminal prohormone of brain natriuretic peptide at its limit of quantification (17 pM)[186]. Incomplete digestion can also arise from protein structures that affect the accessibility of tryptic sites. In such case, optimal denaturation protocol of the analyte protein must be developed[177]. In addition, different digestion protocols[239] and protease[173] may also affect digestion efficiency, therefore these factors must be evaluated to enable efficient signature peptide production. However, such studies are not frequently performed and the denaturation, reduction, alkylation and digestion (DRAD) protocol is not always optimized for protein of interest at low concentration.

In this study, we aimed to develop an efficient DRAD protocol for brain derived neurotrophic factor (BDNF) at trace concentrations. BDNF is selected as the model protein for two reasons. First, BDNF is highly stable in structure, containing 70% β-sheet, 20% β-turn[240] and a cystine knot[241]. The protein exists as tightly folded homodimer in physiological condition, which is stable even in 8 M urea[240]. Exploration for an optimal DRAD protocol for BDNF may provide insights in developing signature peptide method for structurally related proteins, especially for the neurotrophin family. Second, BDNF is

an important neurotrophin that plays critical role in neuron cell survival, differentiation and neuronal plasticity[92]. Measuring *in vivo* concentration of BDNF can provide important information regarding location and mechanism of its modulation function in the living brain, however its extracellular concentration in the brain is low pM and challenging to measure[32,100]. Currently all BDNF *in vivo* detections are achieved by ELISA, which can reach LOD as low as 0.6-1 pM (mass LOD 60-100 amol). A signature peptide method with comparable LOD may serve as promising alternative for ELISA because of its potential in multiplexing.

We conducted a systematic study to evaluate the enzyme selection, denaturing condition and enzyme concentration to achieve highly sensitive detection of BDNF. We discovered that chymotrypsin had higher signature peptide yield than trypsin; and immobilized chymotrypsin yielded better signature peptide signal than solution phase digestion. In addition, a preconcentration step during the denaturation, reduction and alkylation process was found to be necessary in yielding higher signature peptide signal. Combining all the optimization during the digestion and LC-MS analysis process, BDNF was able to be digested at 5 pM. When using the optimal DRAD protocol for BDNF, LOD was approximately 5 pM for BDNF, neurotrophin-3 (NT-3) and 10 pM for glial cell derived neurotrophic factor (GDNF) from 8 µL digest, correspsonding to 40-80 amol injected onto the column. This result shows that signature peptide method might be a promising alternative to ELISA to detect several low abundance neurotrophins from one sample fraction with high sensitivity.

4.2 Materials and methods

4.2.1 Chemical and materials:

Recombinant BDNF (rat, human, mouse, sequence MHSDPARRGELSVCDSISE WVTAADKKTAVDMSGGTVTVLEKVPVSKGQLKQYFYETKCNPMGYTKEGCRG IDKRHWNSQCRTTQSYVRALTMDSKKRIGWRFIRIDTSCCTLTIKRGR), NT-3 (rat, human, mouse, sequence MYAEHKSHRGEYSVCDSESLWVTDKSSAIDIRGHQVTV LGEIKTGNSPVKQYFYETRCKEARPVKNGCRGIDDKHWNSQCKTSQTYVRALTS ENNKLVGWRWIRIDTSCVCALSRKIGRT) and GDNF (rat, sequence MSPDKQAA ALPRRERNRQAAAASPENSRGKGRRGQRGKNRGCVLTAIHLNVTDLGLGYETK EELIFRYCSGSCEAAETMYDKILKNLSRSRRLTSDKVGQACCRPVAFDDDLSFLD DSLVYHILRKHSAKRCGCI) were from Peprotech (Rocky Hill, NJ). α-Chymotrypsin (from bovine pancreas, ≥40 units/mg protein), trypsin(from bovine pancreas, ≥10,000 BAEE units/mg protein), dimethyl sulfoxide (DMSO), guanidine, urea, β-octyl-D-glucopyranoside (BOG), iodoacetamide (IAM) and tris(2-carboxyethyl)phosphine (TCEP) were from Sigma-Aldrich (St Louis, MO). Immobilized chymotrypsin gel and 10× digestion buffer (1M triethylamine) was from Princeton Separations (Freehold, NJ). LC-MS grade formic acid was from Fisher Scientific (Waltham, MA), LC grade ACN, MeOH and water were from Honeywell (Muskegon, MI), 5 µm Alltima C18 packing was from Grace Davidson (Columbia, Maryland) and fused silica capillary with 360 µm outer diameter (O.D.) was purchased from Molex (Lisle, IL).

4.2.2 Protein denaturation and digestion

Protein was dissolved in 10 µL artificial cerebrospinal fluid (145 mM NaCl, 2.68 mM KCl, 1.10 mM $MgSO_4$,1.22 mM $CaCl_2$, 0.50 mM NaH_2PO_4, and 1.55 mM Na_2HPO_4, pH

7.4) and concentrated to dryness using Eppendorf Vacufuge (Mt Laurel, NJ). 1 µL solution containing 0.02% BOG, 15 mM TCEP and 75 mM IAM was added to the vial. The vial was incubated in dark for 1 h with sonication to achieve denaturation, reduction and alkylation of the protein. The protein was then diluted with 18 µL digestion buffer containing 70% (v/v) 100 mM triethylamine (pH 8.0) and 30% (v/v) ACN. 1 µL solution containing free chymotrypsin (for solution phase digestion) or immobilized chymotrypsin with equivalent enzyme concentration to the free chymotrypsin (for chymotrypsin bead digestion) was added to the solution. The reaction was allowed to proceed overnight at 30 ^{o}C in a water bath (for solution phase digestion) or at room temperature on a rotary shaker (for chymotrypsin bead digestion), and quenched by addition of 0.5 µL 10% FA. The resulting supernatant from chymotrypsin bead digestion was transferred to a new vial and the digest was dried in vacufuge and re-suspended in 10 µL 0.5% FA for LC injection.

4.2.3 Signature peptide LC-MS analysis

The 75 µm inner diameter reverse phase capillary LC column and electrospray emitter tip assembly was made in-house with procedures detailed in our previous publications[19,38]. The column was connected to the LC-MS system which consisted of: a high pressure syringe pump (Teledyne Isco, Lincoln, NE) for fast sample loading; an Agilent 1100 HPLC pump (Santa Clara, CA) with flow-splitting for nano-flow elution; and two 6-port Cheminert valves (Valco, Houston, TX) switching between sample loading/injection and LC injection/elution. Mobile phase A (MPA) was 0.1% FA in water and mobile phase B (MPB) was 0.1% FA in MeOH. The auto sampler (WPS-3000, Thermo Scientific) was incorporated with a 16 µL sample loop and operated at partial

loop mode. 8 µL of digest was injected directly to the analytical column with a program containing 4 min injection time and 2 min rinsing time. After injection the sample needle was washed by 100 µL wash solvent containing 50% MeOH, 50% water and 0.2% FA to prevent carry-over, and peptides were eluted with the following gradient: 0.0-5.0 min: 5%-95% MPB, 5.0-10.0min: 95% MPB, 10.0-10.1 min: 95%-5% MPB, 10.1-13.0min: 5% MPB. Elution flow rate was 150 nL/min.

The LC system was coupled to a linear ion trap (LTQ XL, Thermo Scientific) mass spectrometer operating at positive mode, and peptides were detected in MS/MS mode by collision induced dissociation. Detection was achieved with the following parameters: spray voltage = 2.0 kV, capillary temperature = 150 ^{o}C, automatic gain control (AGC) on, q = 0.25, isolation width = 3 m/z, activation time = 0.25 ms, number of micro scan = 1, normalized collision energy = 35%.

To identify signature peptide, high concentration (500 nM) protein digest with 2:1 protein-to-enzyme ratio was injected using the LC-MS set up and detected by data dependent "triple play" mode. Signature peptide was selected with the following criteria: (1) the peptide has good signal at both MS and MS/MS mode; (2) BLAST search against rodent data base shows that only the analyte protein contains the peptide sequence. The 500 nM digest was also diluted by 0.5% FA to concentrations ranging from 100 pM to 2 nM, and injected in triplicate to confirm that the selected peptide has good MS sensitivity and injection reproducibility at low concentration.

4.3 Results and discussion

4.3.1 Selection of protease for signature peptide production

In initial digestion experiment using trypsin, fragment ALTMDSK and TTQSYVR were selected as potential signature peptide according to the criteria described in the experimental session. Injection of 100 pM digest gave no signature peptide signal, although injection of diluted high concentration tryptic digest confirmed detection of these peptides at 100 pM (Figure 4.1A). This indicated that the poor signal of tryptic signature peptide came from low peptide yield of the digestion reaction at low concentrations, not the low LC-MS sensitivity of these peptides. In contrast to tryptic peptides, a peptide fragment produced by chymotrypsin digestion showed good signal when BDNF was digested at 100 pM (Figure 4.1A), therefore chymotrypsin was selected as protease for BDNF signature peptide method. The MS^2 spectrum of the chymotryptic peptide EKVPVSKGQLKQY is in Figure 4.1B.

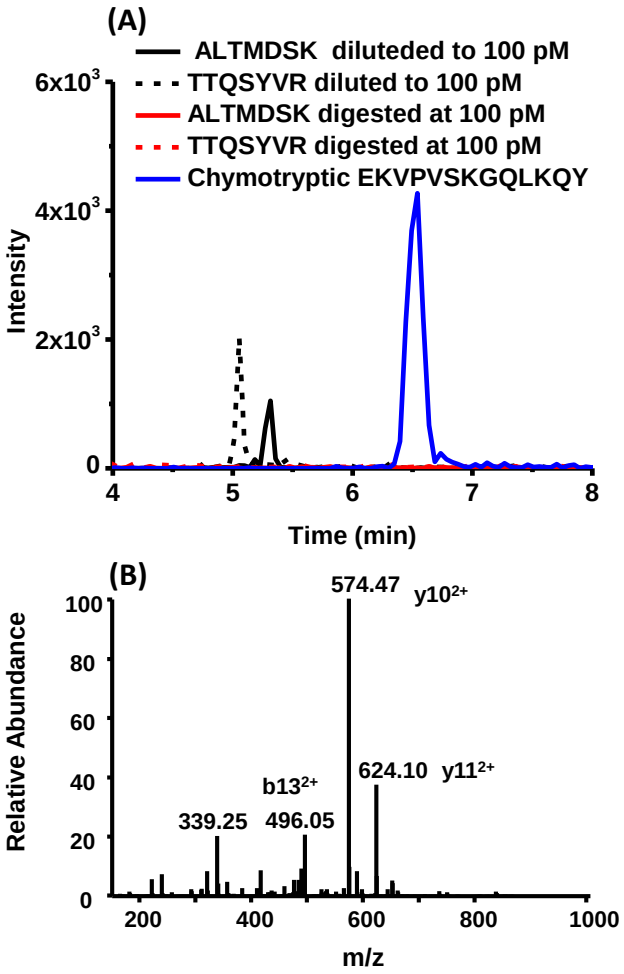

Figure 4.1 Selection of protease for BDNF digestion. (A) Overlaid reconstructed ion chromatogram (RIC) of tryptic peptide ALTMDSK and TTQSYVR and chymotryptic peptide EKVPVSKGQLKQY when 100 pM BDNF digest was injected. BDNF was digested at 100 pM (red chromatograms and blue chromatogram) or digested at 500 nM then diluted to 100 pM (black chromatograms). MS/MS pathway for ALTMDSK was: 383.43 ($[M+2H]^{2+}$)→ 234.15 (y2),514.36(b5-H_2O), 581.28 (y5); for TTQSYVR was: 427.65($[M+2H]^{2+}$)→418.96(b4), 524.28 (y4), 652.42(y5). (B) MS^2 spectrum of chymotryptic peptide EKVPVSKGQLKQY.

The poor tryptic signature peptide yield could be associated with the tightly folded homodimer structure of BDNF[240]. This could have potential impact on the accessibility of cleavage site to protease, and eventually on the yield of certain peptide fragment. Visualization of the structure of a dimer protein containing BDNF (visualization tool: PyMol, protein ID: 1bnd) reveals that its potential tryptic signature peptides sequences all

locate in the β-turn structure, while the chymotryptic peptide sequence is in a region containing mostly random coil, which can possibly explain our observation that chymotrypsin digestion resulted in much higher signature peptide signal.

4.3.2 Evaluation of denaturing condition

Protein denaturation is necessary to achieve complete digestion and the optimal denaturing condition is protein-dependent[177]. Denaturation can be achieved by using high concentration chaotropic agents such as 6 M guanidine and 8 M urea[242,243], or surfactant such as sodium dodecyl sulfate (SDS)[177], or organic solvent such as ACN and MeOH[244,245]. Denaturation is followed by reduction of disulfide bond and alkylation of free cysteine using reducing and alkylation reagents such as TCEP and IAM. The resulting protein solution requires either extensive dilution or clean-up to reduce the concentration of denaturant to preserve protease activity. However, the dilution and clean-up procedures are not favored in low-abundance protein digestion because of even lower digestion rate[238] and potential protein loss during the clean-up procedure. Alternatively, protein can be unfolded by heat which does not introduce additional denaturant that compromises protease activity[179]. In many low abundance protein-signature peptide studies, proteins are also digested directly without denaturation[246].

Based on these considerations, we initially tested four different denaturing conditions on 100 pM BDNF dissolved in 10 µL aCSF: (1) direct digestion without denaturing the protein; (2) digestion after heating the protein at 90 ^{o}C for 1 h; (3) digestion after heating the protein with the presence of TCEP and IAM at 90 ^{o}C for 1 h; (4) denaturing, reducing and alkylating dried protein in 1 µL 0.02% BOG containing TCEP and IAM and diluting it to 20 µL for digestion. In all the four conditions, protein concentration during digestion

were kept at 50 pM (1:1 dilution of starting protein standard) to eliminate possible impact of protein concentration on digestion efficiency.

Figure 4.2 A shows that directly digesting protein without denaturation step produced signature peptide, while heating the protein did not help in increasing its signal, and the presence of TCEP and IAM in the heat-denatured sample dramatically decreased signature peptide signal. This could be due to chymotrypsin deactivation when high concentration of TCEP and IAM were still in the digestion mixture, or IAM modification of BDNF at active sites such as lysine or glutamic acid of the signature peptide sequence[247], which can result in different peptide mass. Concentrating BDNF before denaturation and then diluting it for digestion produced significantly higher ($F=40.686$, $P<0.0001$, one way ANOVA test) signature peptide signal. This may be attributed to the high concentrations of TCEP and IAM during the denaturation, reduction and alkylation step which could effectively reduce and alkylate BDNF to prevent it from refolding, and their lower concentration during the digestion step which maintained chymotrypsin activity. Therefore, in subsequent experiments, 10 µL of BDNF solution was first concentrated to 1 µL for denaturation, reduction and alkylation, followed by dilution to 20 µL for digestion.

In addition to 0.02% BOG, we also tested 0.1% BOG, 6M guanidine and 93% DMSO as denaturants. BOG is a non-ionic surfactant that is used to solubilize membrane protein[248]. It is technically "non-denaturing" but previous study had used it in combination with sonication to dissolve protein prior to reduction and alkylation[249] for signature peptide method using chymotrypsin. 6 M guanidine was reported to fully unfold BDNF while 8 M urea failed to[240]. High concentration DMSO was also reported

to be able to fully unfold protein[250]. 1 µL mixture containing one of the above denaturants, 15 mM TCEP and 75 mM IAM was used to redissolve dried BDNF solution for denaturation. Results showed that 0.1% BOG and 93% DMSO gave comparable signature peptide signal to 0.02% BOG; however, with bigger signal variation. Surprisingly, 6M guanidine gave the lowest signature peptide signal. Removing guanidine by extracting the protein using C18 spin column prior to digestion partially restored the signature peptide signal. Therefore the low signature peptide signal could be due to residual guanidine in the digestion mixture which either caused matrix effect or deactivated chymotrypsin. Compared to the protein samples to which no denaturant was added, 0.02% BOG did not yield significantly higher signature peptide signal (unpaired t-test, p = 0.1623). The statistical insignificancy may origin from the small replicate number of each denaturant (n = 4) and large relative standard deviation within each group (34% for 0.02% BOG, 61% for no denaturant group). Based on the fact that 0.02% BOG gave 70% higher averaged peak area, it was selected as denaturant for the following experiments.

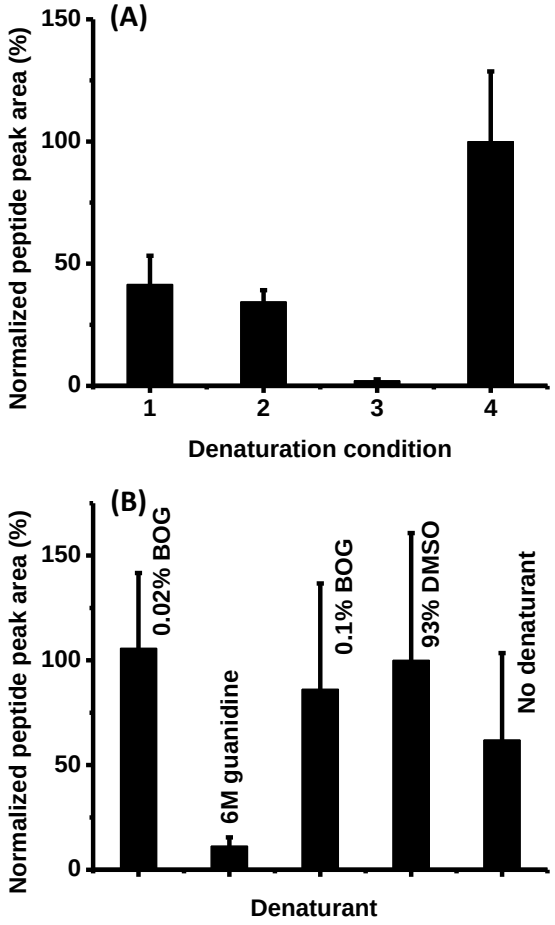

Figure 4.2 Evaluation of denaturation condition. (A) Selection of denaturation protocol for 10 µL protein standard containing 100 pM BDNF. 1: BDNF digested directly without denaturation. 2: BDNF denatured by heating at 90 ^{o}C for 1 hour. 3: BDNF denatured by heating with 10 mM TCEP and 50 mM IAM at 90 ^{o}C for 1 hour. 4: BDNF dried and dissolved in 1 µL buffer containing 0.02% BOG, 15 mM TCEP and 75 mM IAM, sonicated in dark for 1 h and then diluted to 20 µL for digestion. 6 replicates were digested and injected for each condition. (B). Selection of denaturant using protocol 4, 15 mM TCEP and 75 mM IAM was dissolved in 0.02% BOG, 6M guanidine, 0.1% BOG, 93% (v/v) DMSO, or water to re-dissolve the dried protein standard. 4 replicates were digested and injected for each denaturant. The final solution pH for digestion was checked before addition of chymotrypsin to make sure it is approximately 8.0.

4.3.3 Effect of enzyme concentration

In our initial investigation, 100 pM BDNF was reduced and alkylated and then diluted to 50 pM by adding chymotrypsin at a final concentration of 1 nM (enzyme: protein = 20:1). We compared the effect of adding chymotrypsin at once at the beginning of

digestion or every 8 hours for a total of 24 h. Although the final enzyme concentration was 1 nM in both procedures, adding fresh aliquot every 8 hours produced signature peptide signal that was 3 times higher (Figure 4.3A). This result indicates that chymotrypsin might have been deactivated before most BDNF molecule was digested, and supplementing the digestion mixture with fresh enzyme helped to continue the reaction. Adding fresh enzyme every 8 hours can be laborious, therefore other options were also explored, including higher chymotrypsin concentration[238] and chymotrypsin immobilized on beads since the immobilized enzyme has higher local concentration on the bead surface. As shown in Figure 4.3A, a 100:1 enzyme-to-protein ratio gave 2 times higher signal and immobilized chymotrypsin showed 3.5 times increase in signal. Since the equivalent enzyme concentration was still 1 nM in the immobilized chymotrypsin procedure, the enhancement in signature peptide production is likely related to the higher local enzyme concentration that resulted in more complete BDNF digestion before chymotrypsin was deactivated.

The effect of chymotrypsin bead concentration on the signature peptide signal was also studied by varying chymotrypsin bead concentration from 20 pM to 50 nM in 50 pM protein standard (enzyme to protein ratio from 0.4:1 to 1000:1) and evaluating the resulting signature peptide signal. This experiment revealed that the signature peptide signal leveled off above 2 nM chymotrypsin (equivalent to free concentration), corresponding to a 40:1 enzyme-to-protein ratio (Figure 4.3B). A slight decrease of signal at chymotrypsin bead concentration higher than 2 nM was attributed to production of a high concentration of chymotrypsin autolysis fragment KIAKVF (m/z=353.54) which co-eluted with signature peptide and suppressed its signal (Figure 4.3C).

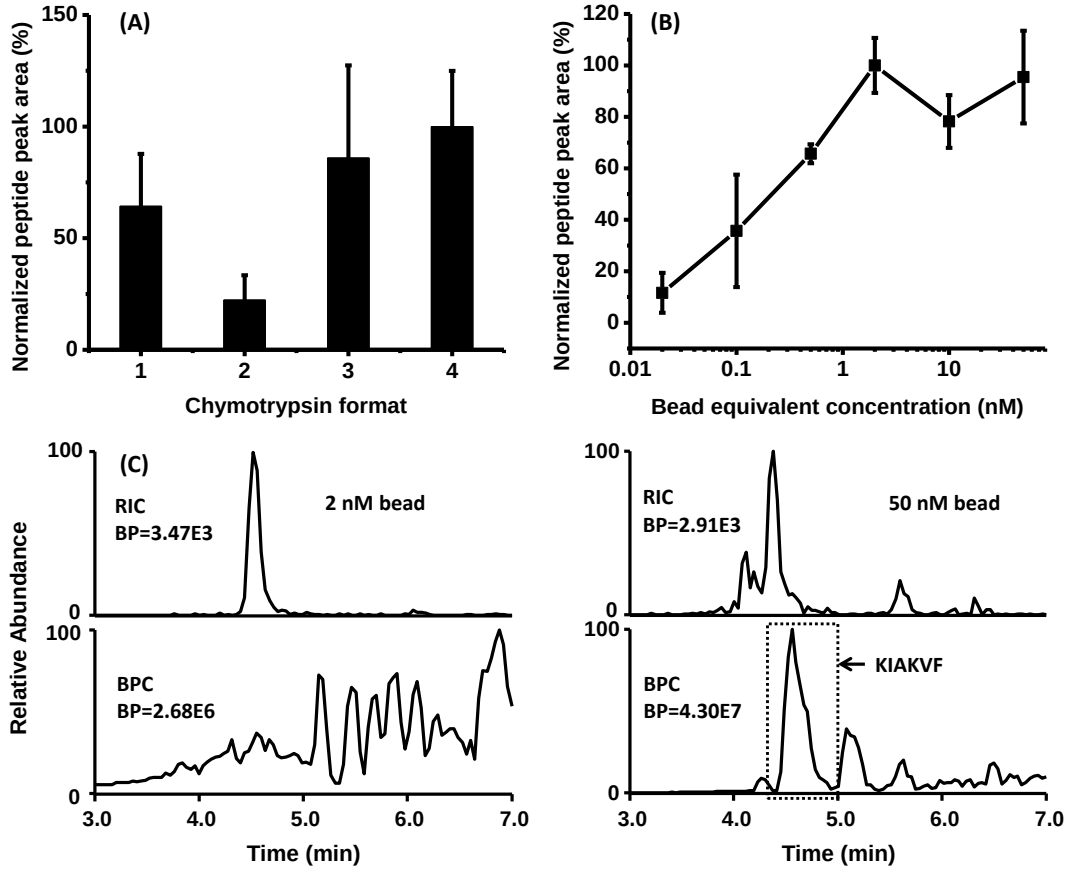

Figure 4.3 Determination of chymotrypsin concentration. (A) Impact of chymotrypsin format on signature peptide signal. 1: 5 nM chymotrypsin, solution phase digestion; 2: 1 nM chymotrypsin, solution phase digestion; 3: Adding 0.33 nM chymotrypsin every 8 hours to a total of 1 nM chymotrypsin; 4. chymotrypsin bead, equivalent enzyme concentration=1 nM. 4 replicates each chymotrypsin format (B) Impact of chymotrypsin bead equivalent concentration on signature peptide signal. 4 replicates each bead concentration. (C) Chromatogram comparison of 2 nM chymotrypsin bead digest and 50 nM chymotrypsin bead digest. Signature peptide was monitored at MS^2 full scan mode, base peak chromatogram (BPC) was recorded with MS full scan mode.

4.3.4 Codigestion with NT-3 and GDNF

One advantage of signature peptide method over immunoassay is its ease in realizing multiplexed detection. Therefore, NT-3 and GDNF was selected in this study to determine if they can be co-digested with BDNF at low concentration. NT-3 and GDNF are members of neurotrophin family and play important role in promoting the growth and differentiation of neurons[251-253]. They are also structurally similar to BDNF, being

homodimers containing predominantly β-sheet structure and cystine knot[241,254]. Injection of digested protein standard containing BDNF, NT-3 and GDNF (100 pM each) showed that NT-3 produced similar signature peptide signal to that of BDNF, while GDNF's signature peptide signal was 10 times lower (Figure 4.4). This could be due to the fact that GDNF's dimer is linked by covalent disulfide bond, therefore it is more difficult to unfold, causing lower signature peptide yield.

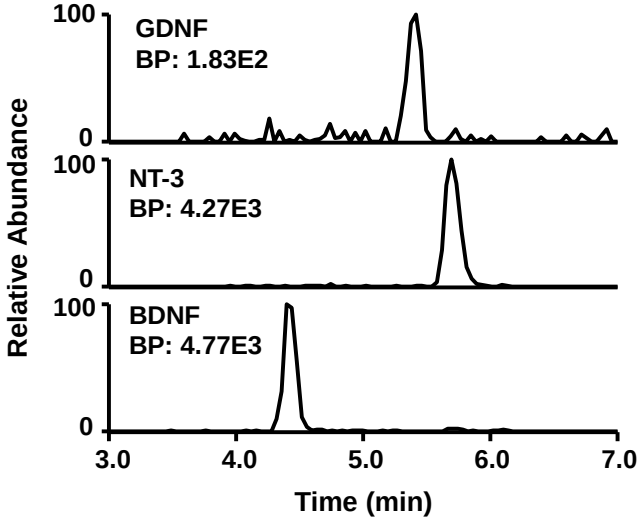

Figure 4.4 RIC and base peak (BP) intensity of BDNF, NT-3 and GDNF's signature peptide when the three proteins were digested together. Protein concentration: 100 pM each. NT-3 signature peptide: VTDKSSAIDIRGHQVTVL, MS^2 pathway: 485.97 ($[M+4H]^{4+}$)→564.63($[b16\text{-}H_2O]^{3+}$), 597.49($[b17\text{-}H_2O]^{3+}$), 603.51($b17^{3+}$);GDNF signature peptide: DKILKNL, MS^2 pathway: 422.39($[M+2H]^{2+}$)→ 487.35(y4), 583.00(y5-NH_3), 600.32(y5) .

4.3.5 Method sensitivity

The signature peptide signal response over concentration change was studied by injecting 8 µL digest produced from 100 pM to 2 nM protein. Resulting calibration curves showed good linearity (Figure 5A) and sample-to-sample reproducibility. LODs were estimated to be ~4 pM for BDNF, 4 pM for NT-3 and ~9 pM for GDNF. 5 pM BDNF and NT-3 or 10 pM GDNF were also digested and analyzed to confirm the

presence of signature peptide signal at calculated LOD (Figure 5B). This corresponds to 50 amol BDNF, NT-3 or 100 amol GDNF in the starting protein standard, and 40 amol BDNF, NT-3 or 80 amol GDNF injected onto the column. Further improvement in reproducibility and quantification can be achieved by including isotopically labeled signature peptide internal standard to reduce the variability introduced after digestion. It is also worth noting that the signature peptides were injected with no addition of ACN because they had no observed carry-over when injected in aqueous solution and addition of ACN, even to 5%, decreased signature peptides' signal.

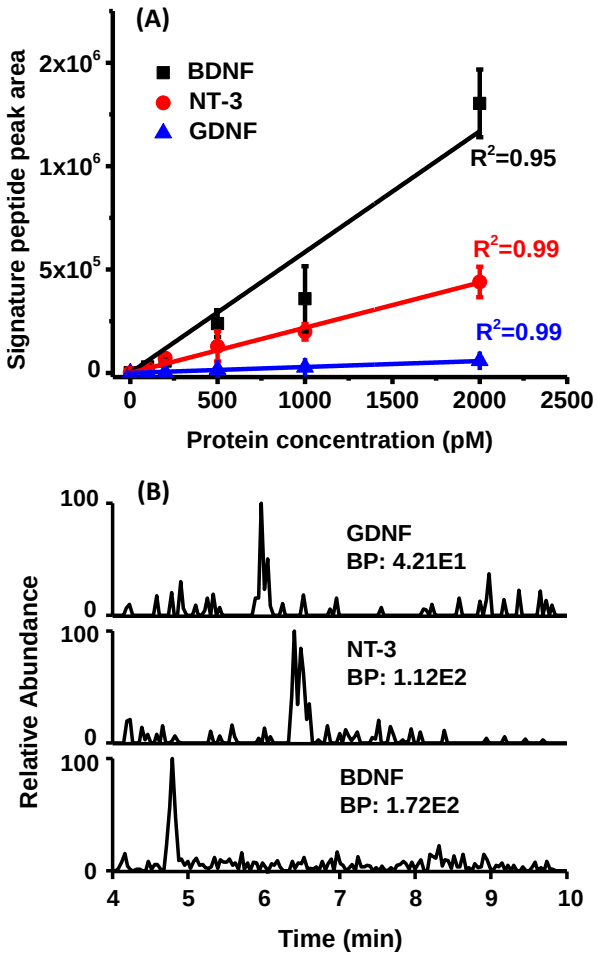

Figure 4.5 Signature peptide method sensitivity for BDNF, NT-3 and GDNF. (A) Calibration curve of BDNF, NT-3 and GDNF using signature peptide produced by digesting these proteins together. 3 replicate digestion each concentration. (B) RIC of signature peptides at concentration close to LOD. GDNF: 10 pM protein digested; NT-3 and BDNF: 5 pM protein digested. LOD was estimated using equation LOD=blank signal+3×standard deviation of blank signal.

4.4 Conclusion

In this chapter, we have developed a signature peptide method for detecting BDNF. Our investigation revealed that in the case of BDNF, chymotrypsin had better signature peptide yield than trypsin, and a concentration step prior to denaturation, reduction and alkylation was necessary for improved signature peptide's yield of this structurally stable protein. In addition, immobilized chymotrypsin bead was shown to result in higher

signature peptide yield. The result had shown necessity of optimizing DRAD protocol of a signature peptide method for structurally stable protein. The selection of enzyme, denaturation condition and enzyme format all affected signature peptide production. With all the optimized digestion procedure for BDNF, NT-3 and GDNF could be co-digested and detected at mid-amol level. Combining with protein purification, this method may be a potential alternative to immunoassay to achieve sensitive detection of several neurotrophins from one sample.

Chapter 5

Conclusions and future directions

In this dissertation, the analytical performance of cLC-MS in neuropeptide detection was improved in terms of speed and sensitivity. The detection speed was enhanced by utilizing 10 µm particulate phase as packing material in a 75 µm bore capillary column. The larger particle diameter and column I.D. compared with previously reported 25 µm bore column packed with 5 µm particle has greatly reduced column backpressure during sample injection and rinsing; therefore, enabling faster sample injection under the same injection pressure. A fast injection flow rate (14 µL/min) combining with low elution flow rate (100 nL/min) was determined to be the optimal for fast sample analysis (4 min/sample compared to previously reported 20-30 min /sample) while still maintaining low LOD of 3 pM for LE, ME and 10 pM for $DynA_{1-8}$ from a 5 µL standard. This method was validated for *in vivo* detection of LE and ME from rat GP.

In terms of sensitivity improvement, we have discovered that the poor LC-MS response of certain big neuropeptides such as β-endorhpin, orexins and Gal can be attributed to its adsorption loss to surfaces prior to being injected onto LC column. ACN was added to sample to prevent adsorption loss and improve sensitivity. Since increased ACN percentage could result in both reduced adsorption loss and lower peptide retention during injection, an optimal ACN percentage that yielded highest peptide signal was determined for each of 10 tested peptides. The optimal ACN percentage had positive

correlation with peptide molecular weight and retention time on a reverse phase column. This method was applied to 10 neuropeptides. LOD was improved by as much as 60 fold and were consistently 0.1-2 pM from 8 µL sample for all neuropeptides tested.

This work also improved *in vivo* recovery of neuropeptides by microdialysis. Hydrophilic, negatively charged microdialysis probe membranes were modified with polycationic PEI to reduce electrostatic interaction between positively charged peptides and the membrane. The modification significantly improved recovery of 7 out of 11 neuropeptides tested. All peptides that were improved had net positive charge at physiological pH illustrating the significance of charge for affecting recovery.

The ACN addition method combined with PEI modification was applied for detecting intact orexin A (MW 3561) and orexin B (MW 2936) from rat arcuate nucleus. This study was the first *in vivo* monitoring of orexin A using mass spectrometry, and first *in vivo* monitoring of orexin B. In this same experiment a peptide fragment from an un-reviewed rat POMC that has identical sequence as mouse β-endorphin was also identified and detected. This result illustrates the high sequence specificity of MS detection. Together the results show that this combined approach enables *in vivo* detection of previously difficult to detect neuropeptides.

In addition to these neuropeptides, we also developed a high sensitivity signature peptide method capable of detecting BDNF and related proteins. These proteins proved challenging to detect because of their low concentration and stable structures that resist ordinary digestion conditions. We discovered that chymotrypsin digestion produced a signature peptide that could be reliably detected at pM level, while trypsin failed to produce such signature peptide due to incomplete digestion. Besides, a concentration step

prior to protein denaturation, reduction and alkylation was found to be necessary for achieving high signature peptide signal. We also found that immobilized chymotrypsin bead produced higher signature peptide signal, even at the same equivalent enzyme concentration. We were able to utilize the digestion protocol optimized for BDNF for co-digesting other 2 structurally similar neurotrophins, NT-3 and glial GDNF. This method has 5 pM LOD for BDNF and NT-3 and 10 pM LOD for GDNF from 8 µL protein standard digest, displaying potential in realizing highly sensitive, multiplexed quantification for neurotrophin.

Future directions based on this dissertation can include both method development and application in biological studies. The improvement in analytical speed and sensitivity in this dissertation can be applied to develop high performance method for other peptides for their *in vivo* applications. Also further method development that overcomes current limitation could also be an important direction.

5.1 ACN addition for improving sensitivity of other big neuropeptides

Adding ACN effectively reduced adsorption loss and allowed high detection sensitivity by cLC-MS for several larger neuropeptides such as orexins, β-endorphin and Gal that had previously been difficult to detect. This can be potentially extended to detecting other biologically important, large neuropeptides. One example is glucagon, which can be detected at 500 pM when injected without ACN addition (Figure5.1).

Glucagon showed good MS intensity when directly infused to an ion trap MS (Figure 5.1 A, B), the signal intensity was comparable to that of LE, which had 0.5-3 pM LOD detected by cLC-MS . However when injecting glucagon onto the same cLC-MS system, the lowest detectable concentration was 500 pM. The good MS response under direct

infusion has suggested that the poor cLC-MS signal could either originate from LC tubing or container vials. Further investigation showed that blank aCSF injection after injecting 5 nM glucagon gave 4 times higher signal than the standard injection, indicating adsorption loss in the LC tubing was a substantial cause for the low cLC-MS signal.

In addition to glucagon, studies in the past 5 years also reported LC-MS detection of other large neuropeptides from biological samples, including parathyroid hormone$_{1\text{-}34}$ (PTH, 4118 Da)[144], salmon calcitonin (3432 Da)[148], Apelin-36 (4196 Da)[149], Aβ_{38} (4132 Da)[146,147], Aβ_{40} (4330 Da) [146,147] and Aβ_{42} (4514 Da)[145-147]. Concentration LOD as low as 3 pM, 11 pM and 12 pM was achieved for salmon calcitonin[148] , Aβ_{42}[145-147] and Apelin-36[149], showing possibility for detecting neuropeptides even larger than orexin A (3561 Da) documented in this dissertation. Although mass LOD was still at mid-to-high fmol range, the sensitivity could potentially be improved by utilizing a capillary column and ACN addition to minimize adsorption loss.

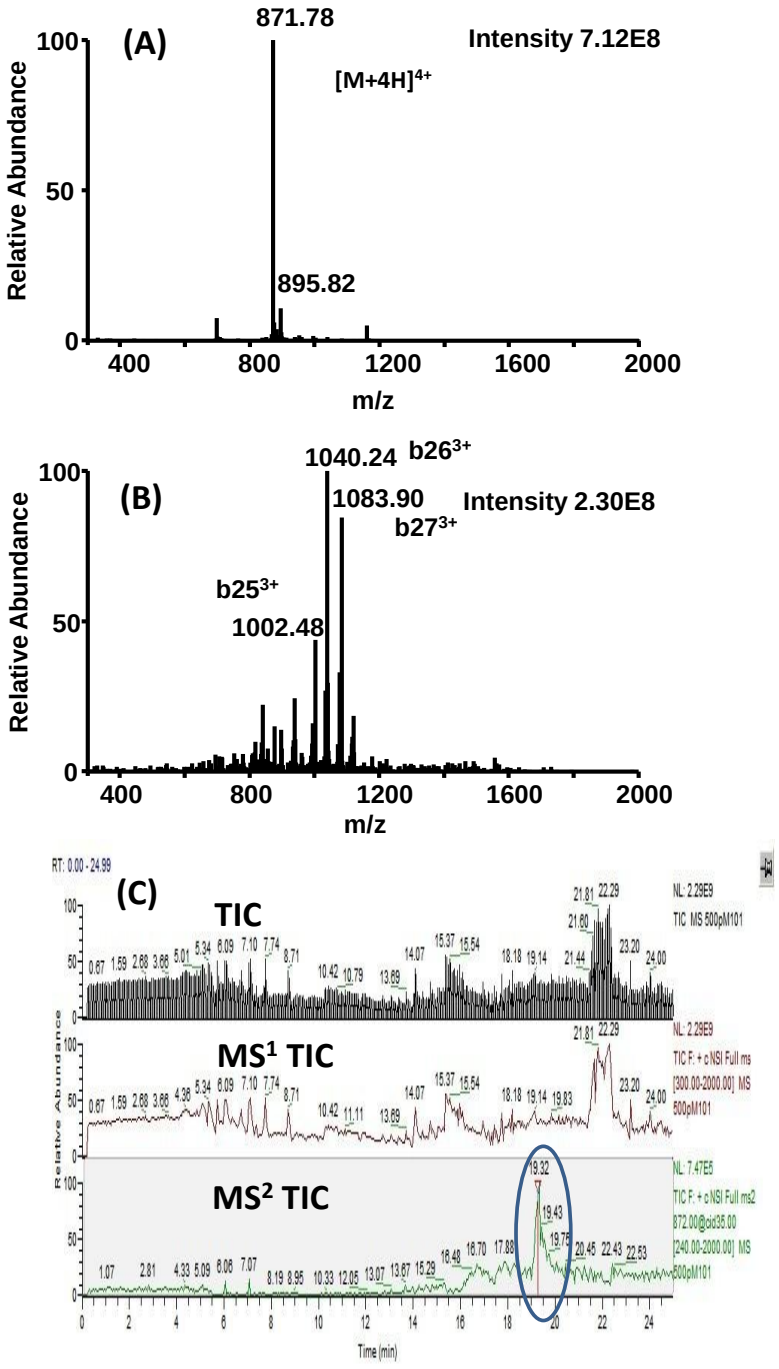

Figure 5.1 LC-MS analysis of glucagon standard without ACN addition**.** (A) MS^1 spectrum of 10 µM glucagon directly infused into LCQ Deca XP Plus. Glucagon was dissolved in 50% MeOH, 50% H_2O with 0.1% FA. (B) MS/MS spectrum of glucagon, mother ion m/z 871.78. (C) MS^2 of 500 pM glucagon injected onto a 50 µm Altima C18 column, injection volume: 5 µL, glucagon standard was dissolved in aCSF with 0.5% FA.

In this dissertation we have demonstrated *in vivo* detection of intact orexins. Therefore another possible project in this direction is to develop methods for orexin fragments. Since current method has good sensitivity for intact orexins, and the optimal ACN% correlates with molecular weight, we expect the optimal ACN% for orexin fragments to be lower than 25%. In addition, since smaller peptides are less prone to adsorption loss, we also expect orexin fragments to have higher microdialysis recovery. The method for orexin fragments could be applied to determine the biologically active form for future *in vivo* studies and to understand the *in vivo* processing of orexins.

5.2 Developing fast detection method for more neuropeptides

In chapter 2, we demonstrated that a 75 µm bore column packed with 10 µm particle was able to maintain good sensitivity and low pM LOD for enkephalins and $DynA_{1-8}$ with 4min/sample analysis rate. The method could be further applied for improving analysis speed for other neuropeptides with established cLC-MS method. For example, the time needed for analyzing 8 µL sample in chapter 3 using a 75 µL column packed with 5 µm particle was 17 min (2 min sample loading into auto sampler+3 min sample injection+2 min sample rinsing+10 min elution), resulting in a total of 12 h analysis time for a regular *in vivo* experiment (3 animals, 10 fractions/animal plus 4 point calibration curve, 3 replicates). If the fast preconcentration method could be applied with similar turn-over rate reported in chapter 2 (4 min/sample), these samples could be analyzed within 3 h instead of 12 h. Chapter 2 also provides some useful guidance on developing fast analysis method from an established, sensitive but "slow" cLC-MS method. First of all, evaluation of the impact of particle size on sensitivity should be performed by comparing peptide signal on a column packed with regular 5 µm material and 10 µm material. This is

because larger particle size may possibly lead to worse separation efficiency and broader peaks, which can compromise sensitivity. Second, optimal injection flow rate should be identified using the column packed with 10 µm particles. The optimal injection flow rate should be the highest injection flow rate without peptide signal decrease. For enkephalins and $DynA_{1-8}$ injected in aCSF this flow rate was 14 µL/min; however, the value may vary with peptides due to differences in hydrophobicity and content of ACN in the sample.

Another option for improving speed while maintaining good separation is to utilize a monolithic column. Monolithic columns are known for improved separation efficiency at reduced back pressure comparing to packed columns. Polymer monoliths are easier to make, and can potentially be patterned into a microfluidic device by photo-initiated polymerization. However this type of column failed to retain peptides when injection flow rate exceeded 0.8 µL/min (Appendix 2), due to its intrinsically low surface area (20-30m^2/g) and lack of meso pores. Silica monolithic column are more challenging to fabricate; however, they contain both macro pores and meso pores, and are suitable for retaining small molecules and peptides. Commercial silica monolithic column with C18 surface functionality (Chromolith^{TM}, Merck Millipore) can achieve 300 m^2/g surface area and carbon load as high as 18% , compared to 200 m^2/g and 12% for Alltima C18 used in this dissertation. Therefore silica monolith can serve as potential alternative for large particulate phase for fast neuropeptide preconcentration and analysis with good separation efficiency.

5.3 Improving microdialysis probe recovery for higher peptide detectability from the brain

As discussed in Chapter 3, enhancement in probe recovery was achieved by PEI modification on an in-house constructed AN69 probe. The modification significantly improved recovery for 7 out of 11 neuropeptides, achieving ~10% recovery for most large neuropeptides carrying four net positive charges. However, the recovery for orexin A was still low (~0.2%). Orexin A carries +1.2 net positive charge at pH 7.4 and has similar size to other better-recovered neuropeptide, such as β-endorphin. The low recovery might still origin from orexin adsorption to the microdialysis catheter, indicating PEI modification did not fully eliminate active sites for adsorption. The slow probe response in Chapter 3 also supports this hypothesis; therefore the probe modification protocol needs further optimization to eliminate peptide adsorption. One possible direction is to investigate the influence of different PEI format on peptide relative recovery. PEI is available in linear and branched format, with average molecular weight ranging from ~1 kDa to 750 kDa. While chapter 3 only tested one PEI (branched, MW 2kDa), other PEIs might be more strongly bound to the negatively charged surface and provide better blockage of negatively charged sites.

The probes used in this dissertation were manually constructed in-house with fused silica capillary, AN69 membrane, stainless steel tubing, epoxy gel and superglue, and the peptide-containing dialysate was in contact with all of the components in its flow path. The complex chemical property of these surfaces may indicate other adsorption mechanism, such as hydrophobic interaction and hydrogen bond in addition to electrostatic interaction. Further blockage of adsorption site could potentially be achieved

by introducing inert functional groups, such as polyethylene oxide (PEO) to the surface, and one possible yet simple approach was to flow Pluronic F-127 (PEO_{98}-PPO_{67}-PEO_{98})[103] or poly L-lysine-PEO[255] through the entire microdialysis catheter including the probe. Pluronic F-127 blocks hydrophobic surface by adsorption of the hydrophobic block polypropylene oxide (PPO), while leaving hydrophilic PEO chain forming a water-swelling layer that repels proteins from the surface. This polymer has been applied for modifying microdialysis probe to improve protein recovery[103]. Poly L-lysine-PEO adsorbs to negatively charged surface by electrostatic interaction between the surface charge and poly-L-lysine chain grafted to PEO, although this method has not been applied to microdialysis yet, it reduced adsorption of serum protein on a surface grafted with negatively charged peptide RGD[255] and therefore can potentially be applied for modifying AN69 probe.

Another possible direction was to improve fabrication protocol to create probe scaffold and membrane that are less prone to absorbing peptides/proteins. Our group has previously reported microfabricated push-pull probe from silicon wafer by lithography and bulk machining[256]. The resulted interior surface of the probe channel was a 3 μm layer of polysilicon, in contrast to the complex inner surface composition of a regular microdialysis probe. This fabrication process is also being applied by our group for constructing microdialysis probes. Although the focus of the on-going study is to develop micro-scale microdialysis probe for improved spatial resolution and reduced tissue damage, it will be interesting to investigate the adsorption property of the microfabricated dialysis probe and see if the more uniform probe inner surface can either reduce peptide adsorption loss or be easily modified to generate peptide/protein repelling surface.

In addition to reducing adsorption loss onto the microdialysis catheter, sampling recovery could also be improved by increasing neuropeptide mass transport into the microdialysis probe. As discussed in Chapter 1, affinity enhanced microdialysis can be applied for neuropeptide detection. Potential issue with affinity enhanced microdialysis is the high level of affinity agent in dialysate that can possibly interfere with LC-MS detection. Besides, bead saturation, settling and clogging also needs to be evaluated for methods using immobilized affinity agents. Future projects in this direction could include feasibility study of incorporating affinity agent (free form or immobilized on bead) into microdialysis perfusion media.

5.4 Improving signature peptide method for detecting BDNF from biological sample

Chapter 4 has discussed the development of a sensitive signature peptide method for BDNF. The study provided insight into BDNF's resistance to protease digestion and gave solutions for overcoming the obstacle in digesting this protein, future projects could continue into testing the method for detecting BDNF from biological samples such as *in vivo* dialysate and CSF. The protein content in dialysate is much lower than that in CSF, therefore dialysate may be less likely to have interference issue caused by high abundance protein, and additional sample cleanup before digestion might not be crucial for dialysate analysis. Including a SIL internal standard for the signature peptide may be necessary for correcting matrix effect in MS analysis and estimating the signature peptide production efficiency at low concentration. In addition, the current method involves two solution drying steps (concentrating the protein for denaturation, reduction and alkylation and removing ACN from the final digest. ACN was added to the immobilized chymotrypsin digestion mixture to prevent BDNF and signature peptide adsorption loss

to the container vial and the beads) and multiple pipetting steps. For practical considerations of biological studies which easily generate 20-30 samples per day, future projects can also be directed to improving digestion protocol to reduce the amount of labor involved. Possible ideas include processing sample using multichannel pipette in 96 well format, or use microwave[257] or ultrasound irradiation[258] to facilitate BDNF digestion without requiring denaturation prior to digestion. Previous study has shown that microwave-enhanced trypsin digestion could produce signature peptide from 17 pM N-terminal prohormone of brain natriuretic peptide within 50 min. Therefore it will be valuable to study if these irradiation formats could potentially enhance BDNF digestion without requiring extensive denaturation.

Appendix A

Signature Peptide and Microchannel ELISA Methods for Measuring Biochemical Indicators of Implantation Success of Tissue-Engineered Oral Mucosa

A.1 Objective

Develop fast and sensitive analytical method for quantifying ultra-low level protein markers in EVPOME spent medium within 2-3 hours to provide assessment on EVPOME viability prior to implantation.

A.2 Approach #1: Signature peptide method for simultaneous quantification of two protein markers

A.2.1 Experiment

A.2.1.1 Protein digestion using trypsin immobilized bead

Recombinant human IL-8 and VEGF (carrier free, R&D systems) was dissolved in a buffer containing 40% (v/v) ACN and 60%(v/v) 100 mM phosphate buffer saline (PBS, pH 2.5) and serially diluted with the buffer to form standard with concentration ranging from 10 pM to 10 nM. 10 µL protein standard was aliquoted to a 500 µL protein LoBind centrifuge tube (eppendorf), and 0.5 µL 200 mM TCEP (Sigma-Aldrich), 0.5 µL 1M IAM (Sigma-Aldrich) were added, 2 µL 1M Tris buffer was also added to adjust solution pH to ~8.0. The reaction was allowed to be incubated in dark under room temperature for 1 h to allow reduction and alkylation of disulfide bonds in IL-8 and VEGF. Then 2.5 µL 200 mM DTT was added and incubated for 40 min to react with the residue IAM, and the

reaction mixture was diluted to 25 µL with 2.5 µL 50 mM ammonium bicarbonate (pH 8.0) and 8 µL ACN. 5 µL immobilized trypsin magnetic bead slurry (Clontech, 500 µL bead slurry was washed by water for 5 times, and excessive supernatant was removed to form ~50 µL 10 ×concentration bead slurry) was added to the protein solution. The reaction was allowed to incubate on a rotary shaker under room temperature for 2.5 h. The ACN% in the reaction mixture was 40% to prevent protein from sticking to the magnetic bead. After 2.5 h the resulted digest was quenched by 0.5% FA and supernatant was separated from the bead by a magnet, dried in a vacufuge and reconstitute in 10 µL 0.5% FA for LC-MS injection.

A.2.1.2 cLC-MS analysis of signature peptides

The cLC-MS system set up and MS detection was detailed in chapter 3 and chapter 4, except that mobile phase B (MPB) was ACN with 0.1% FA. 5 µL reconstituted digest was injected directly under full loop mode onto a 50 µm I.D. column packed with 5 µm Alltima C18 particle to 6 cm. The injection pressure was 4000 psi, the digest was injected for 8 min and washed by loading solvent for another 4 min. Gradient for elution was: 0-1 min: 0%-10% MPB, 1-16 min: 10%-50% MPB, 16-18 min: 50%-95% MPB, 18-21 min: 95% MPB, 21-21.1 min: 95%-0% MPB, 21.1-23 min 0% MPB.

A.2.1.3 Immunoaffinity capture of IL-8

The immunoaffinity column (180 µm I.D.) was packed in house to 5 cm with immobilized antiIL-8 particle (Nucleosil silica support, 7 um diameter, 300 Å pore size) provided by group colleague, Dr. Michelle Johnson. To capture IL-8, 500 µL solution (100 mM PBS, pH 7.0) containing 500 pM IL-8 as target protein and 26 nM VEGF as interfering protein was loaded onto the column. The column was washed by pH 7.0 PBS

at 7 µL/min to remove unbound protein, and the flow-through was collected every 3 min for a total of 15 minues (5 fractions). Then the elution buffer (100 mM PBS, pH 2.0) was pumped through the column at 7 µL/min to release captured IL-8. The flow-through was collected every 3 min for a total of 18 min (6 fractions). All the collected fractions were digested with immobilized trypsin according to the protocol described above.

A.2.2 Result

A.2.2.1 Signature peptide for IL-8 and VEGF

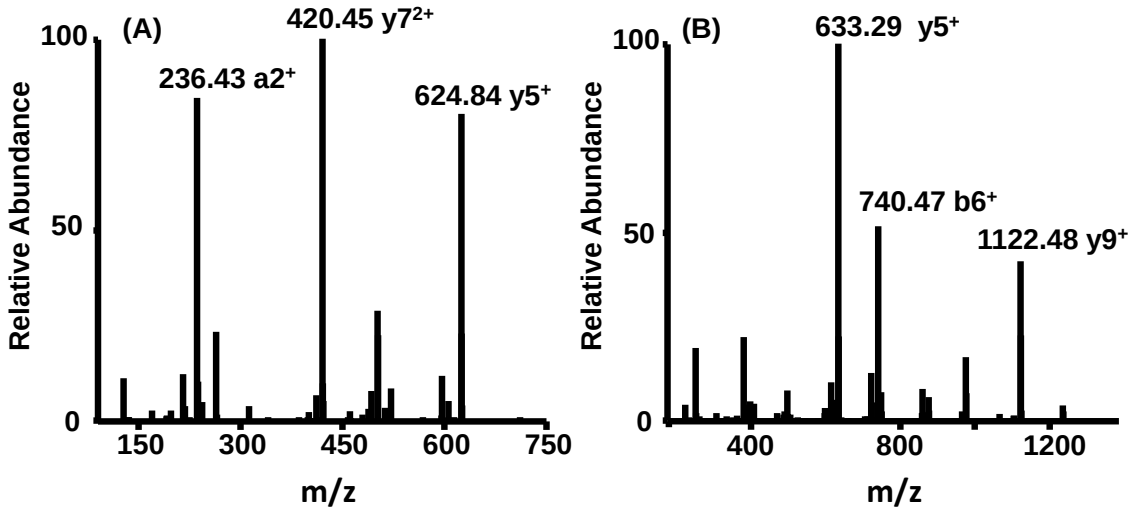

Figure A.1 MS^2 spectra of signature peptide of IL-8 and VEGF. (A) MS^2 spectrum of signature peptide TYSKPFHPK for IL-8, parent ion was $[M+3H]^{3+}$ (m/z 369.0). (B) MS^2 spectrum of signature peptide HLFVQDPQTCK for VEGF, parent ion was $[M+2H]^{2+}$ (m/z 687)

A.2.2.2 Higher signature peptide production and fast digestion achieved by immobilized trypsin

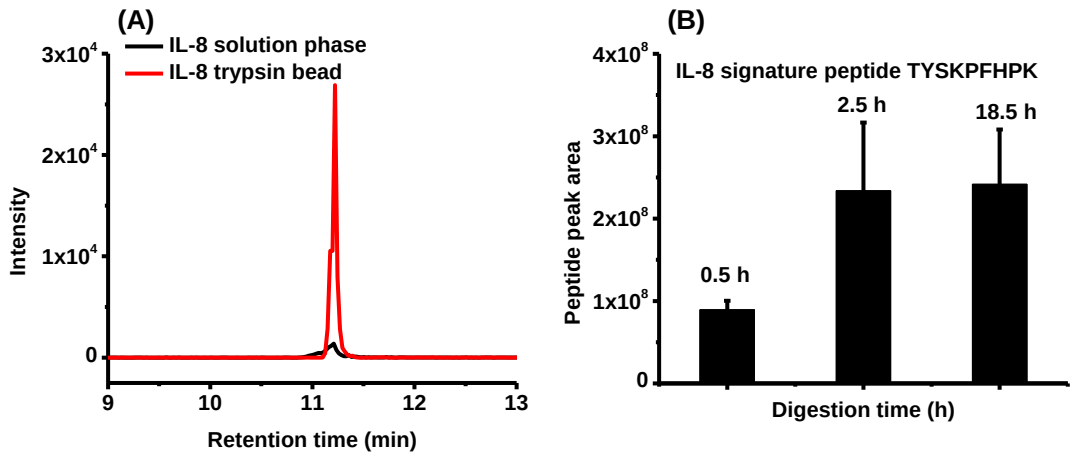

Figure A.2 Immobilized trypsin digestion showed better signature peptide yield than solution phase digestion. (A) Overlaid RIC of IL-8 signature peptide TYSKPFHPK produced from overnight solution phase digestion at 37 ^{o}C (black curve) and 2.5 h immobilized trypsin bead digestion at room temperature (red curve). IL-8 concentrations in both cases were 10 nM, reduction and alkylation protocol used were identical. (B) IL-8 signature peptide signal reached maximum after immobilized trypsin digestion for 2.5h, and remained stable after 18.5h. IL-8 concentration was 10 nM and 3 replicate digestions were analyze for each time point.

A.2.2.3 RIC for IL-8 and VEGF at lowest detectable concentration

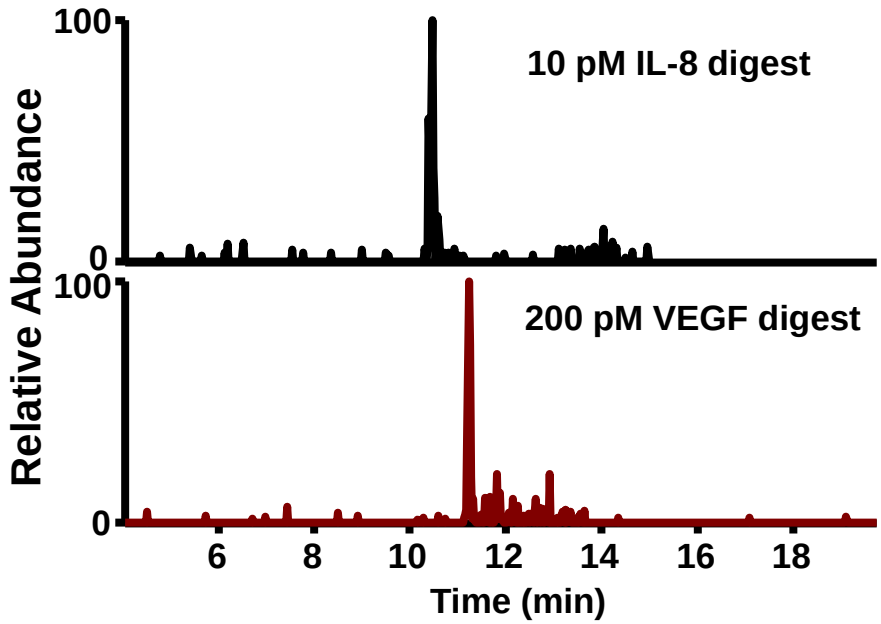

Figure A.3 RIC of IL-8 signature peptide TYSKPFHPK and VEGF signature peptide HLFVQDPQTCK at lowest detectable concentration. The lowest detectable concentration for IL-8 was 10 pM, and for VEGF was 200 pM. Injection volume was 5 µL.

A.2.2.4 Combining with immunocapture to preconcentrate IL-8

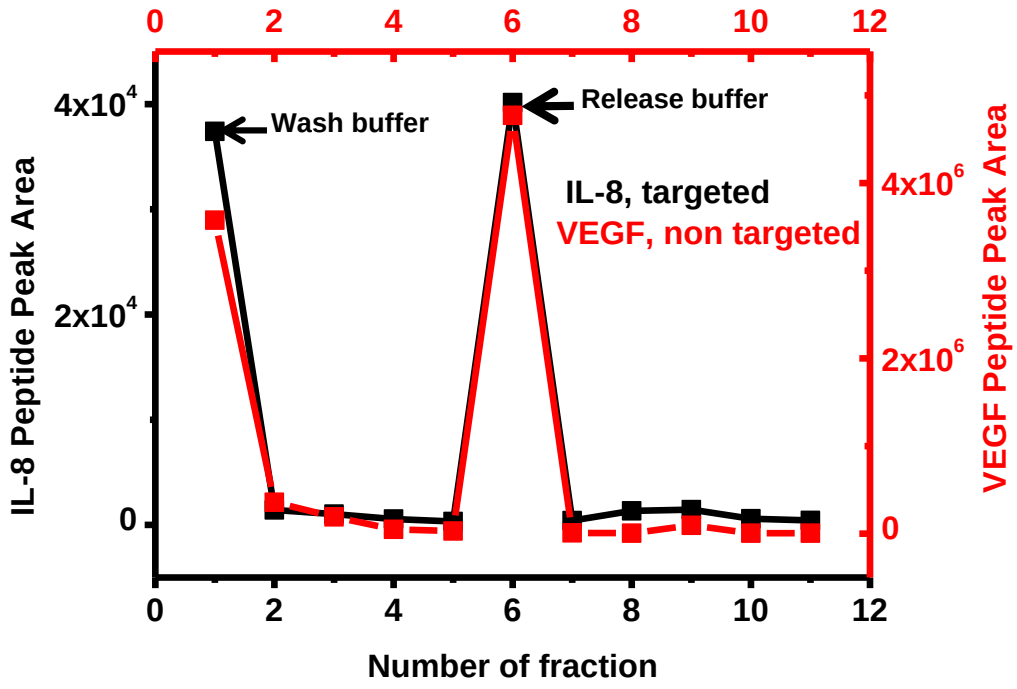

Figure A.4 IL-8 and VEGF signal profile when loading the proteins onto an anti IL-8 column.

A.2.3 Discussion

The digestion time for this method was 2.5 h compared with conventional solution phase overnight digestion, which may potentially fulfill the goal of fast and sensitive protein marker quantification. This approach was not applied for actual detection of IL-8 and VEGF from EVPOME spent medium due to several reasons. First, the antibody column we used showed non-specific binding problem. VEGF (26 nM) was 52 times more concentrated than IL-8 (500 pM) in the solution prior to IL-8 immunoaffinity capture, and after capture, the signal of VEGF's signature peptide in eluent was over 100 times higher than IL-8's signature peptide signal, suggesting the column was non-selectively binding VEGF while the antibody was targeting IL-8. Second, although

digestion time can be reduced to 2.5 h, the time needed for reduction, alkylation (1h 40 min), solution drying (50 min) and LC-MS analysis (40 min) still resulted in an overall analysis time of >5 h. The cLC-MS method developed in Chapter 2 may apply here to improve analysis speed, however highly sensitive and faster sample preparation that produces signature peptide ready for injection within less than 2 hours needs to be developed. Shorten reduction, alkylation time needs to be tested to determine if signature peptide signal is unaffected, and shorter digestion time can be potentially achieved by testing digestion time points between 0.5-2.5 h, or employing microwave or ultrasound irradiation to enhance digestion speed, as discussed in chapter 5. In addition, commercial kits such as Flash Digest (Perfinity Biosciences, West Lafayette, IN) can be potentially useful in increasing digestion speed. Such kits utilize immobilized, high temperature-stable trypsin to achieve complete digestion of protein at protein denaturing temperature (70 ^{o}C) within 1-30 min, eliminating the need for protein denaturation, reduction and alkylation.

A.3 Appoach #2: Microchannel ELISA method for quantifying protein markers in EVPOME spent medium.

A.3.1 Experiment

For microchannel ELISA, Optimser™ microfluidic ELISA plate assembly, buffers, and reagents were from Siloam Biosciences (Cincinnati, OH). IL-8 and VEGF antibody pairs were from Life Technologies (Carlsbad, CA). Human β defensin-1 (hBD-1) and tissue inhibitor of metalloproteinases -1 (TIMP-1) reagent kits were from Peprotech (Rocky Hill, NJ). The TIMP-2 antibody pair was from R&D Systems (Minneapolis, MN). The optimized conditions and LODs for microchannel ELISA measurement are listed in

Table A.1. Measurement was conducted according to the protocol provided by Siloam Biosciences, except for the TIMP-1 assay, whose optimal wash was 0.05% Tween-20 in PBS (pH 7.0). The protein concentration was measured in triplicate based on external calibration.

Table A.1 Optimized ELISA condition and LOD of each protein marker

Protein marker	Coating buffer	Capture antibody concentration	Detection antibody concentration	LOD (pg/ml)
IL-8	OptiBind™-E	2 µg/mL	0.16 µg/mL	1
VEGF	OptiBind™-F	2.5 µg/mL	0.05 µg/mL	2 (20 consecutive additions of 5 µl sample)
hBD-1	OptiBind™-G	2 µg/mL	2 µg/mL	3
TIMP-1	OptiBind™-E	1 µg/mL	1 µg/mL	3(5 consecutive additions of 5 µl sample)
TIMP-2	OptiBind™-D	2 µg/mL	0.4 µg/mL	10(5 consecutive additions of 5 µl sample)

A.3.2 Result

All five protein markers were measurable in the spent medium, and average concentration is listed in table A1.2:

Table A.2 Measured protein marker concentration from 16 EVPOME spent medium, 8 thermally stressed and 8 non-stressed

Protein marker	Tissue culture condition	Mean concentration (pg/mL)	SEM (pg/mL)	P value
IL-8	Control	16.5	4.3	0.04
	Thermally stressed	7.6	1.8	
hBD-1	Control	49.7	12.3	0.03
	Thermally stressed	20.3	8.2	
VEGF	Control	24.1	6.9	0.07
	Thermally stressed	10.7	4.0	
TIMP-1	Control	75.9	26.0	0.15
	Thermally stressed	36.2	13.9	
TIMP-2	Control	168.4	28.4	0.02
	Thermally stressed	88.1	24.8	

Among these protein markers, IL-8, hBD-1 and TIMP-2's concentration was found to significantly correlate with the stress status of EVPOME tissue. The result has been published in *Journal of Dental Research* (2015, Vol 94, 78-84).

Appendix B

Monolithic column fabrication for solid phase extraction of neuropeptides

B.1 Objective

To utilize monolithic column's potential advantage in fast separation and low column back pressure for rapid neuropeptide preconcentration and detection. We selected polymer monolith to start because it is easier to synthesize than silica-based monolith, has better batch-to-batch reproducibility and can potentially achieve photo initiated polymerization to pattern the column for chip-based application. The polymer chosen was polystyrene-divinylbezene (PS-DVB), based on its high chemical inertness and excellent separation performance.

B.2 Experiment

B.2.1 Capillary vinylization

The capillary inner wall needs to be vinylized in order to provide covalent bonding of monolith to the wall. In brief, fused silica capillary was flushed with acetonitrile, water and filled by 1M NaOH solution. The capillary was sealed by septum and placed into 120℃ oven for 2 h to expose fresh silanol groups. The cleaned capillary was then washed with Mili-Q water till pH reached 7, flushed by acetone and allowed to dry in 120℃ for 1 h with nitrogen purging. After drying, vinylization mixture containing 50% (v/v) N, N-dimethylformamide (DMF), 50% (v/v) 3-(trimethoxysilyl) propyl methacrylate, 0.01% w/v 2, 2-diphenyl-1-picrylhydrazyl was loaded into the capillary. Capillary was sealed

again and reacted under 120℃ for 6 h for completion of vinylization. The vinylized capillary was then washed by acetone and stored in the air till use.

B.2.2 Polymerization

The formation of a PS-DVB monolithic column is based on free radical polymerization of monomer styrene and cross-linker divinylbezene in a pore forming solvent (porogen). The morphology of the monolith is controlled by the porogen's solvating power to the growing polymer chain, and poorer (more polar) solvents tend to have earlier phase separation which results in both larger nodule size and pore size. The polymerization mixture contained 1% w/v azobisisobutyronitrile (ratio to volume of monomers) and different compositions of monomer/cross-linker and monomer solvent (porogen) and is listed in Table B.1. The mixture was filtered by 0.2 μm syringe filter (Whatman) and purged with nitrogen for 3 min to remove dissolved oxygen. Vinylized capillary was purged with N_2 for 1h before loaded with mixture. The capillary was then immediately sealed and placed in a 70℃ circulating water bath for 24 h to form the monolith. After that, the monolithic columns were washed with MeOH to remove remaining monomers and dried by N_2. Columns can be made in batch and stored for 2 weeks prior to use.

B.3 Result

B.3.1 Formation of monolithic column and its preconcentration of ME at low injection flow rate

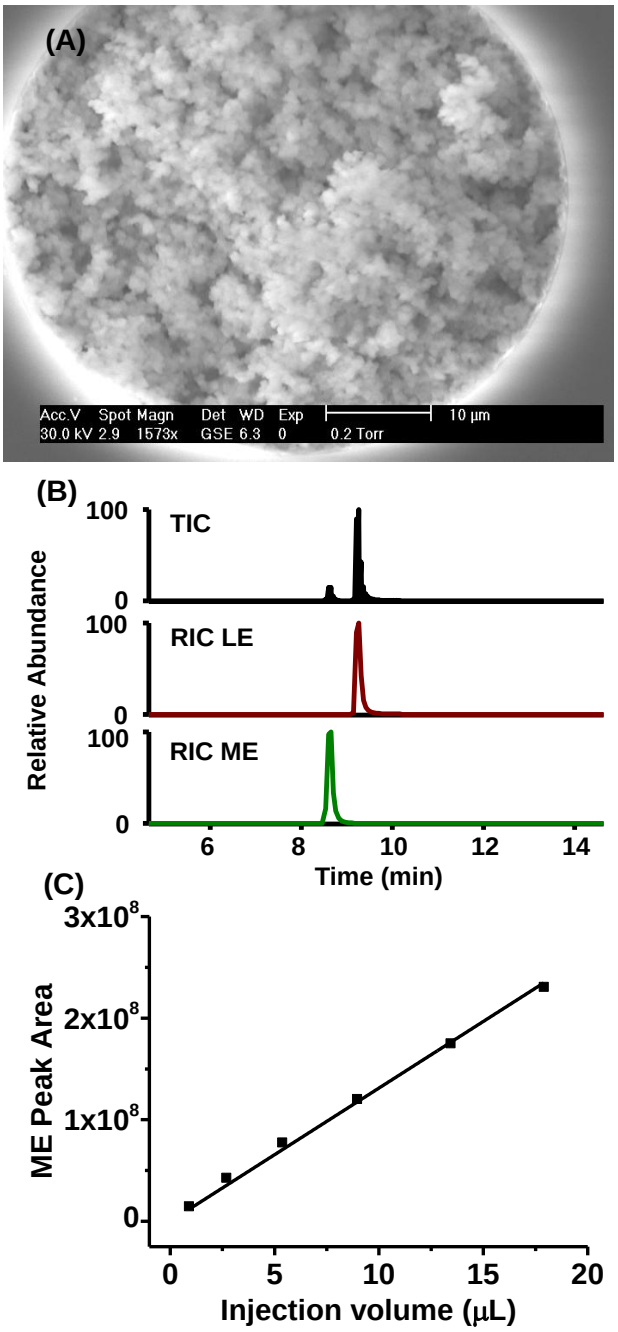

Figure B.1 Characterization of a PS-DVB column using microscopy and LC. (A) Environmental scanning electron microscope image of a monolithic column cross section. (B) HPLC separation of LE and ME on PS-DVB monolithic column. Column length: 5cm; column I.D.: 50 µm. Peptide was 500 nM in 1% HAc, injected volume was ~20 nL. Gradient: 0-0.1 min: 2-10% MPB, 0.1-6 min: 10% -50% MPB, 6-6.5 min:50% -95% MPB, 6.5- 7 min:95% MPB, 7-7.5 min: 95%-2% MPB. MPA: 1% HAc, MPB: 1% HAc in MeOH. (C) Peak area increased linearly as injection volume increased for 3nM ME in 0.5% HAc. Injection flow rate: 0.45 µL/min. Column length: 5 cm; column I.D.: 50 µm; elution flow rate: 122 nL/min, elution solvent: 50% MeOH with 1% HAc.

B.3.2 LE signal decreases with increased injection flow rate

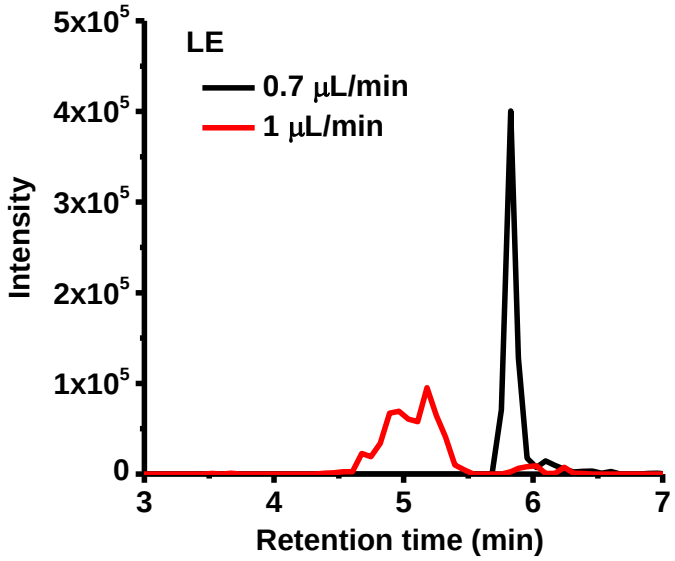

Figure B.2 LE signal decreased as injection flow rate increased from 0.7 μL/min to 1 μL/min. 5 μL 1nM LE dissolved in aCSF was injected, and the injection time was kept at 20 min to allow additional loading solvent (water with 1% HAc) to rinse the column and remove the salt. Column length was 5 cm.

B.3.3 Variation in polymerization mixture component to improve peptide retention

Table B.1 Retention factor (k') and backpressure of different materials derived from polystyrene-divinylbenzene monolith. All columns were 50 μm I.D. column with 10 cm monolithic or packing bed. k' was measured using isocratic gradient of 20% MeOH with 2% HAc.

Polymerization mixture compos ition and reference	Applied pressure, flowrate	k' of ME
column packed with 5 μm Alltima C18 particle	400 psi, 108 nl/min	16.02
styrene: 200 μL, divinylbenzene: 200 μL, 1-decanol: 520 μL, tetrahydrofuran: 80 μL[259]	1120 psi,108 nl/min	1.11
PS-DVB prepared as above and surface grafted with stearyl methacrylate[260]	1020 psi, 104 nl/min	2.77
styrene: 100 μL, octadecene: 100 μL, divinylbenzene: 200 μL, 1-decanol: 500 μL, DMF: 100 μL[261]	1000 psi, 108 nl/min	1.58

B.4 Discussion

In this project PS-DVB column capable of retaining and separating enkephalins was fabricated. The column showed good capacity for concentrating ME when the peptide was injected at 0.45 µL/min (Figure B.1). Since the goal of this project was to fabricate monolithic column with low back pressure that could preconcentrate neuropeptides at elevated flow rate to improve analysis speed, I planned to test peptide signal under a range of injection flow rates. However as shown Figure B.2, slight increase of injection flow rate from 0.7 µL/min to 1 µL/min resulted in significant signal reduction of LE, the wide peak shape and shortened retention also indicated that at1 µL/min the column started to lose retention of LE. In addition, ME's signal was totally lost at this flow rate, indicating the column started to lose retention of enkephalins when injection flow rate increased beyond 0.7 µL/min. Under this flow rate it could take ~20 min to inject and desalt 5 µL peptides, which did not fulfill the requirement of fast sample preconcentration. Altering monomer composition to incorporate C18 moiety was explored for increasing retention, however Table B.1 showed that the retention factor was not significantly enhanced, and was still ten times lower compared to that of a packed column. In the meantime, the back pressure of the monolithic columns was two times higher than that of a packed column with the same dimension. Further literature search has revealed that the claimed "low back pressure" of polymer monolithic column referred to their lower back pressure for achieving same protein separation performance compared to UPLC columns, which employs sub 2 µm packing. However the backpressure of such column is not absolutely lower compared to a standard LC column packed with 5 µm

particles[262]. Therefore, the polymer monolithic column was not applied to fast preconcentration of neuropeptides.

Although PS-DVB monolithic column did not exhibit enough retention for rapid preconcentration of neuropeptides, the column may still be useful for extracting and separating molecules that are highly retained and not fully recovered on a packed C18 column, such as proteins. In addition, as discussed in Chapter 5, silica monolithic column may be another promising extraction media for rapid neuropeptide preconcentration.

Appendix C

ELISA method for BDNF

C.1 Objective

To test ELISA kit's sensitivity in detecting BDNF. I chose Promega BDNF Emax ImmunoAssay System because it claims to generate linear calibration curve within the range of 0.6 pM to 37 pM BDNF from 100 µL standard. In addition, this kit does not precoat wells with capture antibody therefore it offers more flexibility for method modification, eg. using 384 well plate instead of 96 well plate to reduce sample volume and improve mass sensitivity .

C.2 Experiment

ELISA was carried out according to vendor's manual, except that 384 well Corning Costar plate (catalog number 3700) was used instead of a recommended 96 well plate of the same material, therefore 30 µL reagents and sample were used for maintaining same liquid height in the well. Also fluorescent detection was applied instead of absorbance because it was found to generate better linearity and sensitivity.

C.3 Result

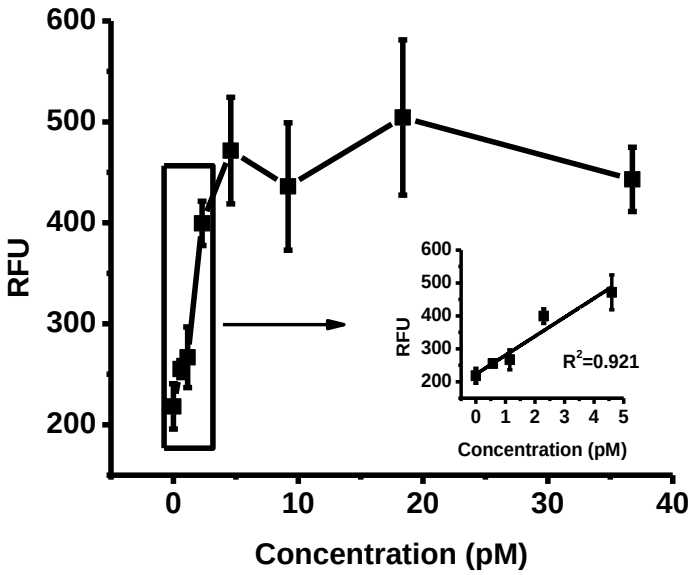

Figure C.1 BDNF calibration curve using Promega BDNF Emax ImmunoAssay System in a 384 well plate

C.4 Discussion

The LOD of this ELISA kit, calculated as blank signal +3×standard deviation of blank, was 1 pM, which was close to the value claimed in vendor's manual. The mass LOD was 30 amol. However the curve reached plateau when BDNF concentration exceeded 5 pM, while the vendor's manual claimed that the linear range should be extended to 37 pM. The fluorescent signal was well below the saturation level of the plate reader. Possible source of the narrow linear range could be the capture antibody's limited capacity to BDNF, therefore longer plate incubation and higher capture antibody concentration was tested, however the observation remained similar. In the meantime we started to develop highly sensitive signature peptide method for BDNF, and the method turned out to have similar mass LOD to the ELISA kit, therefore BDNF's ELISA measurement was not continued.

Appendix D

Supplemental Data for Chapter 3

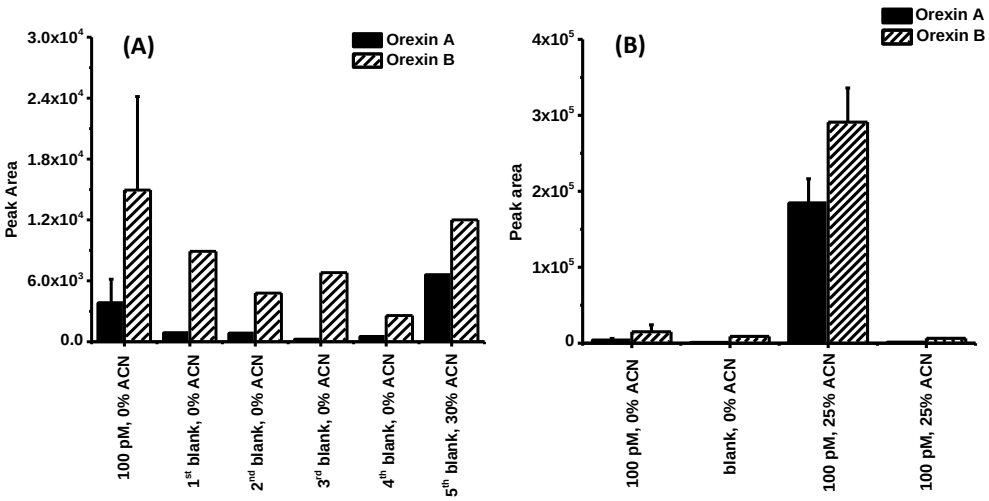

Figure D.1 Adding ACN to peptide sample increased orexin signal by reducing nonspecific adsorption to LC tubing. (A) Indication of peptide adsorption to LC tubing. Triplicate injection of 100 pM orexin A and orexin B in ringer solution, 0.5% FA, followed by 4 repeated injections of blank ringer solution containing 0.5% FA, no ACN (0% ACN blank) and 1 injection of blank ringer solution containing 30% ACN and 0.5% FA (30% ACN blank). (B) Comparison of 100 pM orexins injected with 0% ACN and 25% ACN (3 replicate injection for peptide standard) 1 blank injection after standard injection was also plotted.

The peptides' signal slowly decreased as number of 0% ACN blank injection increased. Orexin A's signal disappeared after two 0% ACN blank injections, while orexin B's signal was still observed in the fourth blank injection. The 30% ACN blank injection after four consecutive 0% ACN injection increased signal for both peptides: for orexin A it was higher than the standard injection and for orexin B the peak area was 80%

of the standard's peak area. This indicated that the LC system was likely to have substantial contribution to adsorption loss.

Carry-over for 0% ACN injection was 20% for orexin A and 60% for orexin B as estimated by peak area from the first blank injection after standard injection. When injected with 25% ACN the carry-over was 0.7 % and 2% for orexin A and orexin B, respectively.

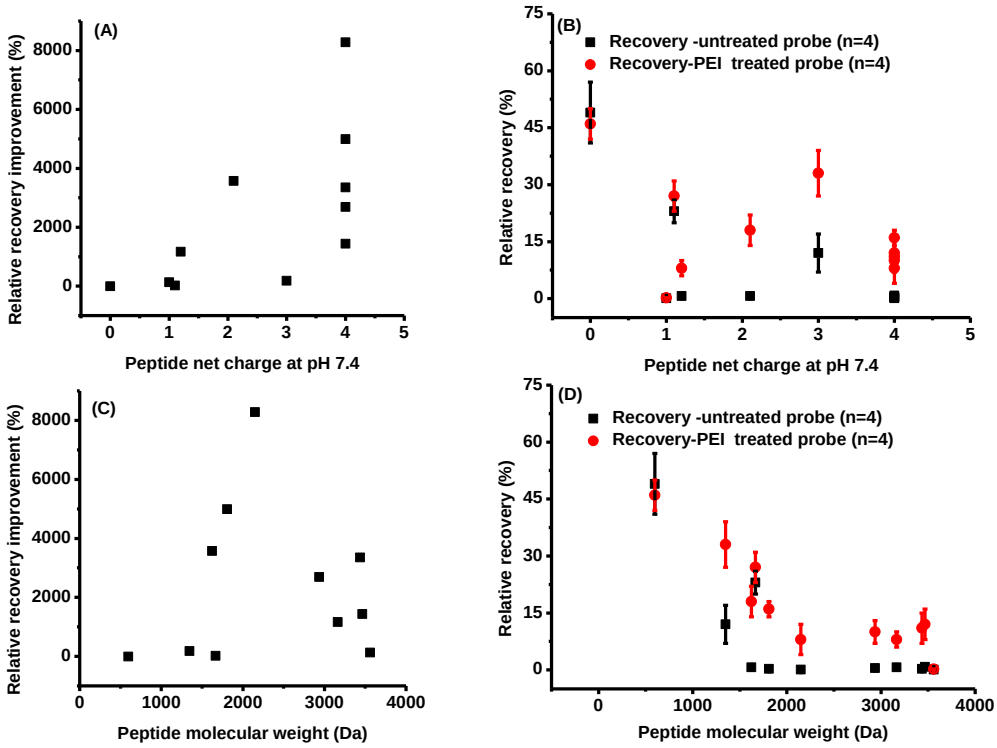

Figure D.2 Correlation between peptide size and charge to probe recovery. (A) Correlation between peptide net charge and improvement of relative recovery when using PEI modified probe; (B) correlation between peptide net charge at pH 7.4 and relative recovery of both PEI modified probe and unmodified probe; (C) correlation between peptide molecular weight and improvement of relative recovery when using PEI modified probe; (D) correlation between peptide molecular weight and relative recovery of both PEI modified probe and unmodified probe.

BIBLIOGRAPHY

(1) Burbach, J. P. H. In *Neuropeptides: Methods and Protocols*; Merighi, A., Ed.; Humana Press Inc: Totowa, 2011; Vol. 789, p 1.

(2) Ogren, S. O.; Kuteeva, E.; Elvander-Tottie, E.; Hokfelt, T. *Eur. J. Pharmacol.* **2010**, *626*, 9.

(3) Le Guen, S.; Nieto, M. M.; Canestrelli, C.; Chen, H. X.; Fournie-Zaluski, M. C.; Cupo, A.; Maldonado, R.; Roques, B. P.; Noble, F. *Pain* **2003**, *104*, 139.

(4) Tsujino, N.; Sakurai, T. *Pharmacol. Rev.* **2009**, *61*, 162.

(5) Yoshida, Y.; Fujiki, N.; Nakajima, T.; Ripley, B.; Matsumura, H.; Yoneda, H.; Mignot, E.; Nishino, S. *Eur. J. Neurosci.* **2001**, *14*, 1075.

(6) DiFeliceantonio, A. G.; Mabrouk, O. S.; Kennedy, R. T.; Berridge, K. C. *Curr. Biol.* **2012**, *22*, 1918.

(7) Blouin, A. M.; Fried, I.; Wilson, C. L.; Staba, R. J.; Behnke, E. J.; Lam, H. A.; Maidment, N. T.; Karlsson, K. A. E.; Lapierre, J. L.; Siegel, J. M. *Nat. Commun.* **2013**, *4*.

(8) Geracioti, T. D.; Carpenter, L. L.; Owens, M. J.; Baker, D. G.; Ekhator, N. N.; Horn, P. S.; Strawn, J. R.; Sanacora, G.; Kinkead, B.; Price, L. H.; Nemeroff, C. B. *Am. J. Psychiat.* **2006**, *163*, 637.

(9) Ratovitski, T.; Gucek, M.; Jiang, H.; Chighladze, E.; Waldron, E.; D'Ambola, J.; Hou, Z.; Liang, Y.; Poirier, M. A.; Hirschhorn, R. R.; Graham, R.; Hayden, M. R.; Cole, R. N.; Ross, C. A. *Journal of Biological Chemistry* **2009**, *284*, 10855.

(10) Castellani, C.; Bimbashi, P.; Ruttenstock, E.; Sacherer, P.; Stojakovic, T.; Weinberg, A. M. *Acta Paediatrica* **2009**, *98*, 1607.

(11) Kolarova, M.; Garcia-Sierra, F.; Bartos, A.; Ricny, J.; Ripova, D. *International journal of Alzheimer's disease* **2012**, *2012*, 731526.

(12) Zilka, N.; Korenova, M.; Kovacech, B.; Iqbal, K.; Novak, M. *Acta Neuropathologica* **2010**, *119*, 679.

(13) Crespi, F. *Anal. Biochem.* **1991**, *194*, 69.

(14) Crespi, F. *Brain Res.* **2011**, *1407*, 27.

(15) Schmidt, A. C.; Dunaway, L. E.; Roberts, J. G.; McCarty, G. S.; Sombers, L. A. *Anal. Chem.* **2014**, *86*, 7806.

(16) Myers, R. D.; Adell, A.; Lankford, M. F. *Neuroscience & Biobehavioral Reviews* **1998**, *22*, 371.

(17) Torto, N.; Gorton, L.; Laurell, T.; Marko-Varga, G. *TrAC Trends in Analytical Chemistry* **1999**, *18*, 252.

(18) Li, Q.; Zubieta, J. K.; Kennedy, R. T. *Anal. Chem.* **2009**, *81*, 2242.

(19) Mabrouk, O. S.; Kennedy, R. T. *J. Neurosci. Methods* **2012**, *209*, 127.

(20) Jacobson, I.; Sandberg, M.; Hamberger, A. *J. Neurosci. Methods* **1985**, *15*, 263.

(21) Smith, A. D.; Justice, J. B. *J. Neurosci. Methods* **1994**, *54*, 75.
(22) Wang, Y.; Wong, S.; Sawchuk, R. *Pharm Res* **1993**, *10*, 1411.
(23) Hershey, N. D.; Kennedy, R. T. *ACS Chem. Neurosci.* **2013**, *4*, 729.
(24) Li, Q., University of Michigan, 2010.
(25) Vasicek, T. W.; Jackson, M. R.; Poseno, T. M.; Stenken, J. A. *ACS Chem. Neurosci.* **2013**, *4*, 737.
(26) Winter, C. D.; Iannotti, F.; Pringle, A. K.; Trikkas, C.; Clough, G. F.; Church, M. K. *J. Neurosci. Methods* **2002**, *119*, 45.
(27) Portnow, J.; Badie, B.; Liu, X. L.; Frankel, P.; Mi, S.; Chen, M. K.; Synold, T. W. *J. Neuro-Oncol.* **2014**, *118*, 169.
(28) Helmy, A.; Carpenter, K. L. H.; Menon, D. K.; Pickard, J. D.; Hutchinson, P. J. A. *J. Cereb. Blood Flow Metab.* **2011**, *31*, 658.
(29) Yamada, K.; Cirrito, J. R.; Stewart, F. R.; Jiang, H.; Finn, M. B.; Holmes, B. B.; Binder, L. I.; Mandelkow, E.-M.; Diamond, M. I.; Lee, V. M. Y.; Holtzman, D. M. *J. Neurosci.* **2011**, *31*, 13110.
(30) Cirrito, J. R.; Yamada, K. A.; Finn, M. B.; Sloviter, R. S.; Bales, K. R.; May, P. C.; Schoepp, D. D.; Paul, S. M.; Mennerick, S.; Holtzman, D. M. *Neuron* **2005**, *48*, 913.
(31) Bero, A. W.; Yan, P.; Roh, J. H.; Cirrito, J. R.; Stewart, F. R.; Raichle, M. E.; Lee, J.-M.; Holtzman, D. M. *Nat Neurosci* **2011**, *14*, 750.
(32) Vaka, S. R. K.; Murthy, S. N.; Repka, M. A.; Nagy, T. *J. Pharm. Sci.* **2011**, *100*, 3139.
(33) Ulrich, J. D.; Burchett, J. M.; Restivo, J. L.; Schuler, D. R.; Verghese, P. B.; Mahan, T. E.; Landreth, G. E.; Castellano, J. M.; Jiang, H.; Cirrito, J. R.; Holtzman, D. M. *Molecular Neurodegeneration* **2013**, *8*.
(34) Emmanouilidou, E.; Elenis, D.; Papasilekas, T.; Stranjalis, G.; Gerozissis, K.; Ioannou, P. C.; Vekrellis, K. *Plos One* **2011**, *6*.
(35) Ebner, K.; Rjabokon, A.; Pape, H. C.; Singewald, N. *Amino Acids* **2011**, *41*, 991.
(36) Takeda, S.; Sato, N.; Ikimura, K.; Nishino, H.; Rakugi, H.; Morishita, R. *Neuroscience* **2011**, *186*, 110.
(37) Francl, J. M.; Kaur, G.; Glass, J. D. *Eur. J. Neurosci.* **2010**, *32*, 1170.
(38) Zhou, Y.; Mabrouk, O. S.; Kennedy, R. T. *J. Am. Soc. Mass Spectrom.* **2013**, *24*, 1700.
(39) Mabrouk, O. S.; Li, Q.; Song, P.; Kennedy, R. T. *J. Neurochem.* **2011**, *118*, 24.
(40) Keen, K. L.; Wegner, F. H.; Bloom, S. R.; Ghatei, M. A.; Terasawa, E. *Endocrinology* **2008**, *149*, 4151.
(41) Frost, S. I.; Keen, K. L.; Levine, J. E.; Terasawa, E. *J. Neurosci. Methods* **2008**, *168*, 26.
(42) Francl, J. M.; Kaur, G.; Glass, J. D. *Neuroreport* **2010**, *21*, 1055.
(43) Lam, M.; Gianoulakis, C. *Psychopharmacology* **2011**, *218*, 229.
(44) Ide, S.; Hara, T.; Ohno, A.; Tamano, R.; Koseki, K.; Naka, T.; Maruyama, C.; Kaneda, K.; Yoshioka, M.; Minami, M. *J. Neurosci.* **2013**, *33*, 5881.

(45) Maes, K.; Béchade, G.; Van Schoors, J.; Van Wanseele, Y.; Van Liefferinge, J.; Michotte, Y.; Harden, S. N.; Chambers, E. E.; Claereboudt, J.; Smolders, I.; Van Eeckhaut, A. *Bioanalysis* **2015**, *7*, 605.

(46) Patterson, C. M.; Wong, J. M.; Leinninger, G. M.; Allison, M. B.; Mabrouk, O. S.; Kasper, C. L.; Gonzalez, I. E.; Mackenzie, A.; Jones, J. C.; Kennedy, R. T.; Myers, M. G., Jr. *Endocrinology* **2015**, *3*.

(47) Jalkanen, A. J.; Savolainen, K.; Forsberg, M. M. *Neuroscience Letters* **2011**, *502*, 107.

(48) Lam, M. P.; Gianoulakis, C. *Alcohol* **2011**, *45*, 621.

(49) Marti, M.; Sarubbo, S.; Latini, F.; Cavallo, M.; Eleopra, R.; Biguzzi, S.; Lettieri, C.; Conti, C.; Simonato, M.; Zucchini, S.; Quatrale, R.; Sensi, M.; Candeletti, S.; Romualdi, P.; Morari, M. *Mov. Disord.* **2010**, *25*, 1723.

(50) Glass, J. D.; Guinn, J.; Kaur, G.; Francl, J. M. *Eur. J. Neurosci.* **2010**, *31*, 1117.

(51) Angulo, J. A.; McEwen, B. S. *Brain Res. Rev.* **1994**, *19*, 1.

(52) Latimer, L. G.; Duffy, P.; Kalivas, P. W. *J. Pharmacol. Exp. Ther.* **1987**, *241*, 328.

(53) Garzon, M.; Pickel, V. M. *Neuroscience* **2002**, *114*, 461.

(54) Kalivas, P. W.; Widerlov, E.; Stanley, D.; Breese, G.; Prange, A. J. *J. Pharmacol. Exp. Ther.* **1983**, *227*, 229.

(55) Marinelli, P. W.; Bai, L.; Quirion, R.; Gianoulakis, C. *Alcoholism* **2005**, *29*, 1821.

(56) Vanderah, T. W.; Laughlin, T.; Lashbrook, J. M.; Nichols, M. L.; Wilcox, G. L.; Ossipov, M. H.; Malan, T. P.; Porreca, F. *Pain* **1996**, *68*, 275.

(57) Bruchas, M. R.; Land, B. B.; Chavkin, C. *Brain Res.* **2010**, *1314*, 44.

(58) Carr, K. D.; Bak, T. H. *Brain Res.* **1990**, *507*, 289.

(59) Leitermann, R. J.; Terashvili, M.; Mizoguchi, H.; Wu, H. E.; Chen, F.; Clithero, A.; Tseng, L. F. *Eur. J. Pharmacol.* **2004**, *504*, 177.

(60) Lam, M.; Marinelli, P.; Bai, L.; Gianoulakis, C. *Psychopharmacology* **2008**, *201*, 261.

(61) Zangen, A.; Herzberg, U.; Vogel, Z.; Yadid, G. *Neuroscience* **1998**, *85*, 659.

(62) Grandison, L.; Guidotti, A. *Neuropharmacology* **1977**, *16*, 533.

(63) Yadid, G.; Zangen, A.; Herzberg, U.; Nakash, R.; Sagen, J. *Neuropsychopharmacology* **2000**, *23*, 709.

(64) O'Donohue, T. L.; Miller, R. L.; Jacobowitz, D. M. *Brain Res.* **1979**, *176*, 101.

(65) Tsujii, S.; Bray, G. A. *Brain Research Bulletin* **1989**, *23*, 165.

(66) Navarro, M.; Cubero, I.; Knapp, D. J.; Breese, G. R.; Thiele, T. E. *Alcoholism* **2008**, *32*, 266.

(67) Patlolla, R. R.; Mallampati, R.; Fulzele, S. V.; Babu, R. J.; Singh, M. *Toxicology letters* **2009**, *185*, 168.

(68) Watanobe, H. *J. Physiol.-London* **2002**, *545*, 255.

(69) Watanobe, H.; Habu, S. *J. Neurosci.* **2002**, *22*, 6265.

(70) Lu, X. Y.; Mazarati, A.; Sanna, P.; Shinmei, S.; Bartfai, T. *Neuropeptides* **2005**, *39*, 147.

(71) Crawley, J. N.; Robinson, J. K.; Langel, U.; Bartfai, T. *Brain Res.* **1993**, *600*, 268.

(72) Narvaez, J. A.; Diaz, Z.; Aguirre, J. A.; Gonzalezbaron, S.; Yanaihara, N.; Fuxe, K.; Hedlund, P. B. *Eur. J. Pharmacol.* **1994**, *257*, 257.

(73) Misawa, K.; Kanazawa, T.; Misawa, Y.; Uehara, T.; Imai, A.; Takahashi, G.; Takebayashi, S.; Cole, A.; Carey, T. E.; Mineta, H. *Transl. Oncol.* **2013**, *6*, 338.

(74) Hilke, S.; Theodorsson, A.; Fetissov, S.; Aman, K.; Holm, L.; Hokfelt, T.; Theodorsson, E. *Eur. J. Neurosci.* **2005**, *21*, 2089.

(75) Blakeman, K. H.; Wiesenfeld-Hallin, Z.; Alster, P. *Exp. Brain Res.* **2001**, *139*, 354.

(76) Lieb, K.; Ahlvers, K.; Dancker, K.; Strohbusch, S.; Reincke, M.; Feige, B.; Berger, M.; Riemann, D.; Voderholzer, U. *Neuropsychopharmacology* **2002**, *27*, 1041.

(77) Ebner, K.; Rupniak, N. M.; Saria, A.; Singewald, N. *Proc. Natl. Acad. Sci. U. S. A.* **2004**, *101*, 4280.

(78) Cador, M.; Kelley, A. E.; Le Moal, M.; Stinus, L. *Neuroscience* **1986**, *18*, 659.

(79) Xin, L.; Geller, E. B.; LiuChen, L. Y.; Chen, C. G.; Adler, M. W. *J. Pharmacol. Exp. Ther.* **1997**, *282*, 1055.

(80) Hanson, G. R.; Bush, L.; Keefe, K. A.; Alburges, M. E. *J. Neurochem.* **2002**, *82*, 1171.

(81) Neubert, J. K.; Matsuka, Y.; Maidment, N. T.; Spigelman, I. *Brain Research Protocols* **2002**, *10*, 102.

(82) Fenzl, T.; Flachskamm, C.; Rossbauer, M.; Deussing, J. M.; Kimura, M. *Behavioural brain research* **2009**, *203*, 143.

(83) Kiyashchenko, L. I.; Mileykovskiy, B. Y.; Maidment, N.; Lam, H. A.; Wu, M. F.; John, J.; Peever, J.; Siegel, J. M. *J. Neurosci.* **2002**, *22*, 5282.

(84) Kastin, A. J.; Akerstrom, V. *J. Pharmacol. Exp. Ther.* **1999**, *289*, 219.

(85) Flores, C. A.; Wang, X. M.; Zhang, K. M.; Mokha, S. S. *Neuroscience* **2001**, *105*, 489.

(86) Witkin, J. M.; Statnick, M. A.; Rorick-Kehn, L. M.; Pintar, J. E.; Ansonoff, M.; Chen, Y.; Tucker, R. C.; Ciccocioppo, R. *Pharmacology & Therapeutics* **2014**, *141*, 283.

(87) Aparicio, L. C.; Candeletti, S.; Binaschi, A.; Mazzuferi, M.; Mantovani, S.; Di Benedetto, M.; Landuzzi, D.; Lopetuso, G.; Romualdi, P.; Simonato, M. *J. Neurochem.* **2004**, *91*, 30.

(88) Javanmard, M.; Shlik, J.; Kennedy, S. H.; Vaccarino, F. J.; Houle, S.; Bradwejn, J. *Biological Psychiatry*, *45*, 872.

(89) Shlik, J.; Koszycki, D.; Bradwejn, J. *Peptides* **1998**, *19*, 969.

(90) Erel, U.; Arborelius, L.; Brodin, E. *Brain Res.* **2004**, *1022*, 39.

(91) Xie, J. Y.; Herman, D. S.; Stiller, C. O.; Gardell, L. R.; Ossipov, M. H.; Lai, J.; Porreca, F.; Vanderah, T. W. *J. Neurosci.* **2005**, *25*, 409.

(92) Numakawa, T.; Suzuki, S.; Kumamaru, E.; Adachi, N.; Richards, M.; Kunugi, H. *Histol. Histopath.* **2010**, *25*, 237.

(93) Ferrer, I.; Marin, C.; Rey, M. J.; Ribalta, T.; Goutan, E.; Blanco, R.; Tolosa, E.; Marti, E. *J. Neuropathol. Exp. Neurol.* **1999**, *58*, 729.

(94) Laske, C.; Stransky, E.; Leyhe, T.; Eschweiler, G. W.; Maetzler, W.; Wittorf, A.; Soekadar, S.; Richartz, E.; Koehler, N.; Bartels, M.; Buchkremer, G.; Schott, K. *J. Psychiatr. Res.* **2007**, *41*, 387.

(95) Faria, M. C.; Goncalves, G. S.; Rocha, N. P.; Moraes, E. N.; Bicalho, M. A.; Cintra, M. T. G.; de Paula, J. J.; de Miranda, L.; Ferreira, A. C. D.; Teixeira, A. L.; Gomes, K. B.; Carvalho, M. D.; Sousa, L. P. *J. Psychiatr. Res.* **2014**, *53*, 166.

(96) Lee, B.-H.; Kim, Y.-K. *Psychiatry Investigation* **2010**, *7*, 231.

(97) Lee, B.-H.; Kim, Y.-K. *Progress in Neuro-Psychopharmacology and Biological Psychiatry* **2009**, *33*, 849.

(98) Rabie, M. A.; Mohsen, M.; Ibrahim, M.; Mahmoud, R. E. S. *J. Affect. Disord.* **2014**, *162*, 67.

(99) Yang, L. L.; Zhang, Z. J.; Sun, D. M.; Xu, Z.; Yuan, Y. G.; Zhang, X. R.; Li, L. J. *Int. J. Geriatr. Psychiatr.* **2011**, *26*, 495.

(100) Arancibia, S.; Lecomte, A.; Silhol, M.; Aliaga, E.; Tapia-Arancibia, L. *Neuroscience* **2007**, *146*, 864.

(101) Dahlin, A. P.; Hjort, K.; Hillered, L.; Sjodin, M. O. D.; Bergquist, J.; Wetterhall, M. *Anal. Bioanal. Chem.* **2012**, *402*, 2057.

(102) Grohganz, H.; Rischer, M.; Brandl, M. *Eur. J. Pharm. Sci.* **2004**, *21*, 191.

(103) Dahlin, A. P.; Wetterhall, M.; Caldwell, K. D.; Larsson, A.; Bergquist, J.; Hillered, L.; Hjort, K. *Anal. Chem.* **2010**, *82*, 4376.

(104) Hasegawa, T.; Iwasaki, Y.; Ishihara, K. *Biomaterials* **2001**, *22*, 243.

(105) Lavaud, S.; Canivet, E.; Wuillai, A.; Maheut, H.; Randoux, C.; Bonnet, J. M.; Renaux, J. L.; Chanard, J. *Nephrol. Dial. Transplant.* **2003**, *18*, 2097.

(106) Qin, H.; Sun, C.; He, C.; Wang, D.; Cheng, C.; Nie, S.; Sun, S.; Zhao, C. *Journal of Membrane Science* **2014**, *468*, 172.

(107) Riyasudheen, N.; Paul, M. J.; Sujith, A. *Chemical Engineering & Technology* **2014**, *37*, 1021.

(108) Thomas, M.; Valette, P.; Mausset, A. L.; Dejardin, P. *Int. J. Artif. Organs* **2000**, *23*, 20.

(109) Vezzani, A.; Ruiz, R.; Monno, A.; Rizzi, M.; Lindefors, N.; Samanin, R.; Brodin, E. *J. Neurochem.* **1993**, *60*, 671.

(110) Gustafsson, H.; de Araujo Lucas, G.; Schött, E.; Stiller, C.-O.; Alster, P.; Wiesenfeld-Hallin, Z.; Brodin, E. *Brain Research Protocols* **1999**, *4*, 192.

(111) Wilson, L. B.; Fuchs, I. E.; Matsukawa, K.; Mitchell, J. H.; Wall, P. T. *J. Physiol.-London* **1993**, *460*, 79.

(112) Ren, J. Z.; Li, Z. S.; Wong, F. S. *Journal of Membrane Science* **2006**, *279*, 558.

(113) Kjellstrom, S.; Lindberg, S.; Laurell, T.; Marko-Varga, G. *Chromatographia* **2000**, *52*, 334.

(114) Winter, C. D.; Iannotti, F.; Pringle, A. K.; Trikkas, C.; Clough, G. F.; Church, M. K. *J. Neurosci. Methods* **2002**, *119*, 45.

(115) Trickler, W.; Miller, D. W. *J. Pharm. Sci.* **2003**, *92*, 1419.

(116) Keeler, G. D.; Durdik, J. M.; Stenken, J. A. *Eur. J. Pharm. Sci.* **2014**, *57*, 60.

(117) Rosenbloom, A. J.; Ferris, R.; Sipe, D. M.; Riddler, S. A.; Connolly, N. C.; Abe, K.; Whiteside, T. L. *J. Immunol. Methods* **2006**, *309*, 55.

(118) Roy, M. C.; Ikimura, K.; Nishino, H.; Naito, T. *Anal. Biochem.* **2010**, *399*, 305.

(119) Fletcher, H. J.; Stenken, J. A. *Anal. Chim. Acta* **2008**, *620*, 170.

(120) Herbaugh, A. W.; Stenken, J. A. *J. Neurosci. Methods* **2011**, *202*, 124.

(121) Wang, Y. X.; Stenken, J. A. *Anal. Chim. Acta* **2009**, *651*, 105.

(122) Ao, X. P.; Stenken, J. A. *Analyst* **2006**, *131*, 62.

(123) Ao, X. P.; Sellati, T. J.; Stenken, J. A. *Anal. Chem.* **2004**, *76*, 3777.

(124) Schmerberg, C. M.; Li, L. J. *Anal. Chem.* **2013**, *85*, 915.

(125) Pettersson, A.; Amirkhani, A.; Arvidsson, B.; Markides, K.; Bergquist, J. *Anal. Chem.* **2004**, *76*, 1678.

(126) Hillman, J.; Aneman, O.; Anderson, C.; Sjogren, F.; Saberg, C.; Mellergard, P. *Neurosurgery* **2005**, *56*, 1264.

(127) Kai, J.; Puntambekar, A.; Santiago, N.; Lee, S. H.; Sehy, D. W.; Moore, V.; Han, J.; Ahn, C. H. *Lab Chip* **2012**, *12*, 4257.

(128) Geissler, D.; Charbonniere, L. J.; Ziessel, R. F.; Butlin, N. G.; Loehmannsroeben, H.-G.; Hildebrandt, N. *Angewandte Chemie-International Edition* **2010**, *49*, 1396.

(129) Jia, M.; Belyavskaya, E.; Deuster, P.; Sternberg, E. M. *Anal. Chem.* **2012**, *84*, 6508.

(130) Li, Y.-Y.; Zhang, C.; Li, B.-S.; Zhao, L.-F.; Li, X.-B.; Yang, W.-J.; Xu, S.-Q. *Clinical Chemistry* **2007**, *53*, 1061.

(131) Mendoza, L. G.; McQuary, P.; Mongan, A.; Gangadharan, R.; Brignac, S.; Eggers, M. *Biotechniques* **1999**, *27*, 778.

(132) Song, E. Y.; VanDunk, C.; Kuddo, T.; Nelson, P. G. *J. Immunol. Methods* **2005**, *300*, 63.

(133) Craig-Schapiro, R.; Kuhn, M.; Xiong, C.; Pickering, E. H.; Liu, J.; Misko, T. P.; Perrin, R. J.; Bales, K. R.; Soares, H.; Fagan, A. M.; Holtzman, D. M. *Plos One* **2011**, *6*.

(134) Wang, J.; Ahmad, H.; Ma, C.; Shi, Q.; Vermesh, O.; Vermesh, U.; Heath, J. *Lab Chip* **2010**, *10*, 3157.

(135) Gorkin, R.; Park, J.; Siegrist, J.; Amasia, M.; Lee, B. S.; Park, J.-M.; Kim, J.; Kim, H.; Madou, M.; Cho, Y.-K. *Lab Chip* **2010**, *10*, 1758.

(136) Honda, N.; Lindberg, U.; Andersson, P.; Hoffman, S.; Takei, H. *Clinical Chemistry* **2005**, *51*, 1955.

(137) Shen, H.; Lada, M. W.; Kennedy, R. T. *J. Chromatogr. B* **1997**, *704*, 43.

(138) Shen, H.; Witowski, S. R.; Boyd, B. W.; Kennedy, R. T. *Anal. Chem.* **1999**, *71*, 987.

(139) Lanckmans, K.; Stragier, B.; Sarre, S.; Smolders, I.; Michotte, Y. *J. Sep. Sci.* **2007**, *30*, 2217.

(140) Baseski, H. M.; Watson, C. J.; Cellar, N. A.; Shackman, J. G.; Kennedy, R. T. *J. Mass Spectrom.* **2005**, *40*, 146.

(141) Haskins, W. E.; Wang, Z. Q.; Watson, C. J.; Rostand, R. R.; Witowski, S. R.; Powell, D. H.; Kennedy, R. T. *Anal. Chem.* **2001**, *73*, 5005.

(142) Andren, P. E.; Caprioli, R. M. *Brain Res.* **1999**, *845*, 123.

(143) Maes, K.; Van Liefferinge, J.; Viaene, J.; Van Schoors, J.; Van Wanseele, Y.; Bechade, G.; Chambers, E. E.; Morren, H.; Michotte, Y.; Heyden, Y. V.; Claereboudt, J.; Smolders, I.; Van Eeckhauta, A. *J. Chromatogr. A* **2014**, *1360*, 217.

(144) Sobhi, H. R.; Vatansever, B.; Wortmann, A.; Grouzmann, E.; Rochat, B. *J. Chromatogr. A* **2011**, *1218*, 8536.

(145) Korecka, M.; Waligorska, T.; Figurski, M.; Toledo, J. B.; Arnold, S. E.; Grossman, M.; Trojanowski, J. Q.; Shaw, L. M. *Journal of Alzheimers Disease* **2014**, *41*, 441.

(146) Lame, M. E.; Chambers, E. E.; Blatnik, M. *Anal. Biochem.* **2011**, *419*, 133.

(147) Pannee, J.; Portelius, E.; Oppermann, M.; Atkins, A.; Hornshaw, M.; Zegers, I.; Hojrup, P.; Minthon, L.; Hansson, O.; Zetterberg, H.; Blennow, K.; Gobom, J. *Journal of Alzheimers Disease* **2013**, *33*, 1021.

(148) Bronsema, K. J.; Bischoff, R.; van de Merbel, N. C. *Anal. Chem.* **2013**, *85*, 9528.

(149) Mesmin, C.; Dubois, M.; Becher, F.; Fenaille, F.; Ezan, E. *Rapid Commun. Mass Spectrom.* **2010**, *24*, 2875.

(150) Liu, Z.; Ren, C.; Jones, W.; Chen, P.; Seminara, S. B.; Chan, Y.-M.; Smith, N. F.; Covey, J. M.; Wang, J.; Chan, K. K. *Journal of Chromatography B-Analytical Technologies in the Biomedical and Life Sciences* **2013**, *926*, 1.

(151) Zhang, G.; Zhang, Y.; Fast, D. M.; Lin, Z.; Steenwyk, R. *Anal. Biochem.* **2011**, *416*, 45.

(152) Balchen, M.; Lund, H.; Reubsaet, L.; Pedersen-Bjergaard, S. *Anal. Chim. Acta* **2012**, *716*, 16.

(153) Wang, H.; Chung-Davidson, Y.-W.; Li, W. *J. Chromatogr. A* **2014**, *1345*, 98.

(154) Rose, R. J.; Damoc, E.; Denisov, E.; Makarov, A.; Heck, A. J. R. *Nat. Methods* **2012**, *9*, 1084.

(155) Sobott, F.; Hernandez, H.; McCammon, M. G.; Tito, M. A.; Robinson, C. V. *Anal. Chem.* **2002**, *74*, 1402.

(156) van den Heuvel, R. H. H.; van Duijn, E.; Mazon, H.; Synowsky, S. A.; Lorenzen, K.; Versluis, C.; Brouns, S. J. J.; Langridge, D.; van der Oost, J.; Hoyes, J.; Heck, A. J. R. *Anal. Chem.* **2006**, *78*, 7473.

(157) Belov, M. E.; Gorshkov, M. V.; Udseth, H. R.; Anderson, G. A.; Smith, R. D. *Anal. Chem.* **2000**, *72*, 2271.

(158) Yan, X. W.; Xu, M.; Yang, L. M.; Wang, Q. Q. *Anal. Chem.* **2010**, *82*, 1261.

(159) Yang, M. W.; Wu, W. H.; Ruan, Y. J.; Huang, L. M.; Wu, Z. J.; Cai, Y.; Fu, F. F. *Anal. Chim. Acta* **2014**, *812*, 12.

(160) Urban, P. L.; Jefimovs, K.; Amantonico, A.; Fagerer, S. R.; Schmid, T.; Madler, S.; Puigmarti-Luis, J.; Goedecke, N.; Zenobi, R. *Lab Chip* **2010**, *10*, 3206.

(161) Borrebaeck, C. A. K.; Ekstrom, S.; Hager, A. C. M.; Nilsson, J.; Laurell, T.; Marko-Varga, G. *Biotechniques* **2001**, *30*, 1126.

(162) Schuerenbeg, M.; Luebbert, C.; Eickhoff, H.; Kalkum, M.; Lehrach, H.; Nordhoff, E. *Anal. Chem.* **2000**, *72*, 3436.

(163) Jespersen, S.; Niessen, W. M. A.; Tjaden, U. R.; Vandergreef, J.; Litborn, E.; Lindberg, U.; Roeraade, J. *Rapid Commun. Mass Spectrom.* **1994**, *8*, 581.

(164) Botting, C. H. *Rapid Commun. Mass Spectrom.* **2003**, *17*, 598.

(165) Hung, K. C.; Ding, H.; Guo, B. C. *Anal. Chem.* **1999**, *71*, 518.

(166) Tu, T.; Sauter, A. D., Jr.; Sauter, A. D., III; Gross, M. L. *J. Am. Soc. Mass Spectrom.* **2008**, *19*, 1086.

(167) Kirkpatrick, D. S.; Gerber, S. A.; Gygi, S. P. *Methods* **2005**, *35*, 265.

(168) Halquist, M. S.; Karnes, H. T. *Biomedical Chromatography* **2011**, *25*, 47.

(169) Anderson, N. L.; Anderson, N. G.; Haines, L. R.; Hardie, D. B.; Olafson, R. W.; Pearson, T. W. *J. Proteome Res.* **2004**, *3*, 235.

(170) Wu, S. T.; Ouyang, Z.; Olah, T. V.; Jemal, M. *Rapid Commun. Mass Spectrom.* **2011**, *25*, 281.

(171) Addona, T. A.; Abbatiello, S. E.; Schilling, B.; Skates, S. J.; Mani, D. R.; Bunk, D. M.; Spiegelman, C. H.; Zimmerman, L. J.; Ham, A.-J. L.; Keshishian, H.; Hall, S. C.; Allen, S.; Blackman, R. K.; Borchers, C. H.; Buck, C.; Cardasis, H. L.; Cusack, M. P.; Dodder, N. G.; Gibson, B. W.; Held, J. M.; Hiltke, T.; Jackson, A.; Johansen, E. B.; Kinsinger, C. R.; Li, J.; Mesri, M.; Neubert, T. A.; Niles, R. K.; Pulsipher, T. C.; Ransohoff, D.; Rodriguez, H.; Rudnick, P. A.; Smith, D.; Tabb, D. L.; Tegeler, T. J.; Variyath, A. M.; Vega-Montoto, L. J.; Wahlander, A.; Waldemarson, S.; Wang, M.; Whiteaker, J. R.; Zhao, L.; Anderson, N. L.; Fisher, S. J.; Liebler, D. C.; Paulovich, A. G.; Regnier, F. E.; Tempst, P.; Carr, S. A. *Nat. Biotechnol.* **2009**, *27*, 864.

(172) van den Broek, I.; Romijn, F. P. H. T. M.; Smit, N. P. M.; van der Laarse, A.; Drijfhout, J. W.; van der Burgt, Y. E. M.; Cobbaert, C. M. *J. Proteome Res.* **2015**, *14*, 928.

(173) Glatter, T.; Ludwig, C.; Ahrne, E.; Aebersold, R.; Heck, A. J. R.; Schmidt, A. *J. Proteome Res.* **2012**, *11*, 5145.

(174) Freije, J. R.; Mulder, P.; Werkman, W.; Rieux, L.; Niederlander, H. A. G.; Verpoorte, E.; Bischoff, R. *J. Proteome Res.* **2005**, *4*, 1805.

(175) Jeng, J.; Lin, M.-F.; Cheng, F.-Y.; Yeh, C.-S.; Shiea, J. *Rapid Commun. Mass Spectrom.* **2007**, *21*, 3060.

(176) Stigter, E. C. A.; de Jong, G. J.; van Bennekorn, W. P. *Anal. Bioanal. Chem.* **2007**, *389*, 1967.

(177) Proc, J. L.; Kuzyk, M. A.; Hardie, D. B.; Yang, J.; Smith, D. S.; Jackson, A. M.; Parker, C. E.; Borchers, C. H. *J. Proteome Res.* **2010**, *9*, 5422.

(178) Russell, W. K.; Park, Z. Y.; Russell, D. H. *Anal. Chem.* **2001**, *73*, 2682.

(179) Park, Z. Y.; Russell, D. H. *Anal. Chem.* **2000**, *72*, 2667.

(180) Barton, C.; Kay, R. G.; Gentzer, W.; Vitzthum, F.; Pleasance, S. *J. Proteome Res.* **2010**, *9*, 333.

(181) Lecchi, P.; Gupte, A. R.; Perez, R. E.; Stockert, L. V.; Abramson, F. P. *Journal of Biochemical and Biophysical Methods* **2003**, *56*, 141.

(182) Wisniewski, J. R.; Zougman, A.; Nagaraj, N.; Mann, M. *Nat. Methods* **2009**, *6*, 359.

(183) Keshishian, H.; Addona, T.; Burgess, M.; Kuhn, E.; Carr, S. A. *Mol. Cell. Proteomics* **2007**, *6*, 2212.

(184) Berna, M.; Ott, L.; Engle, S.; Watson, D.; Solter, P.; Ackermann, B. *Anal. Chem.* **2008**, *80*, 561.

(185) Palandra, J.; Finelli, A.; Zhu, M.; Masferrer, J.; Neubert, H. *Anal. Chem.* **2013**, *85*, 5522.

(186) Berna, M.; Ackermann, B. *Anal. Chem.* **2009**, *81*, 3950.

(187) McAvoy, T.; Lassman, M. E.; Spellman, D. S.; Ke, Z.; Howell, B. J.; Wong, O.; Zhu, L.; Tanen, M.; Struyk, A.; Laterza, O. F. *Clinical Chemistry* **2014**, *60*, 683.

(188) Shi, T.; Fillmore, T. L.; Sun, X.; Zhao, R.; Schepmoes, A. A.; Hossain, M.; Xie, F.; Wu, S.; Kim, J.-S.; Jones, N.; Moore, R. J.; Pasa-Tolic, L.; Kagan, J.; Rodland, K. D.; Liu, T.; Tang, K.; Camp, D. G., II; Smith, R. D.; Qian, W.-J. *Proc. Natl. Acad. Sci. U. S. A.* **2012**, *109*, 15395.

(189) Shi, T. J.; Sun, X. F.; Gao, Y. Q.; Fillmore, T. L.; Schepmoes, A. A.; Zhao, R.; He, J. T.; Moore, R. J.; Kagan, J.; Rodland, K. D.; Liu, T.; Liu, A. Y.; Smith, R. D.; Tang, K. Q.; Camp, D. G.; Qian, W. J. *J. Proteome Res.* **2013**, *12*, 3353.

(190) Willie, J. T.; Chemelli, R. M.; Sinton, C. M.; Yanagisawa, M. *Annu. Rev. Neurosci.* **2001**, *24*, 429.

(191) Heilig, M. *Neuropeptides* **2004**, *38*, 213.

(192) DiLeone, R. J.; Georgescu, D.; Nestler, E. J. *Life Sciences* **2003**, *73*, 759.

(193) Lambert, R. C.; Moos, F. C.; Richard, P. *Neuroscience* **1993**, *57*, 1027.

(194) Guerriero, K. A.; Keen, K. L.; Terasawa, E. *Endocrinology* **2012**, *153*, 1887.

(195) Maidment, N. T.; Brumbaugh, D. R.; Rudolph, V. D.; Erdelyi, E.; Evans, C. J. *Neuroscience* **1989**, *33*, 549.

(196) Kendrick, K. M. *J. Neurosci. Methods* **1990**, *34*, 35.

(197) Freed, A. L.; Cooper, J. D.; Davies, M. I.; Lunte, S. M. *J. Neurosci. Methods* **2001**, *109*, 23.

(198) Kostel, K. L.; Lunte, S. M. *J. Chromatogr. B. Biomed. Sci. App.* **1997**, *695*, 27.

(199) Desiderio, D. M.; Zhu, X. G. *J. Chromatogr. A* **1998**, *794*, 85.

(200) Xu, N.; Qiu, C.; Wang, W.; Wang, Y.; Chai, C.; Yan, Y.; Zhu, D. *J. Pharm. Biomed. Anal.* **2011**, *55*, 101.

(201) Sinnaeve, B. A.; Storme, M. L.; Van Bocxlaer, J. F. *J. Sep. Sci.* **2005**, *28*, 1779.

(202) Dawson, R.; Steves, J. P.; Lorden, J. F.; Oparil, S. *Peptides* **1985**, *6*, 1173.

(203) Marinelli, P. W.; Lam, M.; Bai, L.; Quirion, R.; Gianoulakis, C. *Alcoholism* **2006**, *30*, 982.

(204) Liu, Z. R.; Welin, M.; Bragee, B.; Nyberg, F. *Peptides* **2000**, *21*, 853.

(205) Behrens, H. L.; Chen, R. B.; Li, L. J. *Anal. Chem.* **2008**, *80*, 6949.

(206) Constantopoulos, T. L.; Jackson, G. S.; Enke, C. G. *J. Am. Soc. Mass Spectrom.* **1999**, *10*, 625.

(207) Reed, B.; Bidlack, J. M.; Chait, B. T.; Kreek, M. J. *Journal of Neuroendocrinology* **2008**, *20*, 606.

(208) Giddings, J. C. *Unified separation science*; Wiley: New York, 1991.

(209) Hokfelt, T.; Ljungdahl, A.; Terenius, L.; Elde, R.; Nilsson, G. *Proc. Natl. Acad. Sci. U. S. A.* **1977**, *74*, 3081.

(210) Whistler, J. L.; Chuang, H. H.; Chu, P.; Jan, L. Y.; von Zastrow, M. *Neuron* **1999**, *23*, 737.

(211) Paxinos, G.; Watson, C. J. *The Rat Brain in Stereotaxic Coordinates*; Elsevier, 2007.

(212) Heemskerk, A. A. M.; Busnel, J.-M.; Schoenmaker, B.; Derks, R. J. E.; Klychnikov, O.; Hensbergen, P. J.; Deelder, A. M.; Mayboroda, O. A. *Anal. Chem.* **2012**, *84*, 4552.

(213) Wilm, M.; Mann, M. *Anal. Chem.* **1996**, *68*, 1.

(214) Vandeemter, J. J.; Zuiderweg, F. J.; Klinkenberg, A. *Chemical Engineering Science* **1956**, *5*, 271.

(215) Song, P.; Mabrouk, O. S.; Hershey, N. D.; Kennedy, R. T. *Anal. Chem.* **2012**, *84*, 412.

(216) Siegel, R. E.; Eiden, L. E.; Affolter, H. U. *Neuropeptides* **1985**, *6*, 543.

(217) Richter, J. A.; Wesche, D. L.; Frederickson, R. C. A. *Eur. J. Pharmacol.* **1979**, *56*, 105.

(218) Simantov, R.; Kuhar, M. J.; Uhl, G. R.; Snyder, S. H. *Proc. Natl. Acad. Sci. U. S. A.* **1977**, *74*, 2167.

(219) Wamsley, J. K.; Young, W. S.; Kuhar, M. J. *Brain Res.* **1980**, *190*, 153.

(220) Sirinathsinghji, D. J. S.; Nikolarakis, K. E.; Herz, A. *Brain Res.* **1989**, *490*, 276.

(221) Ungerstedt, U.; Herrera-Marschitz, M.; Jungnelius, U.; Stahle, L.; Tossman, U.; Zetterstrom, T. In *Kohsaka, M. Et Al.* 1982, p P219.

(222) Zhang, M. Y.; Beyer, C. E. *J. Pharm. Biomed. Anal.* **2006**, *40*, 492.

(223) Galvan, A.; Smith, Y.; Wichmann, T. *J. Neurosci. Methods* **2003**, *126*, 175.

(224) Tsai, P.-J.; Wu, J.-P.; Lin, N.-N.; Kuo, J.-S.; Yang, C.-S. *Journal of Chromatography B: Biomedical Sciences and Applications* **1996**, *686*, 151.

(225) Khan, A. S.; Michael, A. C. *TrAC Trends in Analytical Chemistry* **2003**, *22*, 503.

(226) Kottegoda, S.; Shaik, I.; Shippy, S. A. *J. Neurosci. Methods* **2002**, *121*, 93.

(227) Anne, L.; Hu, M.; Chan, K.; Colin, L.; Gottwald, K. *Ther. Drug Monit.* **1989**, *11*, 585.

(228) Emmett, M. R.; Andren, P. E.; Caprioli, R. M. *J. Neurosci. Methods* **1995**, *62*, 141.

(229) Nilsson, C. L.; Karlsson, G.; Bergquist, J.; Westman, A.; Ekman, R. *Peptides* **1998**, *19*, 781.

(230) Hyenstrand, P.; Metcalf, J. S.; Beattie, K. A.; Codd, G. A. *Toxicon* **2001**, *39*, 589.

(231) Warwood, S.; Byron, A.; Humphries, M. J.; Knight, D. *Journal of Proteomics* **2013**, *85*, 160.

(232) van Midwoud, P. M.; Rieux, L.; Bischoff, R.; Verpoorte, E.; Niederlander, H. A. G. *J. Proteome Res.* **2007**, *6*, 781.

(233) Nirogi, R.; Kandikere, V.; Bhyrapuneni, G.; Benade, V.; Saralaya, R.; Irappanavar, S.; Muddana, N.; Ajjala, D. R. *J. Neurosci. Methods* **2012**, *209*, 379.

(234) Sakurai, T.; Amemiya, A.; Ishii, M.; Matsuzaki, I.; Chemelli, R. M.; Tanaka, H.; Williams, S. C.; Richarson, J. A.; Kozlowski, G. P.; Wilson, S.; Arch, J. R.; Buckingham, R. E.; Haynes, A. C.; Carr, S. A.; Annan, R. S.; McNulty, D. E.; Liu, W. S.; Terrett, J. A.; Elshourbagy, N. A.; Bergsma, D. J.; Yanagisawa, M. *Cell* **1998**, *92*, 1 page following 696.

(235) Silva, A. I.; de Matos, A. N.; Brons, I. G.; Mateus, M. *Med. Res. Rev.* **2006**, *26*, 181.

(236) Geng, M. H.; Ji, J. Y.; Regnier, F. E. *J. Chromatogr. A* **2000**, *870*, 295.

(237) Kuzyk, M. A.; Smith, D.; Yang, J.; Cross, T. J.; Jackson, A. M.; Hardie, D. B.; Anderson, N. L.; Borchers, C. H. *Mol. Cell. Proteomics* **2009**, *8*, 1860.

(238) Bender, M. L.; Kezdy, F. J.; Wedler, F. C. *J. Chem. Educ.* **1967**, *44*, 84.

(239) Klammer, A. A.; MacCoss, M. J. *J. Proteome Res.* **2006**, *5*, 695.

(240) Radziejewski, C.; Robinson, R. C.; Distefano, P. S.; Taylor, J. W. *Biochemistry* **1992**, *31*, 4431.

(241) de Young, L. R.; Schmelzer, C. H.; Burton, L. E. *Protein Sci.* **1999**, *8*, 2513.

(242) Jha, S. K.; Marqusee, S. *Proc. Natl. Acad. Sci. U. S. A.* **2014**, *111*, 4856.

(243) Candotti, M.; Esteban-Martin, S.; Salvatella, X.; Orozco, M. *Proc. Natl. Acad. Sci. U. S. A.* **2013**, *110*, 5933.

(244) Sun, L. L.; Zhu, G. J.; Li, Y. H.; Yang, P.; Dovichi, N. J. *Anal. Chem.* **2012**, *84*, 8715.

(245) Sun, L. L.; Zhu, G. J.; Dovichi, N. J. *Anal. Chem.* **2013**, *85*, 4187.

(246) Olah, T. V.; Sleczka, B. G.; D'Arienzo, C.; Tymiak, A. A. *Bioanalysis* **2012**, *4*, 29.

(247) Yang, Z. H.; Attygalle, A. B. *J. Mass Spectrom.* **2007**, *42*, 233.

(248) Mukai, Y.; Kamo, N.; Mitaku, S. *Protein Eng.* **1999**, *12*, 755.

(249) Sturm, R.; Sheynkman, G.; Booth, C.; Smith, L. M.; Pedersen, J. A.; Li, L. J. *J. Am. Soc. Mass Spectrom.* **2012**, *23*, 1522.

(250) Jackson, M.; Mantsch, H. H. *Biochimica Et Biophysica Acta* **1991**, *1078*, 231.

(251) Kearns, C. M.; Gash, D. M. *Brain Res.* **1995**, *672*, 104.

(252) Matheson, C. R.; Carnahan, J.; Urich, J. L.; Bocangel, D.; Zhang, T. J.; Yan, Q. *J. Neurobiol.* **1997**, *32*, 22.

(253) Maisonpierre, P. C.; Belluscio, L.; Friedman, B.; Alderson, R. F.; Wiegand, S. J.; Furth, M. E.; Lindsay, R. M.; Yancopoulos, G. D. *Neuron* **1990**, *5*, 501.

(254) Timm, D. E.; Dehaseth, P. L.; Neet, K. E. *Biochemistry* **1994**, *33*, 4667.

(255) VandeVondele, S.; Voros, J.; Hubbell, J. A. *Biotechnol. Bioeng.* **2003**, *82*, 784.

(256) Lee, W. H.; Slaney, T. R.; Hower, R. W.; Kennedy, R. T. *Anal. Chem.* **2013**, *85*, 3828.

(257) Lin, S. S.; Wu, C. H.; Sun, M. C.; Sun, C. M.; Ho, Y. P. *J. Am. Soc. Mass Spectrom.* **2005**, *16*, 581.

(258) Lopez-Ferrer, D.; Heibeck, T. H.; Petritis, K.; Hixson, K. K.; Qian, W.; Monroe, M. E.; Mayampurath, A.; Moore, R. J.; Belov, M. E.; Camp, D. G., II; Smith, R. D. *J. Proteome Res.* **2008**, *7*, 3860.

(259) Levkin, P. A.; Eeltink, S.; Stratton, T. R.; Brennen, R.; Robotti, K.; Yin, H.; Killeen, K.; Svec, F.; Fréchet, J. M. J. *J. Chromatogr. A* **2008**, *1200*, 55.

(260) Kučerová, Z.; Szumski, M.; Buszewski, B.; Jandera, P. *J. Sep. Sci.* **2007**, *30*, 3018.

(261) Gu, C.; Lin, L.; Chen, X.; Jia, J.; Ren, J.; Fang, N. *J. Sep. Sci.* **2007**, *30*, 1005.

(262) Oberacher, H.; Premstaller, A.; Huber, C. G. *J. Chromatogr. A* **2004**, *1030*, 201.